DISS. ETH NO. 28738

Lineage tracing of CD8 T cells upon asymmetric cell division

A thesis submitted to attain the degree of
DOCTOR OF SCIENCES of ETH ZURICH
(Dr. sc. ETH Zurich)

presented by

FABIENNE OLIVIA GRÄBNITZ

Master of Science, Ludwig Maximilian University of Munich
born on 21.12.1992
in Munich, Germany
citizen of Germany

accepted on the recommendation of

Prof. Dr. Annette Oxenius (examiner)
Prof. Dr. Federica Sallusto (co-examiner)
Prof. Dr. Timm Schroeder (co-examiner)
Dr. Mariana Borsa (co-examiner)

Zurich, 2022

TABLE OF CONTENTS

Summary

English Summary

Efficient clearance of viral infections requires a robust effector CD8 T cell response. Upon acute infection, naïve CD8 T cells are activated and initiate transcriptional and metabolic changes allowing them to enter a vigorous proliferative phase and differentiation into effector and memory cells. Elegant studies have shown that upon initial infection, a single, activated naïve CD8 T cell can give rise to diverse progeny exhibiting different phenotypes and functions, coupled to differential effector and memory cell fates. How divergence between effector and memory fates from a single naïve CD8 T cell is implemented on a mechanistical level, remains incompletely understood. Different models propose various factors or mechanisms that contribute to the establishment of cellular heterogeneity, including the strength of initial T cell receptor (TCR) signaling and asymmetric cell division (ACD).

TCR signal strength is impacted by TCR affinity towards its cognate antigen and antigen abundance and is suggested to modulate the proportional formation of effector and memory CD8 T cells, with strong TCR stimulation preferentially inducing short-lived effector cells and weaker stimulation favoring differentiation of memory precursor cells. Furthermore, it has been shown that strong TCR stimulation induces higher frequencies of cells undergoing ACD compared to weak TCR stimulation.

ACD is characterized by a polarized distribution of specific fate-determining transcription factors, cell organelles and surface receptors and it has been shown that the daughter cell that interacts with the antigen-presenting cell (APC) inherits molecules or organelles related to an effector fate, whereas the other daughter cell inherits molecules related to memory fate. Multiple studies have demonstrated a remarkable impact of asymmetric partitioning of fate-determining molecules on future fate by using bulk sorting of cells either expressing the marker of interest at a high or low level after the first cell division upon activation, followed by *in vivo* transfer in order to investigate their future fate. However, a direct link of ACD with subsequent asymmetric fate on a single cell level is missing, which requires the tracking of individual daughter cells after an ACD and their future differentiation.

As various studies provide evidence for a significant impact on fate diversification for both models - ACD and TCR signal strength - we aimed to combine both and elucidate their interplay and significance in this study. Therefore, we developed experimental systems allowing monitoring the fate of single daughter cell progenies derived from an ACD either induced by weak or strong TCR stimulation by live imaging. We used the combinatorial expression of TCF1 and CD62L as markers indicating fate specification a few days after activation. Using these two markers as predictors of future fate in combination with long-term live imaging approaches, we found that strong TCR stimulation led to elevated ACD rates and single cells undergoing ACD established "mixed-fate" colonies comprising both, effector and memory precursor cells. In contrast, upon weak TCR stimulation, ACD was not associated with different cell fates within the emerging offspring cell population. In this condition, single cells formed either memory or effector precursor colonies, irrespective of the (a)symmetry of their first cell division. We then tested the importance of ACD in fate diversification during the first mitosis after activation versus later cell divisions by transient or permanent inhibition of PKCζ, which prevents ACD. Our data shows that inhibiting ACD during the first cell division after activation upon strong TCR stimulation strongly curtailed the formation of memory precursor cells and this subsequently limited the memory potential of primed antigen-specific CD8 T cells *in vivo*. In opposite, no effect of ACD inhibition was observed on the formation of memory precursor cells upon weak TCR stimulation.

Together, our results indicate that ACD during the first mitosis after activation functions as a safeguard mechanism for CD8 T cell memory formation specifically upon strong TCR stimulation. These findings open new perspectives on vaccination and the development of immunotherapies against tumors.

Furthermore, we established a high-resolution single cell manipulation approach for primary CD8 T cells using Fluidic Force Microscopy (FluidFM) in order to combine imaging data with downstream manipulations. We developed a protocol for isolating single cells after mitosis, followed by monitoring colony formation and fate determination as well as a protocol for the extraction of cytoplasm of asymmetric daughter cells for RNA sequencing. This combinatorial approach allows precise lineage tracing of asymmetrically divided daughter cells at high resolution and opens new

opportunities for analysis of potential functional and transcriptional differences between daughter cells derived from an ACD.

Deutsche Zusammenfassung

Die effiziente Beseitigung viraler Infektionen erfordert eine robuste CD8 T Zell Antwort. Bei einer akuten Infektion werden naive CD8 T Zellen aktiviert, welche transkriptionelle und metabolische Veränderungen initiieren. Diese erlauben es ihnen, in eine starke Proliferationsphase einzutreten und in Effektor- und Gedächtniszellen zu differenzieren. Elegante Studien haben gezeigt, dass eine einzelne, aktivierte naive CD8 T Zelle bei erstmaliger Infektion eine vielfältige Nachkommenschaft mit verschiedenen Phänotypen und Funktionen hervorrufen kann, die mit Effektor- und Gedächtniszell-Charakteristiken verbunden sind. Wie die Aufteilung von Effektor- und Gedächtniszellen, stammend von einer einzelnen naiven CD8 T Zelle auf mechanistischem Level implementiert wird, ist noch nicht ganz verstanden. Verschiedene Modelle schlagen diverse Faktoren oder Mechanismen vor, die zum Entstehen zellulärer Heterogenität beitragen, darunter einerseits die Stärke des initialen T Zell Rezeptor (TZR) Signals und andererseits asymmetrische Zellteilung (AZT).

Die Stärke des TZR Signals wird durch die Affinität des TZRs zu seinem kognaten Antigen sowie durch die Konzentration des Antigens beeinflusst. Es wird angenommen, dass die Intensität des TZR Signals den proportionalen Anteil an Effektor- und Gedächtniszellen moduliert, wobei starke TZR Stimulation bevorzugt die Produktion kurzlebiger Effektorzellen induziert und schwächere Stimulation die Differenzierung von Vorläufergedächtniszellen favorisiert. Des Weiteren wurde gezeigt, dass starke TZR Stimulation zu mehr AZT führt als schwache TZR Stimulation.

Unter AZT wird die polarisierte Verteilung von spezifischen Zellschicksal-assoziierten Transkriptionsfaktoren, Zellorganellen und Oberflächenrezeptoren verstanden. Es wurde gezeigt, dass die Tochterzelle, die mit der antigen-präsentierenden Zelle (APZ) interagiert, Moleküle oder Organelle erbt, die mit der Effektorzell-Identität verbunden sind, während die andere Tochterzelle Gedächtniszell-Identität verbundene Moleküle erhält. Einige Studien haben mit der Sortierung und folgendem *in vivo* Transfer von Zellen, die nach der ersten Zellteilung ein bestimmtes Molekül auf hohem oder niedrigem Niveau exprimieren, einen bemerkenswerten Einfluss asymmetrischer Verteilung von Schicksal-bestimmenden Molekülen auf die zukünftige Zellidentität gezeigt. Allerdings fehlt bisher die direkte Verbindung zwischen AZT und nachfolgender asymmetrischer

5

Zellidentität auf Einzelzell-Level. Hierfür ist man auf die Verfolgung individueller Tochterzellen sowie deren zukünftiger Differenzierung nach einer asymmetrischen Zellteilung angewiesen.

Da mehrere Studien Nachweise für eine signifikante Bedeutung für beide Modelle - AZT und TZR Signalstärke - in Bezug auf Zelldiversifizierung bereitstellen, verfolgten wir in dieser Studie das Ziel, diese beiden Modelle zu kombinieren und ihr Zusammenspiel und ihre Bedeutsamkeit zu untersuchen. Dafür etablierten wir experimentelle Systeme mit bildgebenden Verfahren. Diese ermöglichten die Verfolgung des Zellschicksals von Nachkommen einzelner lebender Tochterzellen nach einer durch starke oder schwache TZR Stimulation erfolgten AZT. Wir nutzten die kombinierte Expression von TCF1 und CD62L, um wenige Tage nach Aktivierung das Zellschicksal identifizieren zu können. Mit Hilfe dieser beiden Moleküle als Indikatoren der zukünftigen Zellidentität in Kombination mit langzeit-bildgebenden Beobachtungsverfahren konnten wir feststellen, dass starke TZR Stimulation zu mehr AZT führte und einzelne Zellen nach einer AZT Kolonien formten, die aus sowohl Effektor- als auch Gedächtniszellen bestanden. Im Gegensatz dazu war AZT nach schwacher TZR Stimulation nicht mit verschiedenen Zellschicksalen in der entstehen Nachkommenpopulation verbunden. Unter dieser Bedingung generierten einzelne Zellen, unabhängig von der (A)Symmetrie ihrer ersten Zellteilung, entweder Effektor- oder Gedächtniszellkolonien. Als nächstes untersuchten wir die Bedeutung von AZT in Bezug auf Zellschicksal-Diversifizierung während der ersten Zellteilung nach Aktivierung verglichen mit möglichen nachfolgenden Zellteilungen durch transiente oder permanente Inhibierung von PKCζ, was zur Inhibierung von AZT führt. Unsere Daten zeigen, dass die Inhibierung von AZT während der ersten Zellteilung nach Aktivierung durch starke TZR Stimulation, die Etablierung von Vorläufergedächtniszellen stark einschränkte. Dies limitierte das Gedächtnispotential von aktivierten antigen-spezifischen CD8 T Zellen *in vivo*. Kein Effekt der AZT Inhibierung auf die Etablierung von Vorläufergedächtniszellen wurde dagegen bei schwacher TZR Stimulation beobachtet.

Zusammenfassend zeigen unsere Ergebnisse, dass AZT, spezifisch bei starker TZR Stimulation, während der ersten Zellteilung nach Aktivierung als Absicherungsmechanismus für die CD8 Gedächtnis-T-Zell-Generierung dient. Diese Erkenntnisse eröffnen neue Perspektiven für die Impfstoffentwicklung sowie für die Entwicklung von Immuntherapien gegen Tumore.

Darüber hinaus etablierten wir eine hochauflösende experimentelle Herangehensweise für Einzelzell-Manipulationen von primären CD8 T Zellen mit Hilfe von Fluidic Force Microscopy (FluidFM). Damit ist es möglich, bildgebende Verfahren mit darauffolgenden Eingriffen zu kombinieren. Wir entwickelten ein Protokoll für die Isolation von einzelnen Zellen nach ihrer Zellteilung, gefolgt von einer Untersuchung der Kolonie-Formation sowie der Bestimmung der angenommenen Zellidentität. Des Weiteren etablierten wir ein Protokoll für die Extraktion von Zytoplasma von asymmetrisch geteilten Tochterzellen für die Sequenzierung ihrer RNA. Diese kombinatorische Herangehensweise erlaubt die präzise Verfolgung von asymmetrisch geteilten Tochterzellen in hoher Auflösung und eröffnet neue Möglichkeiten für die Analyse potenzieller funktionaler und transkriptioneller Unterschiede zwischen Tochterzellen, die von einer AZT stammen.

Aims of the thesis

Understanding how CD8 T cell differentiation proceeds is of fundamental biological interest and of crucial importance in the design of vaccinations. Previous studies demonstrated that upon primary infection, a single, activated naïve CD8 T cell can give rise to distinct progeny with differential fates regarding effector and memory cell identity. However, the underlying mechanisms responsible for fate divergence stemming from a single naïve CD8 T cell remain incompletely understood. Two mechanisms that contribute to cellular diversification are asymmetric cell division (ACD) and the strength of T cell receptor (TCR) signaling.

ACD is defined by the unequal segregation of cell fate determinants leading to two daughter cells that are differentially equipped for future fate. While one daughter cell is destined to differentiate into an effector cell, the other daughter is endowed with memory features. Previous studies provided evidence that ACD is involved in fate diversification by functional analysis of bulk sorted cells either expressing a fate-determining molecule at a high or low level after the first cell division. However, a direct link between ACD and subsequent asymmetric fate on a single cell level remains to be shown. Furthermore, while it is reported that strong TCR stimulation preferentially induces effector cell differentiation at the expense of memory formation, it simultaneously leads to enhanced ACD rates compared to weak TCR stimulation. Yet, the reason for elevated ACD rates upon strong TCR stimulation combined with preferential effector differentiation is not completely understood.

In order to address these questions, we set out to combine both models - ACD and TCR signal strength - and elucidate their interplay. To this end, we aimed at establishing live imaging experimental systems allowing to follow the fate of single ACD-derived daughter cell progenies, either activated by weak or strong TCR stimulation.

Next, we committed to develop a high-resolution single cell manipulation approach for primary CD8 T cells using Fluidic Force Microscopy (FluidFM). We aimed at physically separating single ACD-derived sister cells followed by monitoring colony formation and fate determination. Moreover, we set out to establish image-guided cytoplasm extractions of asymmetric daughter cells followed by single cell RNAseq.

General introduction

CD8 T cell diversification

The importance of scientific research on CD8 T cell differentiation

The current pandemic of acute respiratory disease, named "coronavirus disease 2019" (COVID19), started in December 2019 in Wuhan, China and has caused over 6 million deaths worldwide until now (August 2022) according to the World Health Organization (WHO). COVID19 is caused by SARS-CoV-2, a single-stranded RNA coronavirus (Hu et al., 2021). This outbreak revealed how fast infectious pathogens can spread worldwide and depicted how vulnerable mankind and the system we are living in can be. COVID-19 caused tremendous challenges in all aspects of our life, especially in overwhelmed health care systems, leading to lockdowns and social distancing in order to prevent further viral transmission. Besides economic impacts and significant social challenges, the pandemic globally brought attention to the immune system, how it functions and how research can contribute to vaccine development leading to prevention of severe COVID19 disease and death of millions of people. With the world's globalization and the ever-increasing population's movement into mostly unspoiled natural regions, the risk of getting in contact with new viruses and their distribution all over the world is permanently growing. This has become evident even before the spread of SARS-CoV-2, such as the dreadful outbreaks of Ebola virus between 2014 and 2016 in West Africa.

Edward Jenner, a British physicist and scientist created the basis for the pioneering principle of vaccination in 1798, when he described the protective effect of cowpox against smallpox (Winkelstein, 1992). Vaccination aims at generating efficient and long-lived adaptive immune responses consisting of antibody-producing B cells and memory T cells without causing severe symptoms. Besides their importance in fighting infectious diseases, CD8 T cells play a crucial role in antitumor responses and autoimmunity. In order to develop and improve successful vaccination and immunotherapy strategies, such as adoptive cell transfer therapy (ACT) against tumors and chimeric antigen receptor (CAR) T cell therapy, it is of utmost importance to precisely understand the biology of adaptive immune cells and immune responses, in particular of CD8 T cells.

In the case of an acute viral infection, antigen-specific CD8 T cells are activated by antigen-presenting-cells (APCs), such as dendritic cells. CD8 T cells require three signals for proper activation: The activating interaction of the T cell receptor (TCR) with the peptide-MHC complex is called signal 1. Signal 2 is composed of costimulatory signals, such as the interaction of CD28 on T cells and CD80/CD86 on APCs and promotes survival and expansion of the T cells. Signal 3 is composed of pro-inflammatory cytokines, such as IL-12 or type I interferons and directs T cell differentiation into the different subsets of effector or memory T cells (Figure 3.1) (Mescher et al., 2006; Wiesel et al., 2009). The emerging pool of CD8 T cells upon successful activation consists of a variety of subpopulations that differ in function, phenotype and metabolism.
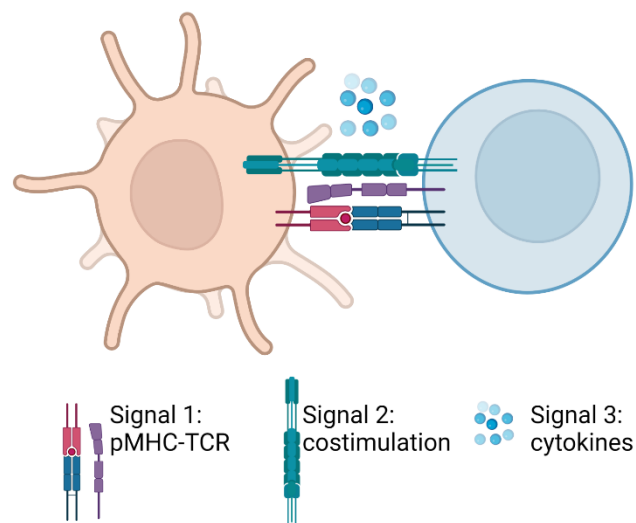

Figure 3.1. A CD8 T cell requires 3 signals for full activation.

A dendritic cell (orange) presents the cognate antigen on MHC-I to the specific TCR of the CD8 T cell (blue) providing signal 1. Signal 2 is composed of the interaction of costimulatory molecules and signal 3 is mediated by cytokines released by the dendritic cell.

Heterogeneity of the CD8 T cell response upon acute infection

The number of naïve T cells (T_n) specific for a given antigen and able to take part in a specific T cell response is 20 000 to 200 000 per person (Alanio et al., 2010). Upon acute infection, these naïve CD8 T cells are activated and initiate transcriptional and metabolic changes allowing them to enter a vigorous proliferative phase, which is described as the expansion phase. Together with the acquisition of effector functions such as cytokine release and cytotoxicity, this expanded effector population can in many cases control a viral infection. This phase is followed by the contraction phase, in which the majority of CD8 T cells undergoes apoptosis and only 5-10% of CD8 T cells enter the memory phase and survive long-term (Figure 3.2).

The main phenotype of CD8 T cells present during the expansion phase are short-lived cytotoxic effector cells (SLECs/T_E). T_E are phenotypically characterized as $KLRG1^{hi}IL7R^{lo}$ expressing cells, by the production of granzymes and perforins in order to efficiently kill infected cells as well as by production of inflammatory cytokines such as IFNγ and TNFα (Arsenio et al., 2015; Kaech and Cui, 2012; Stemberger et al., 2007). In order to meet their energetic demands required for their proliferation and biosynthesis of effector proteins, effector CD8 T cells perform glycolysis (Pearce et al., 2013). However, several studies found early memory cells emerging already throughout the expansion phase. One study characterized memory precursor effector cells (MPECs), which are found at the peak of CD8 T cell expansion and are identified by increased expression of IL7R (Kaech et al., 2003). Another recent study described a small population of $TCF1^+$ CD8 T cells that is already present at day 8 post LCMV infection and gives rise to later central memory CD8 T cells (Pais Ferreira et al., 2020). Similarly, a population of $CD62L^{hi}$ cells that later yield central memory CD8 T cells was recently described to emerge early after acute infection (Johnnidis et al., 2021).

After resolution of acute viral infection, multiple distinct long-lived CD8 T cell subsets varying in migratory and functional properties were described to develop throughout the memory phase: effector memory (T_{EM}), central memory (T_{CM}), stem cell memory (T_{SCM}) and tissue-resident memory (T_{RM}) CD8 T cells (Chung et al., 2021; Jameson and Masopust, 2018, 2009; Lanzavecchia and Sallusto, 2005; Sallusto et al., 2004). Memory T cells are maintained in an antigen-independent,

cytokine dependent manner, mainly relying on sensing IL-7 and IL-15, enabling survival and self-renewal (Surh and Sprent, 2008).

T_{CM} cells can be distinguished from T_{EM} cells by expression of CD62L and CCR7, which both mediate homing to secondary lymphoid organs. While T_{CM} cells express CD62L and CCR7, lack immediate effector functions and retain the potential to give rise to CCR7$^-$ cells, T_{EM} cells do not express CD62L and CCR7 and display immediate levels of effector functions (Sallusto et al., 1999; Wherry et al., 2003). T_{SCM} cells were characterized in humans by enhanced capacity for self-renewal, the ability to give rise to T_{EM}, T_{CM} and T_E cells, increased proliferative capacity and can be identified by the expression of CD45RA$^+$CD45RO$^-$CCR7$^+$CD95$^+$ (Gattinoni et al., 2011). In contrast to circulating memory T cells, T_{RM} cells have been identified to reside in tissues in order to provide a rapid first local response against infections (Masopust David et al., 2001; Mueller and Mackay, 2016). This heterogeneity within the CD8 T cell response is fundamental for efficient immunity.

Even though the diverse offspring of activated CD8 T cells is precisely characterized, it is not yet clearly understood how this heterogeneity is mechanistically generated.
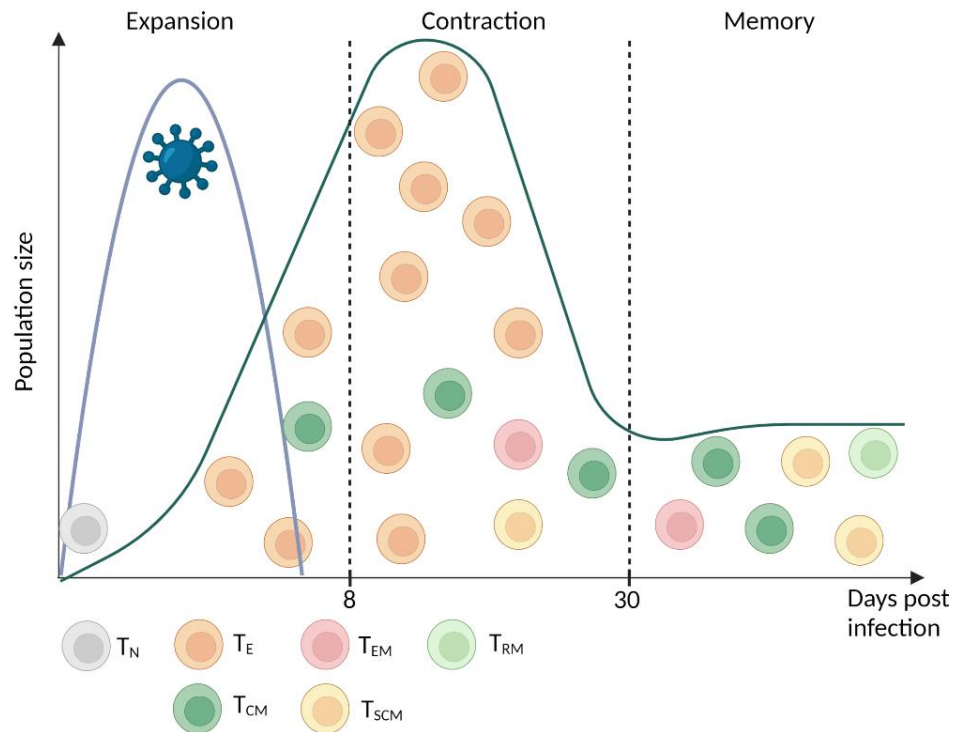
Figure 3.2. Heterogeneity of the CD8 T cell response upon acute infection.

Viral titers are shown in blue; overall virus specific CD8 T cell response is shown in green. Differentially colored cells represent different subsets of effector and memory (precursor) CD8 T cells over time. Upon acute infection, naïve CD8 T cells (T_N) are activated and start to vigorously proliferate during the expansion phase reaching the peak between eight and ten days post infection. The majority of cells during the expansion phase are short-lived effector T cells (T_E), which mediate viral clearance and die shortly after during the contraction phase. However, a small population of memory precursor cells is already present during the expansion phase, giving later rise to long-lived effector memory (T_{EM}), central memory (T_{CM}), stem cell memory (T_{SCM}) and tissue-resident memory (T_{RM}) cells.

CD8 T cell diversification

The well described heterogeneous pool of CD8 T cells emerging upon activation raised the interest in studying the underlying mechanisms and molecular regulation of diversification (Chang et al., 2014). How divergence between the distinct CD8 T cell subsets mechanistically occurs is incompletely elucidated. Several hypotheses on the emergence of CD8 T cell heterogeneity have been addressed in numerous studies. Previous studies have described the early emergence of IL7R$^+$ MPECs, of TCF1$^+$ CD8 T cells and of CD62L^{hi} cells, all of which are present already during the expansion phase upon acute infection and later yield central memory CD8 T cells (Johnnidis et al., 2021; Kaech et al., 2003; Pais Ferreira et al., 2020). These studies provide evidence against a linear differentiation trajectory of $T_N \rightarrow T_E \rightarrow T_{CM}$.

The idea of "pre-programmed" naïve CD8 T cells giving rise to either effector or memory cells has become rather unlikely since studies have elegantly shown that a single naïve CD8 T cell is multipotent and able to give rise to effector and memory CD8 T cells. By using cellular barcoding or adoptive transfer of single CD8 T cells - either by limiting dilution or by using congenic markers allowing the discrimination between single cells - the theory of "one cell - multiple fates" is scientifically well supported (Buchholz et al., 2013; Chang et al., 2007; Gerlach et al., 2013, 2010; Plumlee et al., 2013; Stemberger et al., 2007). Based on this theory, three mechanistic models of CD8 T cell diversification are currently investigated: 1. Decreasing-potential model; 2. Signal-strength model and 3. Asymmetric cell division model (Figure 3.3).

The decreasing-potential model suggests that repetitive stimulation with the cognate antigen, costimulatory signals and cytokines dictates the differentiation state. The accumulating activation signals drive differentiation into terminally effector cells and simultaneously to the loss of memory potential, such as enhanced longevity (D'Souza and Hedrick, 2006; Joshi et al., 2007; Sarkar et al., 2008). Studies supporting this model are based on the findings that curtailing the duration of antigen exposure and limiting inflammation drives memory T cell formation and that latecomers in a T cell response acquire T_{CM} cell characteristics.

The signal strength model, in contrast, is confined to the strength of the first signals 1-3 delivered to the T cell during priming. It is suggested that with increasing TCR signal strength, CD8 T cells will adopt terminally differentiated T_E phenotypes (Kaech and Cui, 2012).

Asymmetric cell division is characterized by the polarized distribution of fate related markers between the emerging daughter cells. It is suggested that the immunological synapse (IS)-proximal daughter (interacting with the APC) inherits molecules related to effector cell properties whereas the IS-distal daughter is endowed with memory cell associated molecules (Kaech and Cui, 2012). Both models - the signal-strength model and asymmetric cell division - will be discussed in more detail in the next chapters.

A Decreasing-potential model

Signals 1, 2, 3

T_N T_{CM} T_{EM} T_E

B Signal-strength model

Increasing strength of signals 1, 2, 3

T_N T_{CM} T_{EM} T_E

C Asymmetric cell division model

T_N T_E T_{CM}
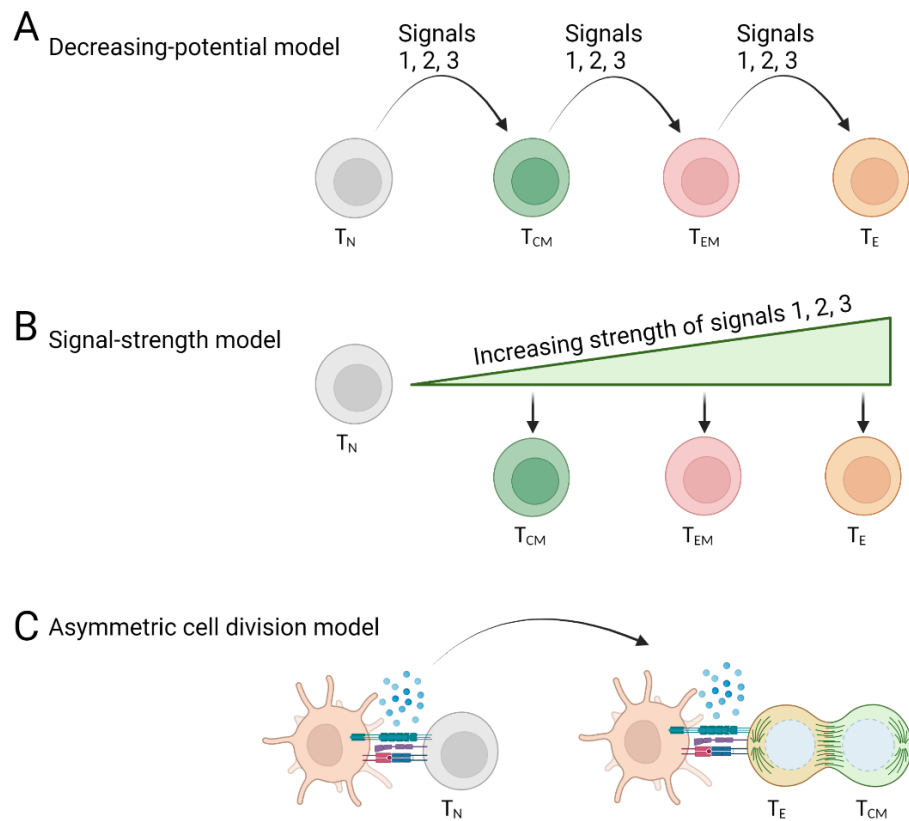
Figure 3.3. Models of CD8 T cell diversification.

A Decreasing potential model. Repetitive signals 1,2 and 3 direct terminal effector differentiation. **B** Signal-strength model. The strength of the first signals 1, 2 and 3 drive differentiation with increased strength favouring the differentiation of terminal effector T cells. **C** Asymmetric cell division model. Polarized distribution of effector and memory related molecules between emerging sister cells leading to one memory precursor and one effector precursor T cell.

Asymmetric cell division

Asymmetric cell division (ACD) is an evolutionary well conserved mechanism for the generation of cellular heterogeneity (Sunchu and Cabernard, 2020), which has also been described to occur in CD8 T cells (Chang et al., 2007). Upon interaction of the TCR with the MHC-antigen complex on an APC, an immune synapse (IS) is formed by the recruitment of receptors and ligands to the cellular interface, providing adherence, stabilization and interaction with their respective counterparts. The formation of an IS leads to the establishment of a polarization axis allowing unequal segregation of specific molecules between the emerging daughter cells, resulting in an asymmetric cell division (Oliaro et al., 2010). Deficiency of the adhesion molecule ICAM1 in CD8 T cells prevents the formation of a stable IS, inhibits ACD and emphasizes the key role of a solid IS as a prerequisite for ACD (Chang et al., 2007).

Previous studies have revealed that the IS-proximal daughter cell (interacting with the APC) is equipped with T cell receptor associated molecules CD3 and CD8 as well as with the integrin LFA-1 (Capece et al., 2017; Chang et al., 2007). Furthermore, the receptor for IFNγ, the Notch signaling inhibitor Numb and Scribble, an important component of a key polarity complex, were shown to localize into the proximal daughter cell (Chang et al., 2007; King et al., 2012). Another study found that CD25, the receptor for IL-2, is enriched on the surface of the proximal daughter cell, suggesting enhanced proliferative potential (Ciocca et al., 2012). The preferential localization of cBAF complex components, the transcription factor c-myc as well as active mTORC1 kinase into the proximal daughter cell leads to enhanced metabolic activity supporting the proliferative burst essential for effector cell differentiation (Guo et al., 2022; Pollizzi et al., 2016; Verbist et al., 2016). Moreover, it was demonstrated that asymmetric activity of the phosphatidylinositol 3-kinase (PI3K) in the proximal daughter cell leads to an enhanced trafficking of Glut1, the receptor for glucose uptake, from recycling endosomes to the cell surface (Y.-H. Chen et al., 2018; Lin et al., 2015). These findings suggest that ACD destines the proximal daughter cell to an effector fate with enhanced metabolic and proliferative capacity.

On the other side, the protein kinase C–ζ (PKCζ) and the proteasome were shown to distribute to the distal daughter cell (Chang et al., 2011, 2007). Interestingly, deficiency of PKCζ inhibits ACD and directs effector fate differentiation at the expense of memory fate (Metz et al., 2015).

Another aspect of asymmetric cell division and fate is the cellular metabolism, which differs between effector and memory CD8 T cells. Memory as well as naive CD8 T cells rely primarily on oxidative phosphorylation for energy production, whereas effector CD8 T cells mainly rely on glycolysis to meet their energetic demands (Pearce et al., 2013). Besides asymmetric partitioning of Glut1, it was shown that sorted bulk first mitosis CD8^{hi} and CD8^{lo} cells differ in their extent of performing glycolysis or oxidative phosphorylation. It was shown that CD8^{hi} cells perform glycolysis, whereas CD8^{lo} cells rely on oxidative phosphorylation (Pollizzi et al., 2016). Moreover, the transcriptional heterogeneity within CD8 T cells that have undergone one cell division after activation emphasizes the potential role of asymmetric cell division in fate diversification (Borsa et al., 2019; Kakaradov et al., 2017).

Taken together, these studies support the hypothesis that the proximal daughter cell displays higher expression of proteins associated with an effector fate, whereas the distal daughter cell inherits proteins that endow it with a memory fate and lends support to the hypothesis that ACD is involved in effector and memory differentiation (Figure 3.4).

Further, a recent study has shown that ACD is a feature of stemness, as preferentially naïve and memory CD8 T cells are able to perform ACDs in contrast to more differentiated cells, such as exhausted or effector CD8 T cells (Borsa et al., 2019). Interestingly, it was described that the ability of naïve CD8 T cells to undergo ACD decreases with age, which might contribute to the impaired ability of diversity generation and decreased vaccination efficacy in the elderly population (Borsa et al., 2021). Furthermore, it has been shown that ACD can be modulated and as a result impacts the formation of memory. The well-described drug rapamycin has been shown to increase the frequency of cells undergoing ACD and thereby increasing the population of functional memory cells. On the other side, it has been shown that aurothiomalate, an inhibitor of PKCζ, decreases the frequency of asymmetrically dividing cells, resulting in less memory potential (Borsa et al., 2019). Mechanistically, it has recently been described that the formation of a diffusion barrier in the ER membrane is closely correlated to asymmetric cell division in CD8 T cells (Emurla et al., 2021).

So far, all studies addressing functional or transcriptional aspects of asymmetrically divided cells in terms of fate used bulk sorting of cells either expressing the marker of interest at a high or low level after the first cell division upon activation, followed by downstream analysis (Borsa et al., 2019; Guo et al., 2022; Pollizzi et al., 2016; Verbist et al., 2016). This approach, however, lacks the precise history and information of whether the investigated cells are truly emerging from an asymmetric cell division.
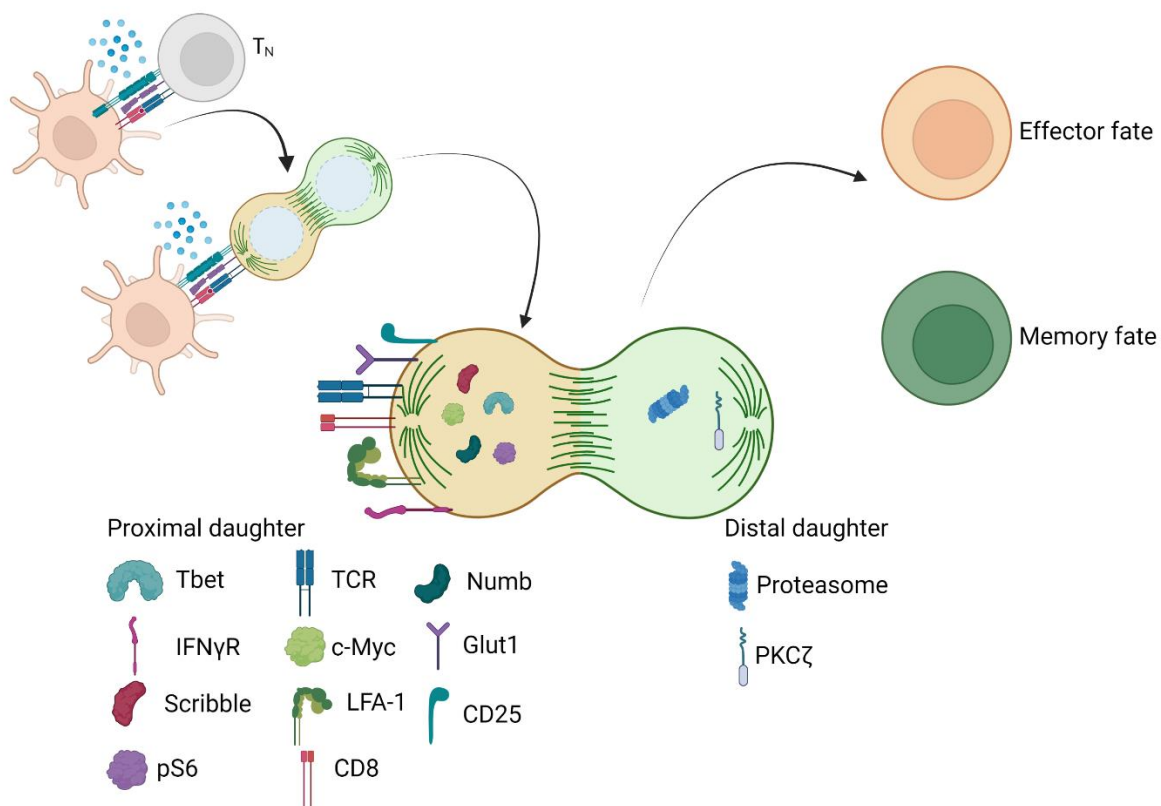
Figure 3.4. Asymmetric CD8 T cell Division.

A naive CD8 T cell recognizes its cognate antigen presented by an APC via MHC-I molecules with its antigen-specific TCR. Interaction of other costimulatory molecules together with sensing of inflammatory cytokines leads to activation of the CD8 T cell and the formation of the immune synapse (IS), which induces a polarization axis. Consequently, key fate determinants segregate asymmetrically between the emerging two daughter cells throughout the process of mitosis leading to an asymmetric cell division (ACD). ACD results in two daughter cells with different potential fates: the IS-proximal cell is committed with an effector fate, while the IS-distal daughter is endowed with a memory fate.

Strength of TCR activation and fate outcome

The pool of naïve CD8 T cells specific for a given antigen within an organism bears T cell clones of diverse TCR sequences leading to different individual TCR affinities towards the cognate antigen. Upon encounter of a naïve CD8 T cell with an antigen presenting cell presenting its specific antigen, the immune synapse is formed and supports TCR signaling. The strength of TCR signaling is regulated by interleukin-2 inducible tyrosine kinase (ITK), acting downstream of the TCR, and is modulated by the affinity of the TCR towards its antigen as well as antigen abundance (Andreotti et al., 2010; Conley et al., 2020, 2016; Huang et al., 2015; Nayar et al., 2012). Affinity of a specific TCR is considered as the strength of interaction with a peptide-MHC (pMHC) complex and is commonly measured by surface plasmon resonance (SPR) (Martinez and Evavold, 2015; Zhang et al., 2016). It is well described that high affinity interactions between the TCR and pMHC result in acquisition of effector functions and establishment of a long-lived memory pool (Corse et al., 2011; Gourley et al., 2004). The survival of naïve peripheral CD8 T cells depends on low affinity interactions with self-peptide-MHC molecules (Jameson, 2005; Sprent et al., 2008). However, there is strong evidence that also low affinity T cell clones take part in the immune response against tumors and pathogens. Similar to the crucial role of functional diversity within the established CD8 T cell pool, it is important to maintain a broad affinity distribution providing advantage for effective immune responses against rapidly evolving and new pathogens (Huseby and Teixeiro, 2022; Martinez and Evavold, 2015).

The strength of TCR signaling is a key determinant for CD8 T cell fate commitment and function and TCR affinity dictates kinetics and magnitude of the T cell response. Studies have shown that both, weak and strong TCR-ligand interactions, lead to full activation of naïve CD8 T cells, induce proliferation and establish effector and memory cells (Prlic et al., 2006; Zehn et al., 2009). However, it has been demonstrated that TCR affinity regulates the proportional abundance of effector and memory precursor cells within the emerging population with high affinity TCR stimulation preferentially inducing short-lived effector cells (SLECs) and weaker stimulation favoring differentiation of memory precursor cells (Chin et al., 2022; King et al., 2012; Smith-Garvin et al., 2010; Solouki et al., 2020). Memory differentiation upon weak TCR stimulation has been

shown to be induced by enhanced expression of Eomes, CD62L, IL7R and BCL6 in contrast to high affinity TCR stimulated cells (Figure 3.5) (Kavazović et al., 2020; Knudson et al., 2013). Differences in migration- and proliferation timing after activation have been observed with low affinity T cell clones exiting lymphoid organs faster and beginning to contract earlier than high affinity T cell clones (Ozga et al., 2016; Zehn et al., 2009). Furthermore, it was described that established low affinity memory cells functionally differ from high affinity memory cells, as they were impaired in their recall response to low but not high affinity ligands for instance (Chin et al., 2022; Knudson et al., 2013). Mechanistically, high and low affinity TCR T cell clones seem to respond differently to persistent antigen exposure with different cell intrinsic features. Using a tumor model, it was recently discovered that PD1^{hi} tumor-specific low affinity CD8 T clones enter a state of functional inertness, while high affinity clones are driven to dysfunction (Shakiba et al., 2022).

Interestingly, it has been shown that strong TCR stimulation induces higher frequencies of cells undergoing asymmetric cell division compared to weak TCR stimulation (Figure 3.5) (King et al., 2012). This observation raises the question whether an interplay between TCR stimulation strength and ACD exists, how this might be regulated and how it impacts fate diversification.
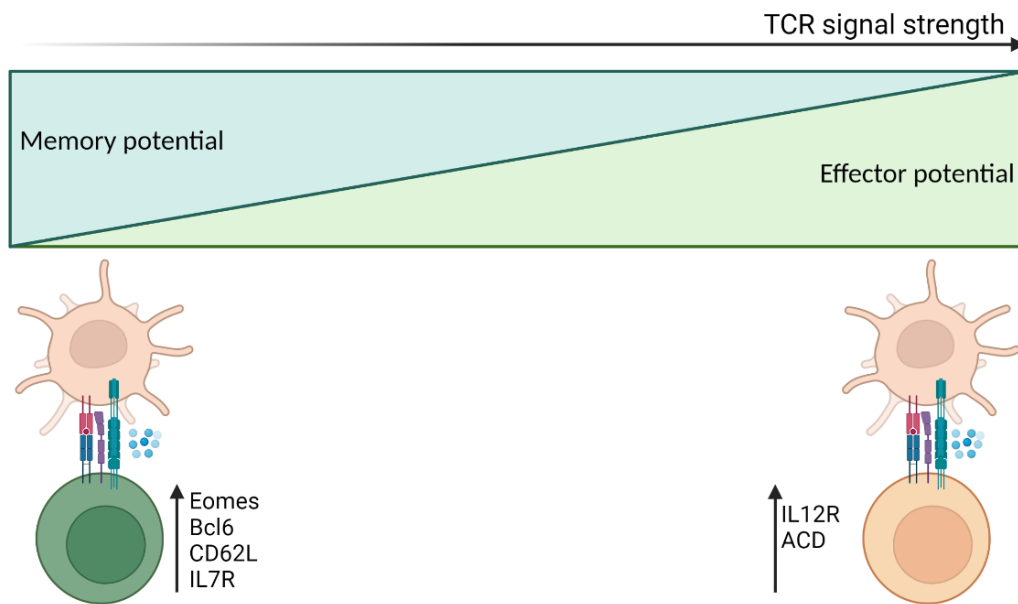
Figure 3.5. The strength of TCR signaling impacts fate outcome.

Upon engagement of the TCR with its cognate antigen presented on MHC-I by an APC, the TCR is activated and signaling downstream of the TCR is initiated. The strength of TCR activation can be modified by the affinity of the TCR towards its ligand and antigen abundance. TCR signal strength further impacts fate diversification of the activated CD8 T cell with strong TCR signaling preferentially inducing effector differentiation and weak TCR stimulation initiating memory differentiation.

Importance of single cell approaches in CD8 T cell differentiation and current limitations

The improvement of existing technologies as well as the establishment of new technologies in combination with high dimensional analysis tools allows for investigations at increasingly higher resolution. The growing knowledge about remarkable cellular heterogeneity between tissues and cell specific subsets emphasizes the need to study cellular function, phenotype and plasticity at the single cell level. In order to establish kinship analysis, fate mapping- and lineage tracing approaches are necessary.

Individual transcriptional differences can be investigated by single cell RNA sequencing (scRNAseq) and bioinformatic approaches can be used to analyze cell differentiation trajectories using the ratio of spliced to unspliced RNA, such as RNA velocity (Wagner and Klein, 2020). Furthermore, TCR sequencing (TCRseq) allows the analysis of which T cells originally emerged from the same naïve T cell clone. RNAseq and TCRseq capture a snapshot - either of the transcriptomic landscape or clonal origin - at a certain point in time. Combining single cell transcriptome sequencing with TCRseq links the transcriptional state to the clonal origin of the cell, providing an elegant method for lineage tracing analysis (Al Khabouri and Gerlach, 2020). However, naïve CD8 T cells bearing the same TCR sequence are present at varying frequencies within the naïve population, ruling out that T cells with the same TCR sequence necessarily originate from a single naïve T cell (de Greef et al., 2020). The immense amount of data stemming from such high-dimensional datasets requires sophisticated bioinformatic analysis to ensure precise interpretation of the data. Moreover, as for the cellular barcoding technology, these two approaches are limited by the viability of cells as these methods require the lysis of cells, preventing downstream experiments (Al Khabouri and Gerlach, 2020; Gerlach et al., 2010). In contrast, single cell transfer experiments allow viability of cells by using congenic markers identified by FACS analysis for kinship investigations. However, the throughput of these experiments is low and especially for the limiting dilution approach, it is not ensured that only one cell is transferred (Buchholz et al., 2013; Stemberger et al., 2007).

In contrast to the discussed *in vivo* technologies to investigate lineage tracing, *in vitro* fate mapping approaches present certain advantages. Live cell imaging in combination with cell manipulations allows for phenotypic, transcriptional, migratory and morphological analyses, which can be followed up by isolation of cells of interest based on the imaging information. One of such approaches is Fluid Force Microscopy (FluidFM) (Guillaume-Gentil et al., 2014a; Meister et al., 2009). FluidFM enables single cell live imaging and based on a microfluidic system allows for micromanipulations such as cell isolation, cell organelle transplantation between living cells and cell content extraction for downstream analysis, such as RNA sequencing, termed Live-seq (Chen et al., 2022; Gäbelein et al., 2022; Guillaume-Gentil et al., 2016).

A major limitation of single cell approaches is the low throughput, which might challenge the significance of the findings. Furthermore, cells are removed from their physiological environment for most of the discussed approaches. *In situ* lineage tracing approaches are technically challenging as cells migrate through their specific tissue and daughter cells might wander into different directions within the tissue upon completed cell division, making it increasingly difficult to follow progeny cells.

However, the ongoing refinements of current technologies together with the establishment of new approaches provide remarkable potential for future investigations and findings at high resolution at the single cell level.

Asymmetric Cell Division safeguards memory CD8 T cell development

Fabienne Gräbnitz[1], Dominique Stark[1], Danielle Shlesinger[2], Anthony Petkidis[3], Mariana Borsa[1,4], Alexander Yermanos[1,2,5], Andreas Carr[1], Niculò Barandun[1], Arne Wehling[2], Miroslav Balaz[6,7], Timm Schroeder[2] and Annette Oxenius[1]

[1] Institute of Microbiology, ETH Zurich, Vladimir-Prelog-Weg 4, 8093 Zurich, Switzerland.

[2] Department of Biosystems Science and Engineering, ETH Zurich, Mattenstrasse 26, 4058 Basel, Switzerland.

[3] Department of Molecular Life Sciences, University of Zurich, Winterthurerstrasse 190, 8057 Zurich, Switzerland.

[4] The Kennedy Institute of Rheumatology, NDORMS, University of Oxford, Roosevelt Drive, Oxford OX3 7FY, UK

[5] Center for Translational Immunology, University Medical Center Utrecht, Utrecht, Netherlands

[6] Department of Metabolic Disease Research, Biomedical Research Center of the Slovak Academy of Sciences, Dubravska cesta 9, 845 05 Bratislava, Slovakia.

[7] Department of Health Sciences and Technology, ETH Zurich, Schorenstrasse 16, 8603 Schwerzenbach, Switzerland.

Abstract

The strength of T cell receptor (TCR) stimulation and asymmetric distribution of fate determinants are both implied to affect T cell differentiation. Here, we uncovered asymmetric cell division (ACD) as a safeguard mechanism for memory CD8 T cell generation specifically upon strong TCR stimulation. Using live imaging approaches, we found that strong TCR stimulation induced elevated ACD rates and subsequent single cell derived colonies comprised both effector and memory precursor cells. The abundance of memory precursor cells emerging from a single activated T cell positively correlated with first mitosis ACD. Accordingly, preventing ACD by inhibition of PKCζ during the first mitosis upon strong TCR stimulation markedly curtailed the formation of memory precursor cells. Conversely, no effect of ACD on fate commitment was observed upon weak TCR stimulation. Our data provide new mechanistic insights into the role of ACD for CD8 T cell fate regulation upon different activation conditions.

Introduction

Robust and heterogeneous antigen-specific CD8 T cell responses are essential for effective host defense against infection. Upon initial acute viral infection, activated naïve CD8 T cells start to clonally expand and differentiate. The majority of generated CD8 T cells within this phase are effector cells (T_E), responsible for rapid elimination of infected cells and viral clearance (Kaech and Cui, 2012). However, also CD8 memory precursor cells develop early during the clonal expansion phase at low frequencies (Johnnidis et al., 2021; Kaech et al., 2003; Pais Ferreira et al., 2020). While T_E are short-lived, leading to contraction of the overall response, memory CD8 T cells establish a long-lived pool composed of multiple distinct self-renewing subsets, which vary in their migratory and functional properties. Reactivation of these memory cells upon secondary encounter with the same pathogen leads to execution of immediate effector functions alongside secondary expansion, thereby providing protection (Chung et al., 2021). Intriguingly, elegant studies have demonstrated that a single, naïve CD8 T cell can give rise to both effector and memory cells upon activation (Buchholz et al., 2013; Gerlach et al., 2013, 2010; Stemberger et al., 2007). However, it remains unknown how divergence between effector and memory fates from a single naïve CD8 T cell is achieved on a mechanistic level. Different models propose various factors or mechanisms that contribute to the establishment of cellular heterogeneity, including the strength of initial T cell receptor (TCR) signaling and asymmetric cell division (ACD) (Y. Chen et al., 2018; Kaech and Cui, 2012). In both models, the immunological synapse (IS), formed between the antigen-presenting cell (APC) and the engaged T cell, orchestrates TCR activation and establishes a polarization axis serving as a prerequisite for ACD. TCR signal strength is impacted by TCR affinity towards its cognate antigen as well as antigen abundance and is suggested to modulate the proportional formation of effector and memory CD8 T cells, with strong TCR stimulation preferentially inducing short-lived effector cells (SLECs) and weaker stimulation favoring differentiation of memory precursor cells (King et al., 2012; Solouki et al., 2020). In addition, it has been shown that strong TCR stimulation induces higher frequencies of cells undergoing ACD compared to weak TCR stimulation (King et al., 2012). ACD is characterized by a polarized distribution of specific fate-determining transcription factors (e.g. Tbet and c-Myc), cell organelles (e.g. proteasomes), and

surface receptors (e.g. CD8, TCR, CD25, IFNγR, Glut1). Further, it has been reported that the IS-proximal daughter cell - interacting with the APC - inherits molecules or organelles related to an effector fate, such as Tbet and CD25, whereas the IS-distal daughter cell inherits components promoting memory fate, such as the proteasome and PKCζ (Capece et al., 2017; Chang et al., 2011, 2007; Y. Chen et al., 2018; Ciocca et al., 2012; King et al., 2012; Liedmann et al., 2022; Metz et al., 2015; Oliaro et al., 2010; Pollizzi et al., 2016; Verbist et al., 2016). Previous studies have demonstrated a remarkable impact of differential expression of fate-determining markers on future fate of first daughter cells by using bulk sorting of cells either expressing the marker of interest at a high or low level after the first cell division upon activation, followed by downstream analyses investigating their future fate (Borsa et al., 2019; Guo et al., 2022; Pollizzi et al., 2016; Verbist et al., 2016). Furthermore, the role of ACD in fate diversification is supported by the reported transcriptional heterogeneity within CD8 T cells that have undergone one cell division after activation (Borsa et al., 2019; Kakaradov et al., 2017). However, a direct link of ACD to subsequent asymmetric fate on a single cell level is missing. Therefore, tracing of individual daughter cells that emerge from an ACD and analysis of their progeny with respect to their differentiation is necessary (Loeffler et al., 2020). As various studies provide evidence for a significant impact on fate diversification for both models - ACD and TCR signal strength - we aimed to elucidate their interplay. To this end, we established experimental systems allowing to follow the fate of single daughter cell progenies derived from an ACD either induced by weak or strong TCR stimulation using live imaging. We validated and used the combinatorial expression of T cell factor 1 (TCF1) and L-selectin (CD62L) as markers indicating effector and memory fate specification a few days after activation. Using these two markers as predictors of future fate in combination with long-term live imaging approaches, we found that strong TCR stimulation led to elevated ACD rates and single cells undergoing ACD established mixed-fate colonies comprising both effector and memory precursor cells. Strikingly, experimental impairment of ACD during the first cell division after activation upon strong TCR stimulation markedly curtailed the development of memory precursor cells, which resulted in limited memory formation *in vitro* and *in vivo*. In contrast, upon weak TCR stimulation, ACD was not associated with different cell fates and single activated cells formed exclusively single-fate colonies, either comprising memory or effector precursor cells, irrespectively of the asymmetry of their first cell division. In addition, no effect of

ACD inhibition was observed on the formation of memory precursor cells. Together, our results indicate that ACD during the first mitosis after activation functions as a safeguard mechanism for CD8 T cell memory formation following strong TCR stimulation.

Results

Expression of TCF1 and CD62L identifies early memory and effector precursor CD8 T cells

To relate divergent cell fates of activated CD8 T cells to ACD, we established an *in vitro* CD8 T cell activation protocol that allows tracking of individual cells and their progeny over several generations by live microscopy. Monitoring of early differentiation states indicative of memory or effector cell differentiation requires the identification of early fate determination markers. Previous studies have shown that CD62L and TCF1 are expressed in naïve and memory CD8 T cells and are both downregulated in effector cells (Chang et al., 2014; Zhao et al., 2010). Furthermore, CD62L$^+$TCF1$^+$ cells generated *in vivo* during the early acute effector phase were shown to give rise to central memory T cells (T$_{CM}$) (Johnnidis et al., 2021; Pais Ferreira et al., 2020). We therefore investigated whether *in vitro* stimulation of CD8 T cells also gives rise to an early establishment of CD62L$^+$TCF1$^+$ cells alongside CD62L$^-$TCF1$^-$ cells, and whether expression of TCF1 and CD62L at these early stages of differentiation serve as reliable markers indicating future fate. To this end, we used TCR transgenic P14 CD8 TCF1-GFP cells, which specifically recognize the gp$_{33-41}$ peptide from the Lymphocytic Choriomeningitis Virus (LCMV) glycoprotein and additionally express a *Tcf7^{GFP}* reporter (Utzschneider et al., 2016). P14 CD8 TCF1-GFP cells were activated by plate bound α-CD3 and α-CD28 antibodies in addition to Fc-ICAM-1 and IL-2 for 36-40 hours (h), then removed from the activation stimuli and further cultured in the presence of IL-2, IL-7 and IL-15 (Fig. 4.1A). 4 days later, we observed marked proliferation and partial downregulation of TCF1 and CD62L, resulting in the development of three populations identified by divergent expression of TCF1 and CD62L (CD62L$^+$TCF1$^+$, CD62L$^+$TCF1$^-$, CD62L$^-$TCF1$^-$, Fig. 4.1A and 4.1B). CD62L required at least 4 cell divisions before downregulation was initiated, while TCF1 downregulation started after 2 - 3 cell divisions (Fig. 4.1C). Next, we dissected the *in vitro* behavior of these three populations. In line with the finding that both markers required several rounds of cell division to initiate downregulation, we found that CD62L$^-$TCF1$^-$ cells proliferated the most, whereas CD62L$^+$TCF1$^-$ cells were slower and CD62L$^+$TCF1$^+$ cells underwent the least rounds of cell division on day 4 and day 7 after activation (Fig. 4.1D). Furthermore, sorting and subsequent individual culture of the three subsets revealed

that the CD62L$^+$TCF1$^+$ subset partially fed into the two other subsets, while CD62L$^+$TCF1$^-$ cells only fed into the CD62L$^-$TCF1$^-$ subset and the CD62L$^-$TCF1$^-$ subset mainly preserved its phenotype 2 days after additional culture, indicating a clear direction of differentiation (Fig. 4.1E). In further analyses, we focused on the most distinct CD62L$^+$TCF1$^+$ and CD62L$^-$TCF1$^-$ cell subsets and wondered whether the observed differences in proliferation and resulting expression of CD62L and TCF1 might be associated with distinct expression profiles of costimulatory and coinhibitory receptors. In line with previous data, showing that early memory precursor cells are maintained by inhibitory signaling (Johnnidis et al., 2021), CD62L$^+$TCF1$^+$ cells expressed elevated levels of PD1. Instead, CD62L$^-$TCF1$^-$ cells showed higher expression of CD25, providing enhanced sensitivity to proliferation inducing IL-2 (Fig. 4.1F). Additionally, TIM3 and ICOS were found to be higher expressed in CD62L$^-$TCF1$^-$ cells compared to CD62L$^+$TCF1$^+$ cells (Fig. 4.S1A and B), whereas for TIGIT, TOX, CTLA-4 and Lag3 no differences were observed (data not shown). The transcription factor FOXO1 was previously described to induce expression of CD62L and TCF1 in addition to other memory specific markers (Adams et al., 2016; Kim et al., 2013; van der Windt and Pearce, 2012). Using confocal microscopy, we investigated the cellular localization of FOXO1 and found that in naïve CD8 T cells and in early establishing CD62L$^+$TCF1$^+$ CD8 T cells upon activation, FOXO1 was mainly localized in the nucleus, enabling transcription of CD62L and TCF1, while in CD62L$^-$TCF1$^-$ cells, FOXO1 was mainly found in the cytoplasm (Fig. 4.1G). We next characterized the functional profiles of CD62L$^+$TCF1$^+$ and CD62L$^-$TCF1$^-$ cells established early after activation. Memory and effector CD8 T cells differ substantially in their metabolic profiles. While naïve and memory CD8 T cells primarily rely on oxidative phosphorylation, effector CD8 T cells rely mainly on glycolysis (Geltink et al., 2018; van der Windt and Pearce, 2012; Zhang and Romero, 2018). To investigate the metabolic profiles of the two subsets, we performed extracellular flux analysis. Interestingly, CD62L$^+$TCF1$^+$ cells demonstrated higher basal mitochondrial respiration and ATP production compared to CD62L$^-$TCF1$^-$ cells, while CD62L$^-$TCF1$^-$ cells had higher extracellular acidification rates (ECAR) over time and significantly higher glycolysis and glycolytic capacity (Fig. 4.1H). Re-stimulation with gp$_{33-41}$ of CD62L$^+$TCF1$^+$ cells resulted in pronounced IL-2 production, whereas CD62L$^-$TCF1$^-$ cells produced more IFNγ and TNFα compared to CD62L$^+$TCF1$^+$ cells (Fig. 4.1I). These results demonstrate that *in vitro* generated CD62L$^+$TCF1$^+$ cells possess characteristics of memory cells, whereas CD62L$^-$TCF1$^-$ cells are endowed with effector cell features.
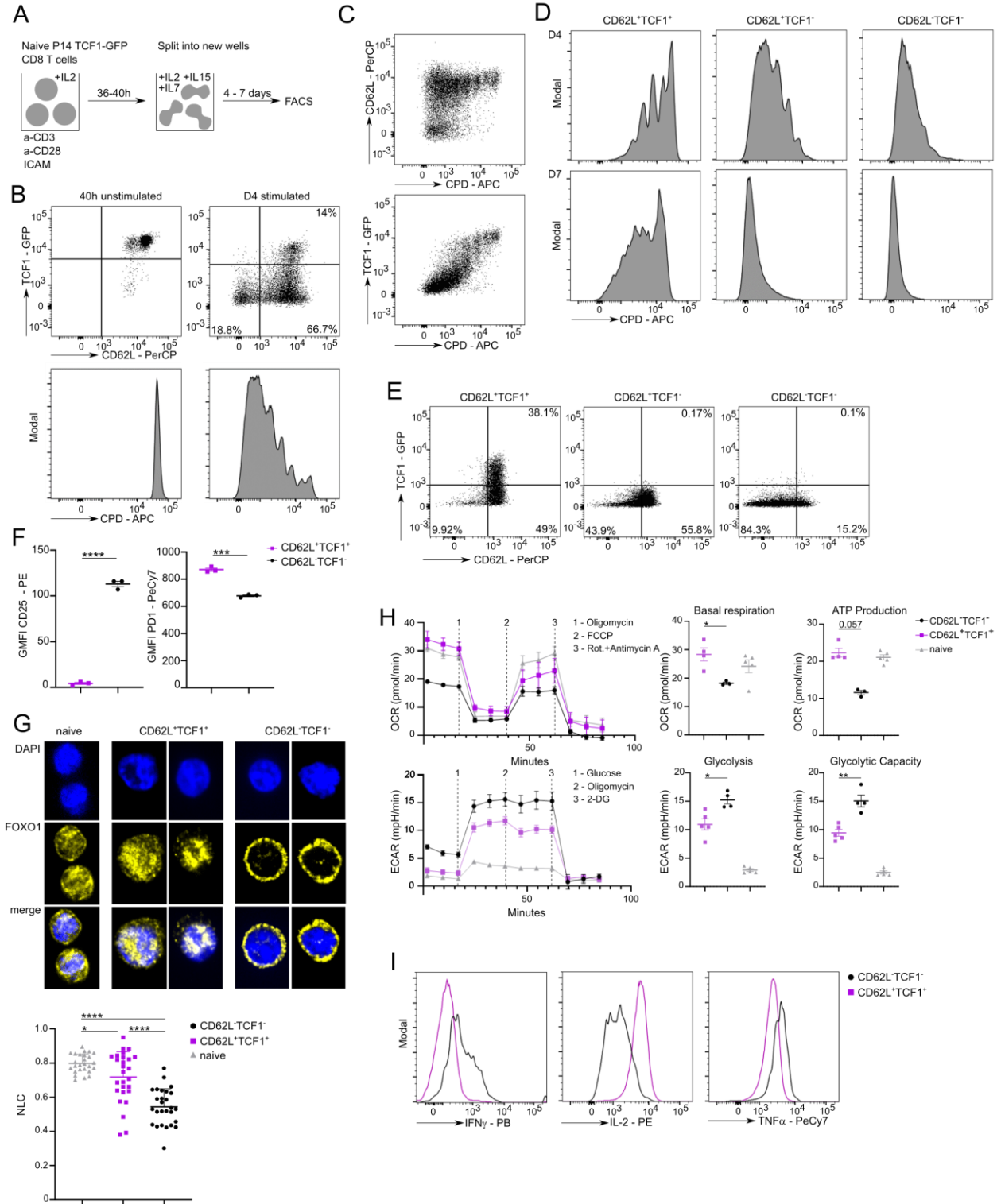
Figure 4.1: *In vitro* differentiation of P14 TCF1-GFP cells and characterization of CD62L$^+$TCF1$^+$ and CD62L$^-$TCF1$^-$ cells.

A Experimental setup. Naïve P14 TCF1-GFP cells were stimulated with plate-bound α-CD3 and α-CD28 antibodies and Fc-ICAM-1 in the presence of IL-2 for 36 – 40 h before cells were transferred to new wells in medium containing IL-2, IL-7 and IL-15. Cells were cultured for 4 – 7 days until FACS analysis. **B** Representative FACS plots of TCF1 and CD62L expression in P14 TCF1-GFP cells and respective cell proliferation dye (CPD) dilution with or without stimulation after 4 days. **C** Representative FACS plots of P14 TCF1-GFP cells expressing CD62L and TCF1 against CPD dilution on day 4 post stimulation. **D** Representative CPD dilution of CD62L$^+$TCF1$^+$, CD62L$^+$TCF1$^-$ and CD62L$^-$TCF1$^-$ cells on day 4 and 7 post stimulation. **E** Representative FACS plots of TCF1 and CD62L expression. P14 TCF1-GFP cells were stimulated for 4 days and sorted into CD62L$^+$TCF1$^+$, CD62L$^+$TCF1$^-$ and CD62L$^-$TCF1$^-$ cells. Subsets were individually re-cultured for 2 days before CD62L and TCF1 expression was re-assessed. **F** Geometric Mean of Fluorescence Intensity (GMFI) of CD62L$^+$TCF1$^+$ and CD62L$^-$TCF1$^-$ P14 TCF1-GFP cells expressing CD25 and PD1 on day 4 post stimulation. **G** Cellular localization of FOXO1. Representative confocal microscope images of fixed naïve (n=26), CD62L$^+$TCF1$^+$ (n=27) and CD62L$^-$TCF1$^-$ (n=27) cells. Distribution of nuclear localization coefficient (NLC) in all three cell subsets. **H** Oxygen consumption rate (OCR) (upper panel) and extracellular acidification rate (ECAR) (lower panel) of naïve, d5 sorted CD62L$^+$TCF1$^+$ and CD62L$^-$TCF1$^-$ cells was measured under basal conditions and in response to indicated drugs. **I** Representative histograms depicting production of IFNγ, IL-2 and TNFα by CD62L$^+$TCF1$^+$ and CD62L$^-$TCF1$^-$ cells. P14 cells were stimulated and sorted on day 4 into the two subsets followed by re-stimulation with gp$_{33-41}$ for 6 h at 37°C. (B to D) Representative data from one of four experiments. (H) Representative data from one of two experiments. (E) Representative data from one of two experiments. (F) Representative data from one of two experiments. (I) Representative data from one of three experiments. Statistical analysis was performed using the unpaired two-tailed Student's *t* test or, when data did not pass the Shapiro-Wilk normality test, the unpaired two-tailed Mann-Whitney test. *$P <$ 0.05; **$P <$ 0.01; ***$P <$ 0.001; ****$P <$ 0.0001.

Adoptively transferred CD62L⁺TCF1⁺ cells home better to lymphoid organs and give rise to memory cells upon LCMV challenge

As *in vitro* generated CD62L⁺TCF1⁺ cells were characterized by memory features and CD62L⁻TCF1⁻ cells by effector hallmarks, we next addressed the *in vivo* behavior of the two subsets upon adoptive transfer. To this end, P14 TCF1-GFP cells were activated as described in Figure 4.1A, sorted on day 4 post activation into CD62L⁺TCF1⁺ and CD62L⁻TCF1⁻ cells and adoptively transferred into naïve recipient B6 mice at equal numbers. First, we assessed homing to lymphoid and peripheral organs 8h post cell transfer (Fig. 4.2A). While significantly more CD62L⁺TCF1⁺ cells localized to the lymph nodes compared to CD62L⁻TCF1⁻ cells, no significant differences were observed in the abundance of the two subsets in the spleen and lung (Fig. 4.2B). Interestingly, when we investigated the phenotype of the transferred cells 8h post transfer, we found that both subsets had altered expression of CD62L and TCF1 in an organ-dependent manner, which was more pronounced in the CD62L⁺TCF1⁺ population. While cells from both subsets found in the lymph nodes were predominantly CD62L⁺TCF1⁻, the main phenotype of transferred cells in the lung was CD62L⁻TCF1⁻, potentially due to partial ongoing proliferation-dependent downregulation of both markers after transfer (Fig. 4.2B and Fig. 4.S2A). TCF1 and CD62L expression of transferred cells found in the spleen was heterogeneous but mainly resembled the phenotype of initially transferred CD62L⁺TCF1⁺ and CD62L⁻TCF1⁻ cells. Furthermore, we prepared fixed spleen slices and analyzed *in situ* localization of transferred P14 cell subsets by confocal microscopy. CD62L⁺TCF1⁺ cells entered the T cell zone at significantly higher numbers compared to CD62L⁻TCF1⁻ cells, which were positioned mostly outside of the T cell zones (Fig. 4.2C). We next wondered whether enhanced homing capacity of CD62L⁺TCF1⁺ cells to the lymph nodes resulted in improved long-term survival. To this end, we adoptively transferred the two subsets individually into recipient B6 mice at equal numbers and quantified their abundance and phenotype in lymph nodes and spleens 30 days later (Fig. 4.2D). Surprisingly, we found higher frequencies of CD62L⁻TCF1⁻ derived cells in the spleen of recipient mice, while no difference was observed in the lymph nodes nor in total numbers in spleen or lymph nodes (Fig. 4.2E). Interestingly, adoptively transferred CD62L⁻TCF1⁻ cells were able to reacquire expression of CD62L and TCF1 over the period of 30 days in naïve

38

hosts, as the major phenotype of the offspring stemming from both subsets was CD62L$^+$TCF1$^+$ (Fig. 4.2E). These data indicate that CD62L$^+$TCF1$^+$ cells have an advantage in homing to the lymph nodes, specifically to the T cell zones, early after adoptive transfer. However, in particular, cells from the CD62L$^-$TCF1$^-$ subset could re-express CD62L and TCF1, potentially mediated by the microenvironment they are facing when residing in tissues and thereby establishing a phenotype that enables long-term survival. We next determined the re-expansion and differentiation into secondary effector and memory cells of the two subsets after adoptive transfer followed by acute LCMV WE challenge one day later (Fig. 4.2F). 31 days post infection, the offspring of CD62L$^+$TCF1$^+$ cells were found at significantly higher numbers in lymph nodes and spleens of recipient mice. Furthermore, CD62L$^+$TCF1$^+$ cells gave rise to significantly higher numbers of memory cells (IL7R$^+$KLRG1$^-$) in lymph nodes and spleens (Fig. 4.2G). This trend was also observed in the lungs. As already reported in the survival experiments, but also in response to viral challenge, we observed altered expression of CD62L and TCF1 31 days post infection when compared to the phenotype on the day of initial transfer (Fig. 4.2H). While the predominant phenotype of progeny cells coming from both subsets in the lung and spleen of recipient mice was CD62L$^-$TCF1$^-$, the phenotype of cells in the lymph nodes was more heterogeneous with mainly CD62L$^+$TCF1$^+$ and CD62L$^-$TCF1$^+$ cells coming from the CD62L$^+$TCF1$^+$ group, while the less abundant progeny of the CD62L$^-$TCF1$^-$ group mainly comprised cells with a CD62L$^-$TCF1$^+$ and CD62L$^-$TCF1$^-$ phenotype (Fig. 4.2H). Altogether, these findings indicate that *in vitro* generated CD62L$^+$TCF1$^+$ cells, as early as on day 4 post activation, can be characterized as memory precursor cells, whereas CD62L$^-$TCF1$^-$ cells at the same time can be classified as effector precursor cells, although a considerable level of plasticity was noticed upon *in vivo* transfer of these subsets.
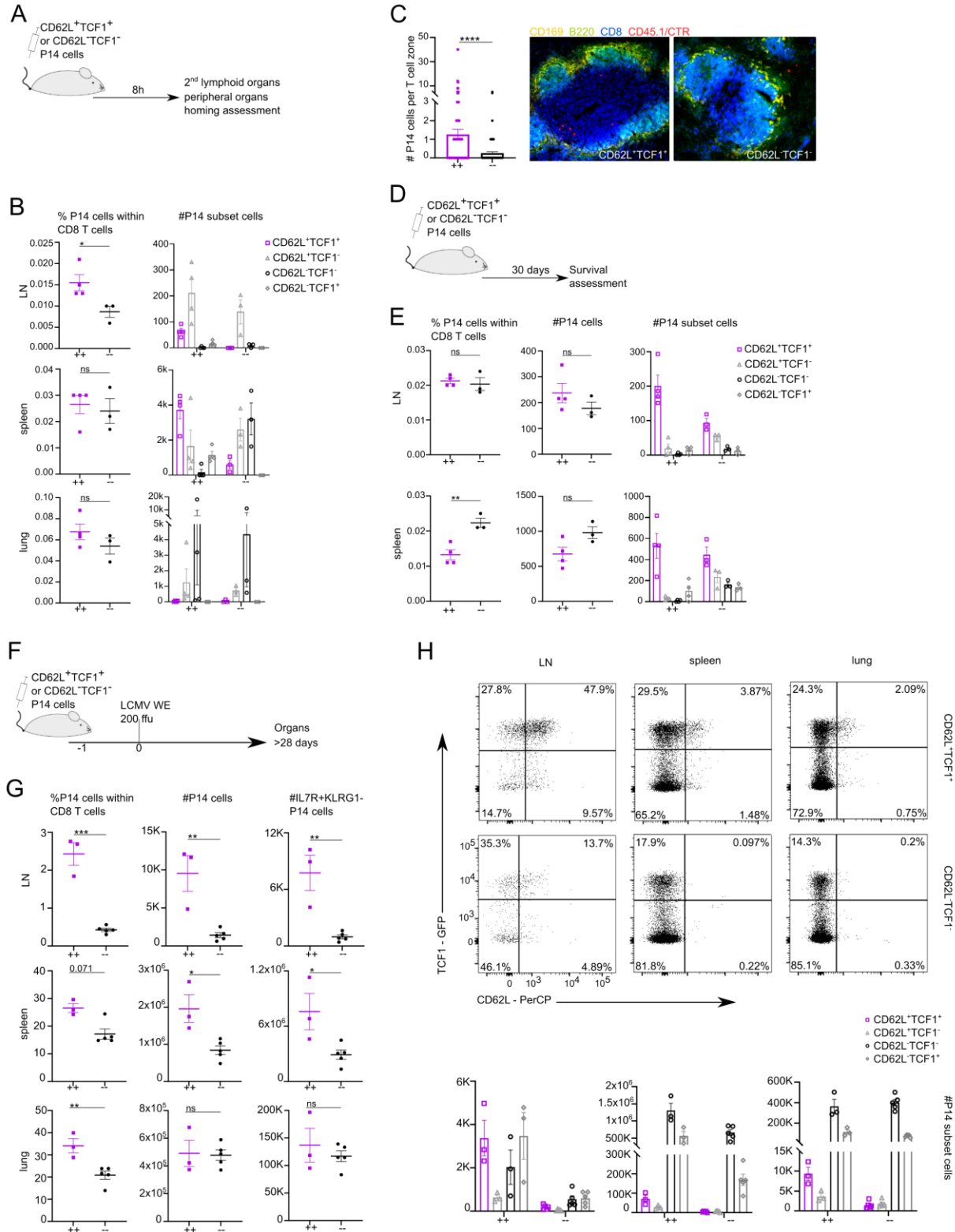
Figure 4.2: Adoptively transferred CD62L$^+$TCF1$^+$ cells home better to lymphoid organs and give rise to memory cells upon LCMV challenge.

P14 TCF1-GFP cells were activated as described in Figure 4.1A and sorted on day 4 post activation into CD62L$^+$TCF1$^+$ and CD62L$^-$TCF1$^-$ cells. Sorted subsets were individually transferred at equal numbers into B6 recipient mice. **A** Experimental setup. Spleens, lymph nodes and lungs were harvested 8h post transfer and homing of transferred cells was investigated. **B** Frequencies and absolute numbers of P14 subset cells within spleen, lymph nodes and lung of recipient mice. **C** Left: Absolute numbers of splenic P14 cells localized in T cell zones. Right: Representative confocal microscopy images of 10-µm fixed splenic sections. Tissues were stained for the localization of metallophilic macrophages (CD169), B cells (B220), and CD8 T cells (CD8). P14 cells could be identified by CD45.1 and preserved CTR staining. **D** Experimental setup. Spleens and lymph nodes of recipient mice were harvested on day 30 post transfer. **E** Frequencies and absolute numbers of P14 cells and CD62L$^+$TCF1$^+$, CD62L$^+$TCF1$^-$, CD62L$^-$TCF1$^-$ and CD62L$^-$TCF1$^+$ cells in spleens and lymph nodes of recipient mice. **F** Experimental setup. Mice were infected with acute LCMV WE (200 ffu/mouse intravenously) one day after adoptive transfer. Spleens, lymph nodes and lungs were harvested 31 days post infection. **G** Frequencies and absolute numbers of P14 cells within spleens, lymph nodes and lungs of recipient mice. Absolute numbers of IL7R$^+$KLRG1$^-$ cells. **H** Representative FACS plots of TCF1-GFP and CD62L expressing P14 cells in lymph nodes, spleens and lungs of recipient mice. Absolute numbers of CD62L$^+$TCF1$^+$, CD62L$^+$TCF1$^-$, CD62L$^-$TCF1$^-$ and CD62L$^-$TCF1$^+$ cells. (A - C) Representative data from one of three experiments. (D - H) Representative data from one of two experiments. Statistical analysis was performed using the unpaired two-tailed Student's *t* test or, when data did not pass the Shapiro-Wilk normality test, the unpaired two-tailed Mann-Whitney test. *$P < 0.05$; **$P < 0.01$; ***$P < 0.001$; ****$P < 0.0001$.

ACD does not promote diversity upon stimulation with TCR agonistic antibodies

The identification of the two early fate indicating CD62L$^+$TCF1$^+$ and CD62L$^-$TCF1$^-$ cell subsets allowed us to investigate whether ACD might be a key determinant in effector and memory precursor cell generation originating from one naïve mother cell. To this end, we activated naïve P14 TCF1-GFP cells with plate-bound α-CD3, α-CD28, Fc-ICAM-1 and IL-2 for 32 − 34 h before the first cell division occurred (Fig. 4.3A and B). Such activation was sufficient to induce full activation of the cells, indicated by high CD44 expression (Fig. 4.3B). The subset of unstimulated CD44$^-$ P14 cells (~30%) present in the activation condition was neglected and excluded from downstream analyses, as CD44$^-$ cells did not proliferate until day 4 post activation (Fig. 4.S3A). After 32 − 34 h, we harvested the P14 cells and transferred them onto imaging slides in medium containing IL-2, IL-15 and IL-7, and started time-lapse imaging for 3 days (Fig. 4.3A) (Loeffler et al., 2022, 2019). To facilitate precise tracking (Hilsenbeck et al., 2016), we established a coating with α-CD44 and α-CD43 antibodies, which was applied to the imaging slides prior to adding the cells. This coating led to adherence of the cells (Loeffler et al., 2018) and therefore allowed precise tracing of individual single cells without inducing further activation signals assessed by unaltered phospho-Akt (pAkt) staining, or inducing changes of the proliferation profile or alterations of expression of TCF1 and CD62L (Fig. 4.3C). We analyzed asymmetry between the daughter cells of first mitoses by differential expression of the surface marker CD8, which has been described as a reliable readout for asymmetric CD8 T cell division in previous studies (Borsa et al., 2021, 2019; Chang et al., 2007). Cell divisions were defined as asymmetric when the CD8 signal was 1.5-fold greater in one daughter cell compared to the other, corresponding to an asymmetry rate of 0.2. P14 cells divided asymmetrically as well as symmetrically in their first cell division (Fig. 4.3D). The frequencies of asymmetrically dividing cells were similar to those observed when ACD was measured in mitotic cells from fixed samples by confocal microscopy (Borsa et al., 2019). Of note, CD8 asymmetry was reduced within the following 40 - 80 min of culture, potentially due to re-expression of CD8 on the distal daughter cell (Fig. 4.S3B). Throughout the time-lapse movie, we observed the occurrence of "big" (> 6 cell divisions) and "small" (2 - 5 cell divisions) colonies (Movie 4.1 and 4.2). Small colonies contained cells of comparably small individual cell size, while the cells within big colonies showed

a larger cellular size (Fig. 4.S3C). Furthermore, while cells giving rise to big colonies divided throughout the entire imaging period every $6-8$ h, cells within small colonies stopped dividing after 3 - 4 cell divisions and entered a quiescent state (Fig. 4.S3D). Continuous cell division of cells within big colonies prevented precise tracking after the 4th - 5th cell division as the cells were positioned around and on top of each other. We then investigated the phenotype of the evolving colonies and found that in line with the described proliferation profile (Fig. 4.1D), small colonies exclusively contained $CD62L^+TCF1^+$ cells, whereas big colonies were strictly composed of $CD62L^-$ $TCF1^-$ cells (Fig. 4.3E). In accordance with the described "intermediate" population (Fig. 4.1D and E), we also observed colonies consisting of $CD62L^+TCF1^-$ cells. Interestingly, we did not observe any mixed-fate colonies, i.e. family trees that would comprise both cells with a $CD62L^+TCF1^+$ and $CD62L^-$ $TCF1^-$ phenotype, which would be compatible with an ACD-induced bifurcation of fates. Instead, the evolving colonies stemming from one mother cell were strictly homogeneous in expression of CD62L and TCF1. We then correlated the CD8 (a)symmetry of the first cell division of each individual cell with fate outcome of their emerging progeny and found that differentiation into either an effector precursor or memory precursor population was independent of the degree of asymmetry of the first cell division (Fig. 4.3F). The frequency of first symmetric and asymmetric cell divisions was similar between the ensuing $CD62L^-TCF1^-$, $CD62L^+TCF1^-$ and $CD62L^+TCF1^+$ colonies, indicating no direct impact of ACD on fate determination under the applied stimulation conditions.
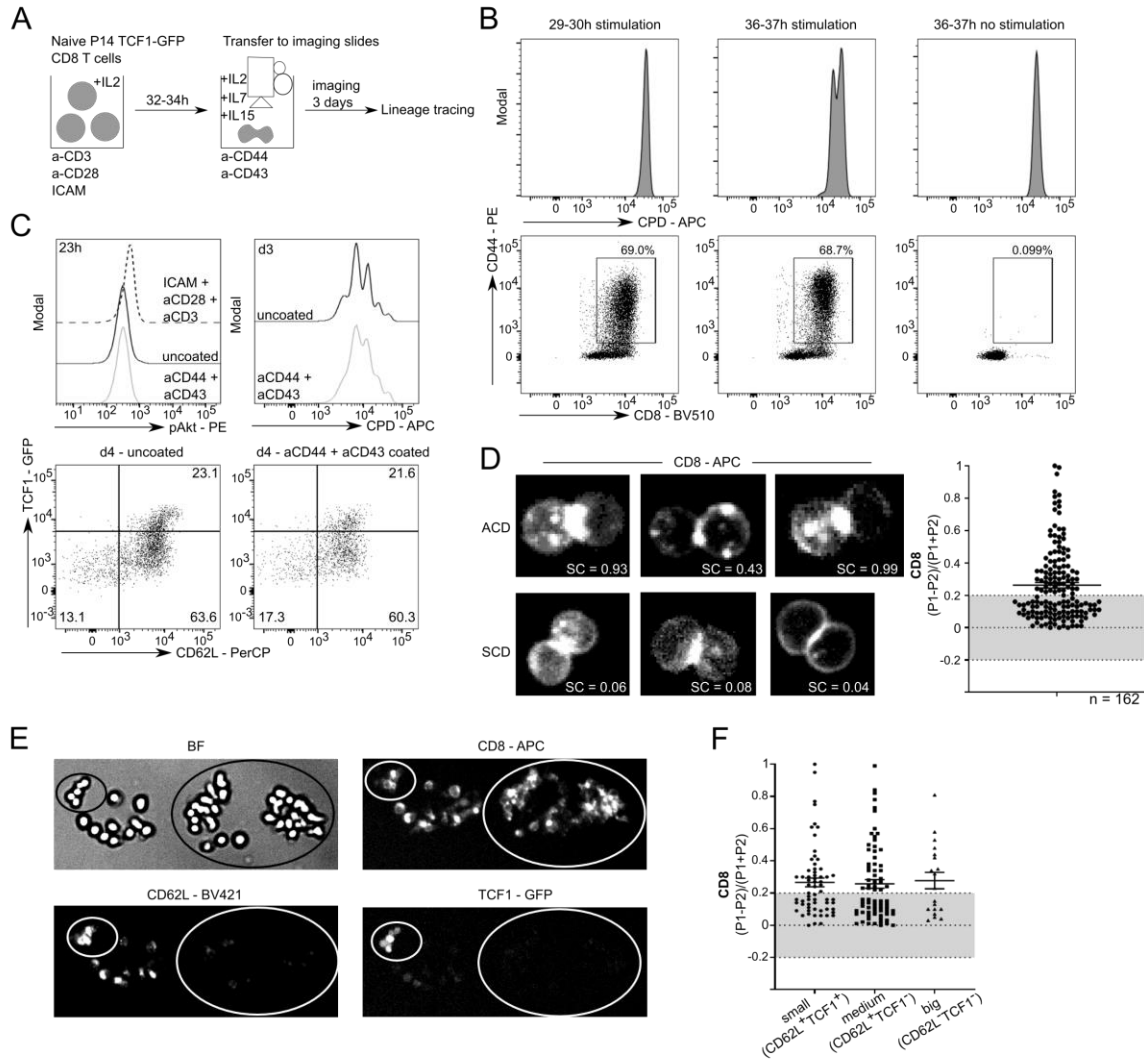
43

Figure 4.3: ACD does not promote diversity upon stimulation with TCR agonistic antibodies.

A Experimental setup. P14 TCF1-GFP cells were activated as described in Figure 4.1A for 32 − 34 h. Cells were harvested and transferred onto imaging slides pre-coated with α-CD44 and α-CD43 antibodies in imaging medium containing IL-2, IL-7 and IL-15. Time-lapse imaging was performed for 3 days with 10× magnification. BF and far red channels were acquired every 40 min, blue and green channels were acquired every 90 min. **B** Representative plots of CPD dilution and CD44 expression of unstimulated and activated P14 TCF1-GFP cells after 29 − 30 h and 36 − 37 h. **C** P14 TCF1-GFP cells were activated as described in Figure 4.1A for 34 h and further cultured on uncoated or α-CD44 and α-CD43 antibody coated surfaces. Representative plots of pAkt (23 h post seeding), CPD dilution (day 3 post seeding) and TCF1 and CD62L expression (day 4 post seeding). As a positive control for pAkt staining, naïve P14 TCF1-GFP cells were stimulated on Fc-ICAM-1, α-CD3 and α-CD28 in the presence of IL-2. **D** Representative time-lapse images of asymmetric (ACD) and symmetric cell divisions (SCD) and quantified ACD rates based on CD8-APC surface

expression. CD8 staining was quantified in both daughter cells and P1 was arbitrarily defined as the pole with higher amounts of CD8. Cell division was classified as asymmetric when the amount of CD8 was 50% higher in one daughter cell compared to the other one, defining the threshold of 0.2 (dashed line). Data are represented as mean ± SEM. **E** Representative time-lapse images of colonies on day 3 depicted in BF, CD8-APC (far red channel), CD62L-BV421 (blue channel) and TCF1-GFP (green channel). Circles are drawn around colonies stemming from one cell. **F** ACD rates from P14 TCF1-GFP cells that later formed small-sized (CD62L$^+$TCF1$^+$), medium-sized (CD62L$^+$TCF1$^-$) and big-sized (CD62L$^-$TCF1$^-$) colonies. Data are represented as mean ± SEM. (D to G) Data pooled from two independent experiments.

The strength of TCR stimulation impacts ACD and fate

As ACD did not lead to different fates within the emerging progeny of single cells under the above applied stimulation conditions (i.e. α-CD3, α-CD28 and Fc-ICAM-1), we wondered whether varying the strength of initial TCR stimulation might have an impact on ACD promoting bifurcation of fates. TCR stimulation strength can be modulated by both TCR-pMHC affinity and pMHC density on antigen-presenting cells, leading to differences in the kinetics and magnitude of the CD8 T cell response (Conley et al., 2016; Denton et al., 2011; King et al., 2012; Ozga et al., 2016; Shakiba et al., 2022; Skokos et al., 2007; Zikherman and Au-Yeung, 2015). We decided to use two distinct peptide modalities of the LCMV glycoprotein, the variant C6 (KAVYNCATC), providing low peptide affinity for the P14 TCR, and the wild-type high affinity variant gp33 (KAVYNFATC) (Utzschneider et al., 2016). Moreover, we used the high affinity peptide variant gp33 at two concentrations (10^{-6} M and 10^{-11} M) to additionally probe for an effect of antigen abundance. The C6 variant was used at 10^{-6} M. To provide optimal CD8 T cell activation, we stimulated adherent dendritic cells (DCs) from the MutuDC1940 cell line (Fuertes Marraco et al., 2012) with CpG to induce expression of costimulatory molecules CD80, CD86 and CD40 (Fig. 4.S4A), thus facilitating the establishment of an IS, and loaded the peptides onto their MHC molecules. Then, we added naïve P14 TCF1-GFP T cells for 28 – 30 h before we transferred them into new wells containing medium with IL-2, IL-7 and IL-15 for further culture (Fig. 4.4A). Compared to P14 CD8 T cells activated by plate-bound antibodies, pMHC/DC-activated P14 cells already performed their first cell division 28 – 30 h post activation (Fig. 4.4B). This was true for both peptide variants. We then investigated proliferation and phenotype of the P14 cells on day 4 or 6 post stimulation. Interestingly, while P14 cells activated by gp33 at 10^{-6} M proliferated the most, gp33 at 10^{-11} M and C6 stimulated P14 cells proliferated slower but in a comparable manner (Fig. 4.4C). Furthermore, gp33 at 10^{-11} M and C6 activation induced comparable frequencies of CD62L$^+$TCF1$^+$ and CD62L$^-$TCF1$^-$ cells whereas gp33 at 10^{-6} M induced significantly fewer CD62L$^+$TCF1$^+$ cells but more CD62L$^-$TCF1$^-$ cells (Fig. 4.4D and E). Overall, expression levels of activation markers such as CD25, PD-1 and ICOS were higher after gp33 10^{-6} M stimulation compared to gp33 10^{-11} M and C6 stimulation (Fig. 4.S4B) and CD62L$^-$TCF1$^-$ cells expressed higher levels compared to CD62L$^+$TCF1$^+$ cells. Only after weak TCR stimulation, PD1

expression was found to be slightly higher on $CD62L^+TCF1^+$ cells compared to $CD62L^-TCF1^-$ cells. Comparing the phenotype and proliferation data of P14 cells between plate-bound antibody stimulation (Fig. 4.1) and pMHC/DC-activation, indicates that the outcome of plate-bound antibody stimulation resembles the two low TCR stimulation strength conditions, i.e., gp33 at 10^{-11} M and the C6 variant. We then assessed the emerging subpopulations regarding TCF1 and CD62L expression in more detail. Proliferation analyses indicated that $CD62L^-TCF1^-$ cells proliferated the most, whereas $CD62L^+TCF1^-$ cells cycled slightly slower and $CD62L^+TCF1^+$ cells showed the lowest number of cell divisions (Fig. 4.4F). To determine the behavior of $CD62L^+TCF1^+$ and $CD62L^-TCF1^-$ cells after *in vivo* stimulation, we sorted P14 TCF1-GFP cells 6 days after initial activation, provided either by the high or the low affinity peptide, into the two subsets, and adoptively transferred them into recipient mice followed by acute LCMV WE infection. Consistent with our previous findings, the frequencies and absolute numbers of P14 cells deriving from $CD62L^+TCF1^+$ cells were significantly higher in spleens and lymph nodes of recipient mice on day 35 post infection compared to $CD62L^-TCF1^-$ derived P14 cells (Fig. 4.S4C). The absolute number of P14 $IL7R^+KLRG1^-$ memory cells deriving from $CD62L^+TCF1^+$ cells was also significantly higher compared to $CD62L^-TCF1^-$ derived P14 cells in spleens and lymph nodes (Fig. 4.S4C). These findings were observed for both peptide stimulations. TCF1 and CD62L expression of P14 cells in spleens and lymph nodes was comparable to P14 cells stimulated with TCR agonistic antibodies (Fig. 4.S4C and Fig. 4.2F). To compare memory potential upon strong versus weak TCR stimulation on a bulk population level, we adoptively transferred P14 TCF1-GFP cells into recipient mice on day 6 after activation by pMHC/DC. Mice were challenged immediately with LCMV WE one day later. At day 35 post infection, frequencies and numbers of P14 cells derived from C6 and gp33 10^{-11} M were significantly higher in lymph nodes of recipient mice compared to gp33 10^{-6} M derived P14 cells, presumably due to the diminished abundance of $CD62L^+TCF1^+$ cells within the transferred bulk population (Fig. 4.4G). Accordingly, absolute numbers of $IL7R^+KLRG1^-$ P14 memory cells were significantly higher in recipient mice that received C6 or gp33 10^{-11} M stimulated cells (Fig. 4.4G). P14 cells derived from both weak TCR stimulation conditions were mainly either $CD62L^+TCF1^+$ or $CD62L^-TCF1^+$, whereas P14 cells derived from the strong TCR stimulation condition had similar numbers of $CD62L^+TCF1^+$, $CD62L^-TCF1^+$ and $CD62L^-TCF1^-$ cells (Fig. 4.4G).

We next addressed the frequency of ACDs after activation by pMHC/DC with different affinities and concentrations. In line with previous reports (King et al., 2012), we found that activation with high concentrations of the high affinity gp33 (10^{-6} M) peptide induced increased frequencies of ACD compared to activation with the C6 variant or gp33 at 10^{-11} M (Fig. 4.4H and I). To exclude a P14-specific effect, we additionally analyzed first mitosis ACD rates and differentiation after stimulation of OT-I TCF1-GFP cells with their respective high affinity (SIINFEKL "N4") and low affinity (SIILFEKL "L4") peptide variants (Turner et al., 2008). Also here, stimulation with N4-loaded DCs led to higher frequencies of ACDs compared to stimulation with L4-loaded DCs (Fig. 4.S4D). Additionally, the frequency of CD62L$^+$TCF1$^+$ cells was lower after N4-stimulation compared to L4-stimulation (Fig. 4.S4E and 4.S4F). Taken together, strong TCR stimulation resulted in increased ACD rates with a preferential path of differentiation into an effector fate. Weak TCR stimulation, in contrast, either provided by low affinity peptides or low antigen concentration, resulted in lower ACD rates and in uniform differentiation into memory or effector precursor cells.
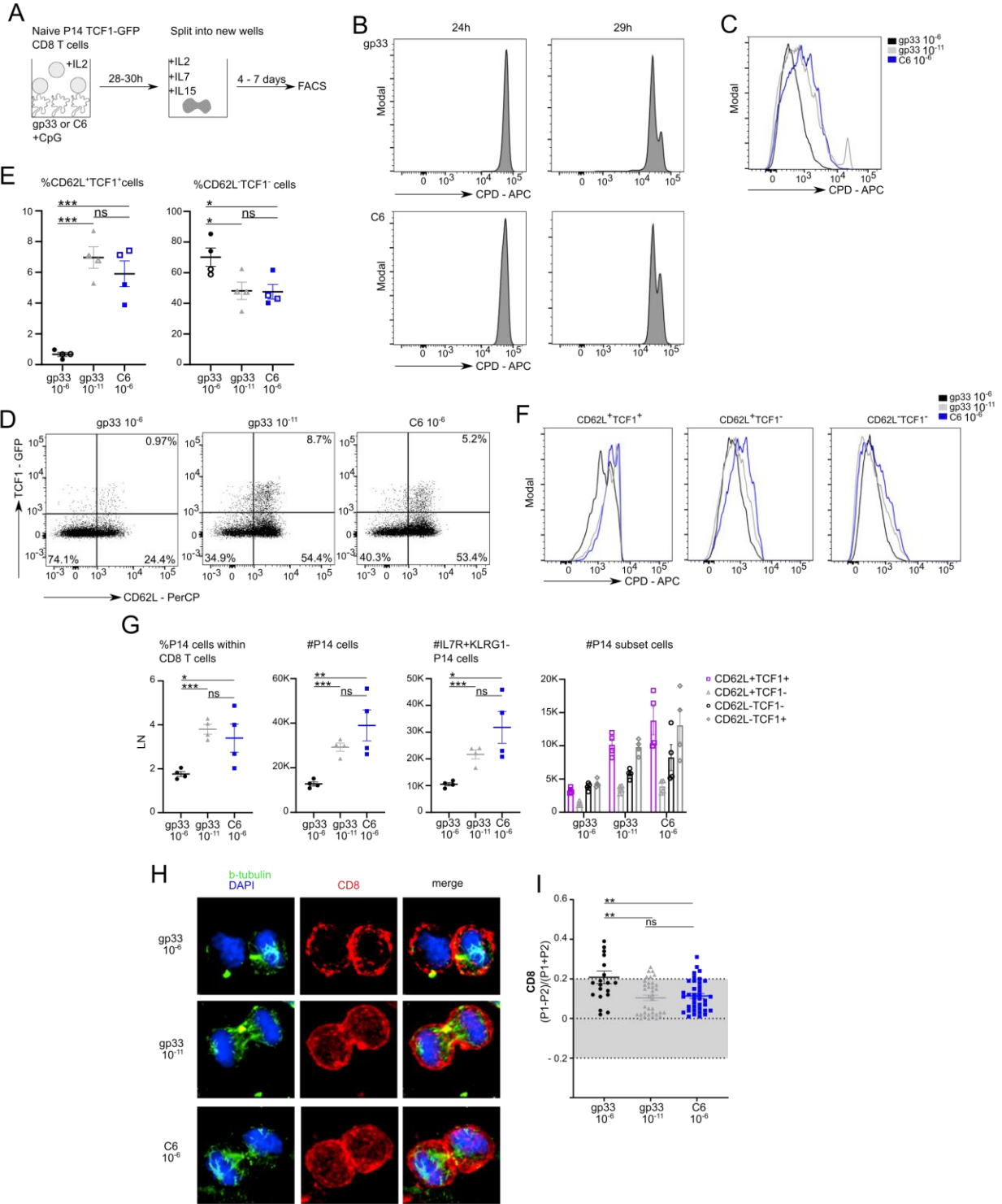
Figure 4.4: The strength of TCR stimulation impacts ACD and fate.

A Experimental setup. MutuDC1940 cells were stimulated with CpG and pulsed with either gp33 (high affinity) or C6 (low affinity) peptides before P14 TCF1-GFP cells were added. P14 cells were activated in the presence of IL-2 for 28 − 30 h before cells were either analyzed for ACD or transferred to new wells in medium containing IL-2, IL-7 and IL-15. Cells were cultured for 4 - 7 days. **B** Representative histograms of CPD dilution of gp33 or C6 activated P14 TCF1-GFP cells after 24 and 29 h. **C** Representative histograms of CPD dilution of gp33 at 10^{-6} M, gp33 at 10^{-11} M or C6 at 10^{-6} M activated P14 TCF1-GFP cells on day 6. **D** Representative FACS plots of TCF1 and CD62L expression. P14 TCF1-GFP cells were analyzed on day 6 after activation. **E** Frequencies of CD62L$^+$TCF1$^+$ and CD62L$^-$TCF1$^-$ cells on day 4 (empty symbol) or day 6 (filled symbol) after stimulation. **F** Histograms of CPD dilution of CD62L$^+$TCF1$^+$, CD62L$^+$TCF1$^-$ and CD62L$^-$TCF1$^-$ cells on day 6 post activation. **G** P14 TCF1-GFP cells were activated with gp33 at 10^{-6} M, 10^{-11} M or C6 at 10^{-6} M and sorted on day 6 post activation. Sorted cells were individually transferred at equal numbers into recipient mice followed by acute LCMV WE infection (200 ffu/mouse intravenously) one day later. Lymph nodes were harvested 35 days post infection. Frequencies and absolute numbers of P14 cells within lymph nodes of recipient mice. Absolute numbers of IL7R$^+$KLRG1$^-$, CD62L$^+$TCF1$^+$, CD62L$^+$TCF1$^-$, CD62L$^-$TCF1$^-$ and CD62L$^-$TCF1$^+$ cells. **H** Confocal images from fixed samples of naïve P14 cells 27 − 30 h after *in vitro* stimulation with gp33 or C6 loaded MutuDCs at 10^{-6} M or 10^{-11} M. Mitotic cells were identified based on β-tubulin and nuclear structures and imaged from late anaphase to cytokinesis. **I** ACD rates from P14 cells activated with gp33 at 10^{-6} M (n=20), gp33 at 10^{-11} M (n=36) or C6 at 10^{-6} M (n=38). Data are represented as mean ± SEM. (B) Representative data from one of two experiments. (C, D and F) Representative data from one of three experiments. (E) Data pooled from three independent experiments. (G) Representative data from one of two experiments. Statistical analysis was performed using the unpaired two-tailed Student's *t* test or, when data did not pass the Shapiro-Wilk normality test, the unpaired two-tailed Mann-Whitney test. *$P < 0.05$; **$P < 0.01$; ***$P < 0.001$.

In vitro generated CD62L⁺TCF1⁺ and CD62L⁻TCF1⁻ cells are transcriptionally similar to in vivo generated memory and effector cells

Following the observation that strong TCR stimulation leads to enhanced ACD rates and preferential generation of CD62L⁻TCF1⁻ effector precursor cells at the expense of CD62L⁺TCF1⁺ memory precursor cells, which results in curtailed memory formation, we next aimed to dissect the role of ACD on fate diversification specifically upon strong TCR stimulation. To complement the *in vitro* and *in vivo* characterization of CD62L⁺TCF1⁺ and CD62L⁻TCF1⁻ cells derived from different strengths of TCR stimulation on a transcriptional level, we analyzed the transcriptional profiles of *in vitro* generated CD62L⁺TCF1⁺ and CD62L⁻TCF1⁻ cells derived from either antibody-induced (AB) activation or from gp33/C6 peptide stimulation and compared them to *in vivo* generated effector and memory cells, respectively. Thus, we sorted CD62L⁺TCF1⁺ and CD62L⁻TCF1⁻ cells on day 6 post activation, followed by RNA extraction and bulk RNA sequencing. Using multidimensional scaling, we found that biological replicates from each condition clustered closely together and that CD62L⁺TCF1⁺ and CD62L⁻TCF1⁻ samples occupied distinct areas, indicating differential transcriptional profiles. Interestingly, independent of their initial activation stimulus, samples within each subset showed overall transcriptional similarity (Fig. 4.5A and 4.S5A). Next, we analyzed gene expression of known memory- and effector-specific genes. As expected, *Sell* (encoding CD62L) and *Tcf7* (encoding TCF1) were expressed at higher levels in CD62L⁺TCF1⁺ cells (Fig. 4.5B and 4.S5B). Effector genes, such as *Gzma*, *Gzmb* and *Tnf* were found to be enriched in CD62L⁻TCF1⁻ cells in all activation conditions (Fig. 4.5B and 4.S5B). Interestingly, while expression patterns of *Tbx21* and *Ezh2* were similar between AB and C6 activation conditions with higher expression in CD62L⁻TCF1⁻ cells, gp33 activation showed an altered expression pattern with higher or similar expression in CD62L⁺TCF1⁺ cells. Furthermore, genes related to terminal differentiation and inhibitory regulation (e.g., *Pdcd1*, *Ctla4* and *Prdm1*) were predominantly expressed in cells derived from strong gp33 activation, with CD62L⁻TCF1⁻ cells displaying higher expression (Fig. 4.5B and 4.S5B). Differential gene expression (DEG) analysis between CD62L⁺TCF1⁺ and CD62L⁻TCF1⁻ cells further confirmed transcriptional differences between CD62L⁺TCF1⁺ and CD62L⁻TCF1⁻ cells (Fig. 4.5C). To investigate whether the DEG relate to *in vivo* generated effector and memory cell

transcriptional profiles, we performed gene set enrichment analysis (GSEA) using gene sets from effector CD8 T cells 8 days post infection (dpi) with acute LCMV Armstrong and >40 dpi memory cells, respectively (Kaech et al., 2002). We found a significant overlap of DEG of CD62L$^+$TCF1$^+$ cells (positive fold change (FC)) with downregulated DEG of 8 dpi effector cells versus >40 dpi memory cells in all activation conditions (Fig. 4.5D). Accordingly, we observed a significant enrichment of DEG of CD62L$^-$TCF1$^-$ cells (negative FC) in upregulated DEG of 8 dpi effector cells versus >40 dpi memory cells in all activation conditions (Fig. 4.5D). To confirm our findings, we performed another GSEA with gene sets from IL7R^{lo} short-lived effector cells (SLECs) and IL7R^{hi} memory precursor effector cells (MPECs) 6/7 days post LCMV infection, respectively. Similarly, we found a significant overlap of DEG of CD62L$^+$TCF1$^+$ cells (positive (FC)) with downregulated DEG of IL7R^{lo} SLECS versus IL7R^{hi} MPECS in all activation conditions (Fig. 4.S5C). In accordance, we observed a significant enrichment of DEG of CD62L$^-$TCF1$^-$ cells (negative FC) in upregulated DEG of IL7R^{lo} SLECS versus IL7R^{hi} MPECS in all activation conditions (Fig. 4.S5C) (Joshi et al., 2007). Thus, these findings confirm that CD62L$^+$TCF1$^+$ cells transcriptionally resemble *in vivo* generated memory cells, whereas CD62L$^-$TCF1$^-$ cells are similar to *in vivo* generated effector cells and this is independent of the strength of the initial TCR stimulation. Of note, overall gene expression patterns appeared to be more similar between CD62L$^+$TCF1$^+$ and CD62L$^-$TCF1$^-$ cells derived from AB and C6 stimulation compared to the more distinct transcriptional profile of both subsets derived from gp33 activation, once more supporting the notion that AB stimulation can be classified as rather weak compared to high affinity peptide stimulation. Further, as gp33 stimulated cells show a more "effector-oriented" transcriptional profile compared to AB or C6 stimulated cells, it might be possible that a safeguard process might be beneficial, which prevents some cells from adopting a "full effector program". This seems much less in demand for a low affinity stimulation.
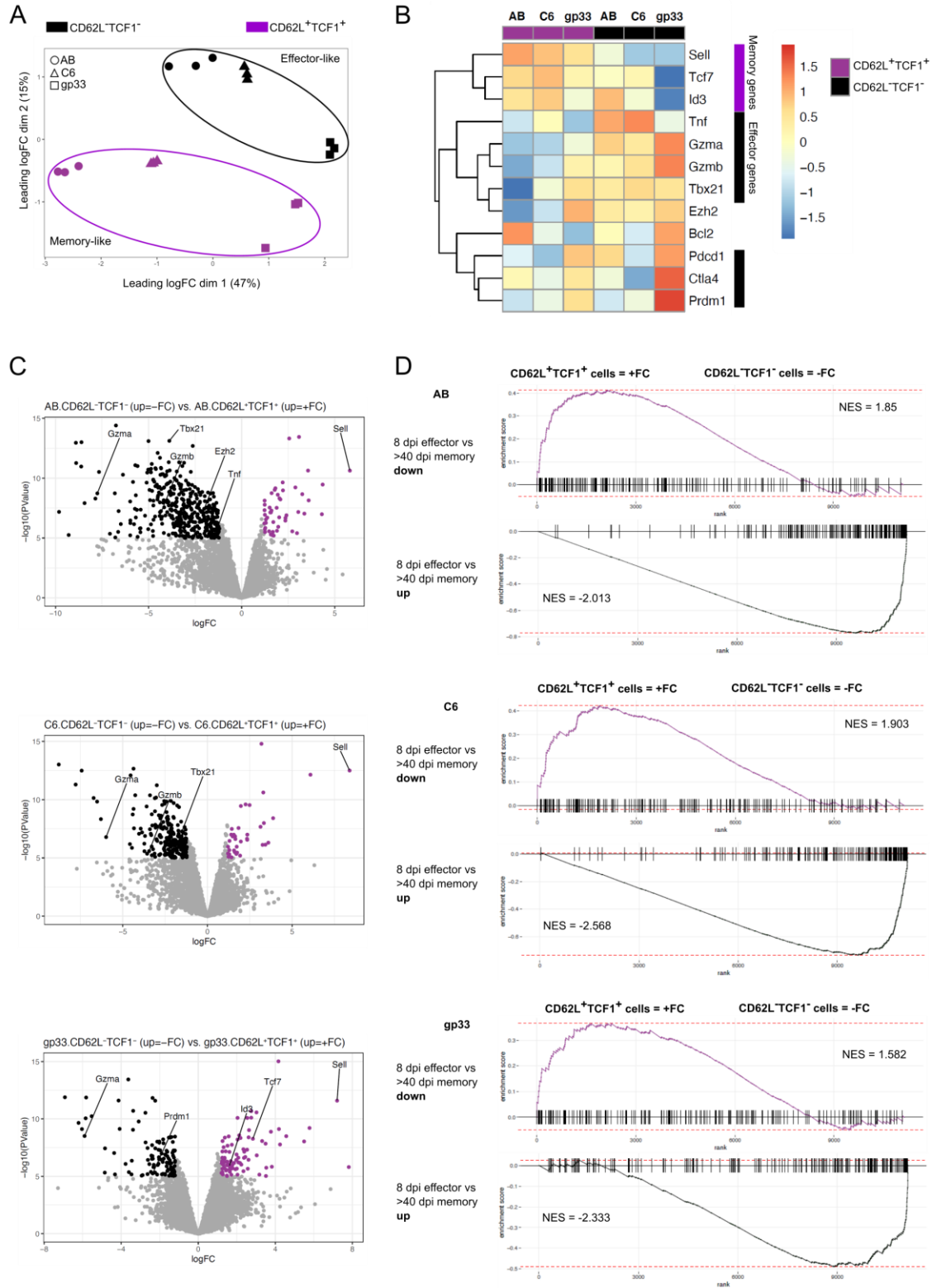
Figure 4.5: Transcriptional profiling of *in vitro* generated memory and effector precursor cells upon weak and strong TCR stimulation.

P14 TCF1-GFP cells were activated by plate-bound Fc-ICAM-1, α-CD3 and α-CD28 (AB) or by MutuDC1940 cells, which were stimulated with CpG and either pulsed with gp33 or C6 peptides. P14 cells were activated in the presence of IL-2 for 30 h before cells were transferred to new wells in medium containing IL-2, IL-7 and IL-15. Cells were cultured for 6 days and CD62L$^+$TCF1$^+$ and CD62L$^-$TCF1$^-$ cells were sorted for RNAseq. 3 biological replicates were used for each condition. **A** Multidimensional scaling (MDS) plot depicting sample variation between CD62L$^+$TCF1$^+$ and CD62L$^-$TCF1$^-$ cells derived from different stimulation conditions. **B** Heatmap of gene expression of selected memory- and effector-specific genes among CD62L$^+$TCF1$^+$ and CD62L$^-$TCF1$^-$ cells derived from AB, C6 or gp33 activation. Averages of pooled biological replicates are shown. **C** Volcano plots displaying differentially expressed genes between CD62L$^+$TCF1$^+$ and CD62L$^-$TCF1$^-$ cells per activation condition. Points colored in purple or black are differentially expressed (p-value < 10^{-6} and average log fold change (FC) > 1.2). **D** Gene set enrichment analysis (GSEA) plots and normalized enrichment score (NES) of differential gene expression displayed in C using gene sets describing 8 days post acute infection (dpi) with LCMV Armstrong effector cells and >40 dpi memory cells, respectively (Kaech et al., 2002).

ACD enables the establishment of single cell-derived mixed-fate colonies upon strong TCR stimulation

To investigate the role of ACD in fate divergence specifically upon strong TCR stimulation at high resolution, we next addressed on a single-cell level whether ACD gives rise to differential cell fates within a single cell-derived colony in this setting. To this end, we activated P14 TCF1-GFP cells by gp33- or C6-loaded DCs for 24 h before we sorted single, undivided but blasted cells into wells of a 384 well plate (sorting strategy shown in Fig. 4.S6A). We then performed a high-throughput microscopy approach using time-lapse imaging with an interval of 60 minutes (min) for the following 24 h to record the first cell division (Movie 4.3). Cells were then incubated for another 3 days before formed colonies were imaged and analyzed for fate acquisition (Fig. 4.6A). Quantifying the CD8 surface expression within the first 24 h of imaging demonstrated that cells divided both asymmetrically and symmetrically (Fig. 4.6B). Strikingly, upon strong TCR stimulation (gp33), we observed that some single cell-derived colonies consisted of both $TCF1^+$ memory and $TCF1^-$ effector precursor cells on day 5 after stimulation (Fig. 4.6C and 4.S6C). To exclude that the detected green signal was the result of potential auto-fluorescent debris of dead cells, we performed a propidium iodide (PI) staining, which revealed that the detected signal was not associated with dead cells (Fig. 4.S6B). We next analyzed whether mixed fate colonies were preferentially derived from mother cells undergoing ACD in their first mitosis. Compared to control day 5 sorted and subsequently imaged $TCF1^+$ memory precursor cells (green dots) and $TCF1^-$ effector precursor cells (brown dots), we observed a significant enrichment of $TCF1-GFP^+$ memory precursor cells in colonies stemming from an initial ACD (red dots) compared to colonies emerging from an initial symmetric cell division (SCD) (black dots) (Fig. 4.6C). However, colonies stemming from a SCD also contained sometimes very few $TCF1-GFP^+$ cells (Fig. 4.6C-E). When comparing the ratio of $TCF1-GFP^+$ cells per colony (defined as cells with a GFP signal above the mean value of control sorted $TCF1-GFP^+$ cells) to total cell number of the colony, a significant difference was observed between ACD- and SCD-derived colonies with ACD-derived colonies containing more $TCF1-GFP^+$ memory precursor cells (Fig. 4.6D). Consequently, when comparing the ratio of $TCF1-GFP^-$ cells per colony (defined as cells with a GFP signal below the mean value of control sorted $TCF1-GFP^-$ cells) to total cell number of the colony, SCD-derived colonies contained more TCF1-

GFP⁻ effector precursor cells compared to ACD-derived colonies (Fig. 4.6D). This approach, however, is impacted by the fact that effector precursors proliferate faster than memory precursor cells and therefore influence the absolute cell number per colony. This might lower the ratio of TCF1-GFP⁺ cells and increase the ratio of TCF1-GFP⁻ cells within a colony. We therefore compared the absolute numbers of TCF1-GFP⁺ or TCF1-GFP⁻ cells per colony and found that ACD-derived colonies indeed contained significantly more TCF1-GFP⁺ memory precursor cells compared to SCD-derived colonies (Fig. 4.6E). SCD-derived colonies, concomitantly, contained significantly more TCF1-GFP⁻ effector cells compared to ACD-derived colonies (Fig. 4.6E). In addition, we found that single cells, which established mixed-fate colonies, underwent more ACDs during their first cell division compared to those that established single-fate colonies (Fig. 4.6F). To strengthen our hypothesis and confirm the findings from the plate-bound antibody induced stimulation conditions (Fig. 4.3, representing a weak TCR stimulation), we repeated the experiment using C6 stimulation. Indeed, single cell-derived colonies preferentially induced either small colonies comprising TCF1-GFP⁺ memory precursor cells or large colonies consisting of TCF1-GFP⁻ effector precursor cells and no mixed-fate colonies (Fig. 4.6G and 4.S6D). As for the antibody-induced stimulation condition (Fig. 4.3E and F), we did not observe any correlation between first mitosis ACD or SCD with subsequent fate diversification (Fig. 4.6H-J). Taken together, our data suggest that ACD serves as a mechanism for the generation of memory precursor cells, specifically upon strong TCR stimulation.
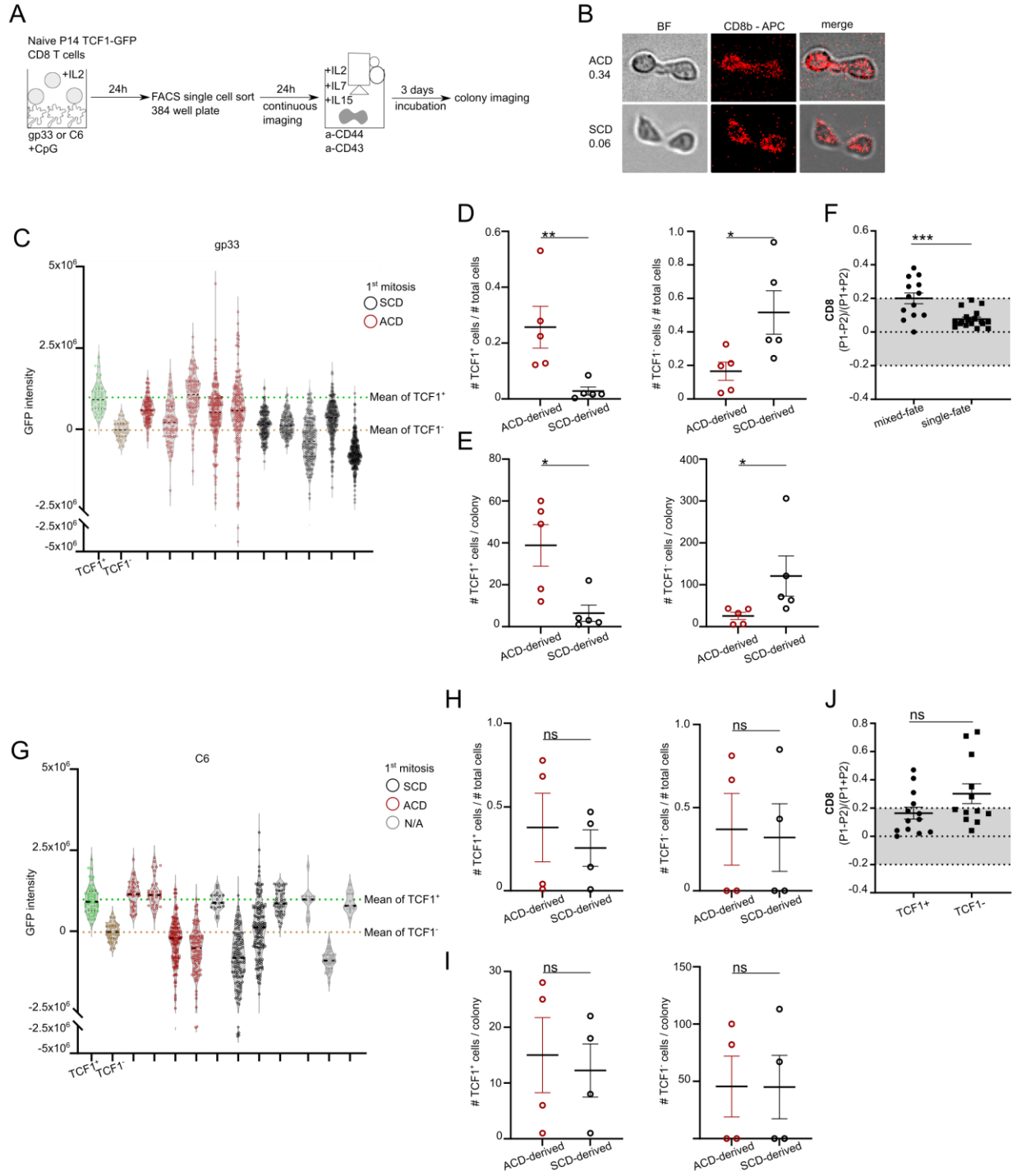
Figure 4.6: ACD enables the establishment of single cell-derived mixed-fate colonies upon strong TCR stimulation.

A Experimental setup. MutuDC1940 cells were stimulated with CpG and pulsed with gp33 or C6 peptide before P14 TCF1-GFP cells were added. P14 cells were activated in the presence of IL-2 for 24 h before blasted single cells were sorted into a 384-well plate containing medium supplemented with IL-2, IL-7 and IL-15. Cells were imaged in BF and red channel (CD8b-APC) every 60 min for 24 h and then further incubated. On day 5 post activation established colonies were imaged and analyzed for TCF1 expression. **B** Representative images of P14 TCF1-GFP cells in BF and red channel (CD8b-APC) taken from the time-lapse movie at the first time-point after cell division. **(C-F)** Data derived from gp33 stimulation. **(G-J)** Data derived from C6 stimulation. **C+G** GFP intensities of single cells within established colonies stemming from an initial ACD (red) or SCD (black). N/A indicates that no reliable asymmetry determination was possible. Green dots: control sorted and imaged TCF1$^+$ cells from day 5 post *in vitro* activation. Brown dots: control sorted and imaged TCF1$^-$ cells from day 5 post *in vitro* activation. **D+H** Ratio of cell numbers of TCF1$^+$ and TCF1$^-$ cells divided by total cell numbers per colony. **E+I** Absolute cell numbers of TCF1$^+$ and TCF1$^-$ cells per colony. **F** ACD rates from P14 cells activated with gp33 resulting in mixed-fate (n=13) or single-fate (n=18) colonies. A colony was characterized as mixed-fate when more than 10 TCF1$^+$ cells were identified. **J** ACD rates from P14 cells activated with C6 resulting in single-fate TCF1$^+$ (n=13) or TCF1$^-$ (n=12) colonies. Statistical analysis was performed using the unpaired two-tailed Student's *t* test or, when data did not pass the Shapiro-Wilk normality test, the unpaired two-tailed Mann-Whitney test. *$P < 0.05$, **$P < 0.01$, ***$P < 0.001$.

Inhibition of ACD markedly curtails memory precursor formation upon strong TCR stimulation

Following the hypothesis that ACD is of particular importance in memory cell generation upon strong TCR stimulation, we postulated that ACD might function as a safeguard mechanism for memory cell generation, specifically upon strong TCR stimulation. To test this assumption, we set out to modulate the ability of cells to undergo ACD in order to investigate the effect on memory formation. We hypothesized that interfering with the ability of cells to perform ACD would not influence fate outcome in conditions of weak TCR stimulation, whereas it would have a clear impact in conditions of strong TCR stimulation. Previous studies have demonstrated that atypical PKC is involved in the regulation of ACD and that PKCζ inhibition impairs the establishment of asymmetry (Borsa et al., 2019; Chang et al., 2011; Metz et al., 2015; Oliaro et al., 2010). To this end, we used a myristolated PKCζ inhibitor (PKCi) to prevent ACD. P14 cells were activated as described in Figure 4.4A and transiently treated with PKCi for the first 30 h of activation. We observed a significant decrease in ACD rates based on CD8 surface distribution between two daughter cells upon gp33 stimulation in the presence of PKCi compared to gp33 stimulation without PKCi. No effect of PKCi treatment on ACD rates was observed upon C6 stimulation (Fig. 4.7A and B). Additionally, we treated P14 cells with FTY720, a sphingosine-1-phosphate receptor agonist, previously described to inhibit long chain fatty acid ceramide synthesis, altering lymphocyte trafficking and decreasing ACD rates (Berdyshev et al., 2009; Borsa et al., 2019; Emurla et al., 2021; Mandala et al., 2002; Matloubian et al., 2004). Similar to PKCi treatment, ACD rates were significantly reduced upon FTY720 treatment in the gp33 stimulation condition. No impact of FTY720 on ACD rates in the C6 stimulation condition was observed (Fig. 4.S7A). Next, we investigated the expression profile of TCF1 and CD62L on progenies of activated P14 cells to determine potential effects of ACD inhibition on effector and memory precursor cell development. We discriminated between transient (only for the first 30 h) and permanent (throughout the entire culture period) PKCi treatment of P14 cells upon gp33 and C6 stimulation to inhibit ACD not only during first mitoses but also during all subsequent ones. Transient (t) and permanent (p) PKCi treatment significantly decreased the frequency of CD62L$^+$TCF1$^+$ cells and increased the frequency of CD62L$^-$TCF1$^-$ cells upon gp33 stimulation. Interestingly, no difference was observed between transient and permanent PKCi

treatment (Fig. 4.7C and D). Transient PKCi treatment upon C6 stimulation had no effect on the generation of $CD62L^+TCF1^+$ cells and $CD62L^-TCF1^-$ cells compared to untreated cells. Interestingly, and in contrast to gp33 stimulation, permanent PKCi treatment upon C6 stimulation slightly increased the frequency of memory precursor cells at the expense of effector cells (Fig. 4.7C and D). However, the observed effects of PKCi treatment were more pronounced in the setting of strong TCR stimulation. To confirm these findings on a functional level, we adoptively transferred P14 cells, either untreated, with transient or permanent PKCi treatment on day 6 after gp33 or C6 stimulation into recipient mice, which were subsequently infected with LCMV WE. In line with the *in vitro* findings, transient and permanent PKCi treatment upon gp33 stimulation significantly decreased the frequencies and absolute numbers of transferred P14 cells in lymph nodes and spleen of recipient mice on day 35 post infection, due to the diminished generation of memory precursor cells (Fig. 4.7E). Consequently, absolute numbers of $IL7R^+KLRG1^-$ P14 cells were also significantly reduced upon transient and permanent PKCi treatment after gp33 activation (Fig. 4.7E). Neither transient nor permanent PKCi treatment led to alterations in memory formation upon C6 stimulation (Fig. 4.7E). Thus, ACD during the first mitosis after activation indeed serves as a safeguard mechanism for the establishment of memory precursor cells in conditions of strong TCR stimulation and prevention of ACD in this setting markedly curtails memory formation *in vitro* and *in vivo*.
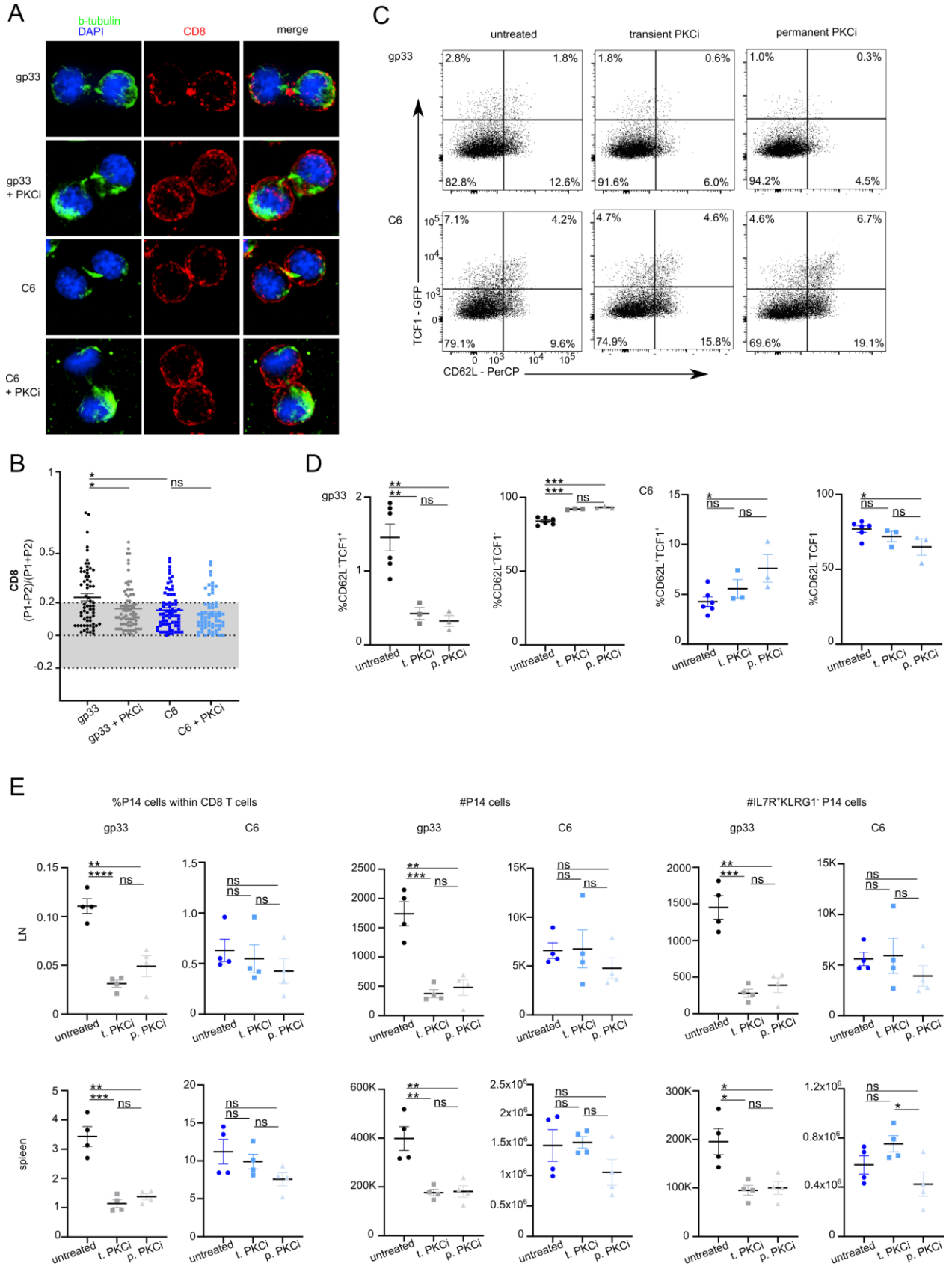
Figure 4.7 Inhibition of ACD markedly curtails memory precursor formation upon strong TCR stimulation.

A Confocal images from fixed samples of murine naïve P14 T cells 27 − 30 h after *in vitro* stimulation on gp33 or C6 loaded MutuDCs at 10^{-6} M with or without PKCi treatment. Mitotic cells were identified based on β-tubulin and nuclear structures and imaged from late anaphase to cytokinesis. **B** ACD rates of P14 cells activated with gp33 without (n=65) or with (n=76) PKCi, or with C6 at 10^{-6} M without (n=69) or with (n=65) PKCi. Data are represented as mean ± SEM. **C+D** Representative FACS plots and frequencies of $CD62L^{+}TCF1^{+}$ and $CD62L^{-}TCF1^{-}$ cells on day 6 post *in vitro* stimulation with gp33 or C6 at 10^{-6} M in the presence or absence of PKCi. PKCi treatment was either transiently (t) performed during the first 30 h of activation or permanently (p) throughout the entire culture period. **E** P14 cells were activated with gp33- or C6-loaded DCs at 10^{-6} M with or without PKCi treatment, either transiently (t) or permanently (p), and sorted on day 7 post activation. Sorted cells were individually transferred at equal numbers into recipient mice followed by acute LCMV WE infection (200 ffu/mouse intravenously) one day later. Lymph nodes and spleens were harvested 35 days post infection. Frequencies and absolute numbers of P14 cells within lymph nodes and spleens of recipient mice. Absolute numbers of $IL7R^{+}KLRG1^{-}$ cells. Representative data from 2-3 experiments. Statistical analysis was performed using the unpaired two-tailed Student's t test or, when data did not pass the Shapiro-Wilk normality test, the unpaired two-tailed Mann-Whitney test. *P < 0.05; **P < 0.01; ***P < 0.001.

Discussion

The establishment of a heterogeneous pool of CD8 T cell subsets differing in functional, phenotypic and metabolic features is an essential hallmark of effective adaptive immune responses. During acute infections, vigorous proliferation and diversification occur in parallel and it has been reported that a single activated CD8 T cell is able to give rise to both effector and memory cells (Buchholz et al., 2013; Chang et al., 2007; Gerlach et al., 2013, 2010; Plumlee et al., 2013; Stemberger et al., 2007). How fate diversification is implemented on a mechanistic level is not fully understood so far. Besides transcriptional and epigenetic regulation, the strength of initial TCR signaling and ACD have gained interest as contributors to the establishment of heterogeneous cell populations. ACD is an evolutionarily well-conserved mechanism for the generation of cellular heterogeneity (Sunchu and Cabernard, 2020). In CD8 T cells, ACD is initiated by a stable IS inducing a polarization axis, which allows for unequal distribution of fate-related markers resulting in two daughter cells that differ phenotypically, transcriptionally and metabolically (Borsa et al., 2019; Chang et al., 2011, 2007; King et al., 2012; Pollizzi et al., 2016; Verbist et al., 2016). Moreover, TCR signaling is mediated via the IS, and modulating the intensity of TCR stimulation has been shown to impact fate diversification, with strong TCR stimulation preferentially inducing effector differentiation and weak TCR stimulation leading to memory precursor formation due to high levels of Eomes and Bcl-6 (Chin et al., 2022; Kavazović et al., 2020; King et al., 2012; Knudson et al., 2013; Solouki et al., 2020). In the present study, we investigated the interplay between ACD and TCR activation signal strength and analyzed their impact on future fate divergence of CD8 T cells on the single cell level. Although previous studies identified remarkable contributions of ACD and TCR signal strength to CD8 T cell differentiation on a bulk population, analysis on the single cell level as well as their interactive contribution was missing. By using different *in vitro* imaging approaches linked with functional *in vivo* analysis and transcriptional profiling, we report a specific safeguarding role for ACD in CD8 memory T cell generation upon strong TCR stimulation. The determination of effector and memory differentiation early after *in vitro* activation requires reliable markers as indicators of fate. In contrast to a recent study describing two separate *in vitro* protocols for the generation of effector and memory precursor cells, respectively, here we established an *in vitro* stimulation

protocol which allows for early effector and memory fate discrimination by differential expression of CD62L and TCF1 within the same activation condition (Neitzke-Montinelli et al., 2022). On day 5 post *in vitro* activation, we found that CD62L⁺TCF1⁺ cells show typical hallmarks of memory precursor cells, whereas CD62L⁻TCF1⁻ cells possess features of effector cells. Metabolically, CD62L⁺TCF1⁺ cells relied on oxidative phosphorylation (OXPHOS), whereas CD62L⁻TCF1⁻ cells used glycolysis for energy production. It is well-described that *in vivo* generated memory cells use OXPHOS, while effector cells depend on glycolysis (Pearce et al., 2013). Consistent with previous studies investigating the proliferation of effector and memory precursor cells, we found that CD62L⁺TCF1⁺ cells divided slower compared to CD62L⁻TCF1⁻ cells (Buchholz et al., 2013; Gerlach et al., 2013; Kinjyo et al., 2015; Kretschmer et al., 2020; Plambeck et al., 2021). This finding corresponds to the observed elevated expression levels of CD25 of the CD62L⁻TCF1⁻ cell subset allowing for IL-2 induced proliferation. Furthermore, CD62L⁺TCF1⁺ cells showed nuclear localization of FOXO1, a transcription factor that induces the expression of TCF1 and CD62L and that contributes to orchestrating metabolic regulation favoring the OXPHOS pathway (Adams et al., 2016; Kim et al., 2013; van der Windt and Pearce, 2012). By *in vivo* analysis of CD62L⁺TCF1⁺ cells upon adoptive transfer, we found that these cells home better into the T cell zones of lymphoid organs and possess enhanced re-expansion and memory formation potential upon LCMV infection compared to their CD62L⁻TCF1⁻ cell counterpart. Furthermore, the transcriptional profiles of CD62L⁺TCF1⁺ and CD62L⁻TCF1⁻ cells significantly overlapped with *in vivo* established memory and effector cells, respectively. Thus, CD62L⁺TCF1⁺ and CD62L⁻TCF1⁻ cells resemble *in vivo* generated memory and effector cells, respectively, according to phenotypic, transcriptional and functional criteria. Using two LCMV derived peptides with different affinities towards the P14 TCR - gp33 (high affinity) and C6 (low affinity) - allowed us a combined analysis of TCR signal strength and ACD on fate determination (Daniel T Utzschneider et al., 2016). Specifically, our established *in vitro* differentiation protocol enabled us to determine the fate of progenies stemming from a single CD8 T cell a few days after activation - either induced by weak or strong TCR activation - and link the phenotypic composition of the emerging colony to the (a)symmetry of the first cell division of the mother cell. As reported in previous studies, we found that high affinity stimulation induced increased rates of ACD and preferential effector differentiation at the expense of memory formation compared to low affinity stimulation (King et al., 2012), suggesting a potential specific

role of ACD within this condition. Therefore, we hypothesized that in contrast to weak TCR stimulation, either induced by low affinity peptides or by plate-bound antibodies, strong TCR stimulation would cause single activated CD8 T cells to generate mixed-fate colonies following ACD. Indeed, we found single cell-derived colonies consisting of effector and memory precursor cells after strong TCR activation. The abundance of TCF1$^+$ memory precursor cells was significantly increased if the first performed cell division was asymmetric, while single cell-derived colonies derived from a symmetrically dividing mother cell comprised either none or very few memory precursor cells. In contrast, activation of naïve CD8 T cells by plate-bound Fc-ICAM-1 and α-CD3 and α-CD28 antibodies or by the low affinity C6 peptide did not establish single cell derived mixed-fate colonies. Instead, single cells formed single-fate colonies either consisting of effector (CD62L$^-$ TCF1$^-$) or memory precursor (CD62L$^+$TCF1$^+$) cells, independent of the (a)symmetry of the first cell division. To confirm a strong TCR stimulation dependent impact of ACD on future fate diversification, we introduced a PKCζ inhibitor into our experimental protocol, leading to inhibition of ACD (Chang et al., 2011; Metz et al., 2015). We hypothesized that PKCζ inhibition should only impact memory formation after strong TCR stimulation with gp33 and not upon C6 stimulation. Indeed, we found that PKCζ inhibition led to significantly lower ACD rates and strongly curtailed memory formation *in vitro* and *in vivo* after gp33 stimulation, whereas no effect was observed upon C6 stimulation. Lastly, by analyzing permanent versus transient inhibition of ACD by PKCζ inhibitor treatment, we found that ACD during the first mitosis after activation in contrast to potential subsequent ACDs played a key role in fate diversification during CD8 T cell differentiation. Taken together, we report that ACD during the first mitosis after activation functions as a safeguard mechanism for the generation of a robust CD8 memory T cell pool, specifically upon strong TCR stimulation.

Our data and other studies show that strong TCR stimulation induces quantitatively fewer memory precursor cells compared to weak TCR stimulation (King et al., 2012; Solouki et al., 2020). It remains to be elucidated, however, whether high-affinity stimulation-derived memory CD8 T cell clones are qualitatively similar or different from low affinity stimulation-derived clones in terms of their responsiveness following recall (i.e. generating potent cytotoxic effector cells and robust secondary memory cells) and are therefore able to compensate for the lower abundance.

Interestingly, on a transcriptional level, cells derived from weak TCR stimulation (AB and C6) clustered more closely compared to the more distinct gp33 stimulated cell cluster, which was overall more effector-like. Previous studies provide evidence for differential behavior of low and high affinity memory T cell clones during recall responses, with low affinity memory clones poorly responding to low affinity ligands upon rechallenge (Knudson et al., 2013). Further, it remains elusive which mechanisms drive ACD upon high versus low affinity stimulation. Even though ACD occurs after weak TCR stimulation at low levels, it does not lead to single cell derived mixed fate colonies, suggesting a differential downstream mechanism that allows fate diversification specifically upon strong TCR stimulation. One option would be the described prolonged interaction between the T cell and the APC, potentially leading to an enforced polarization axis (Ozga et al., 2016). Whether the recently reported establishment of an ER diffusion barrier forms differentially upon varying TCR signal strengths and thereby potentially contributes to fate divergence remains to be investigated (Emurla et al., 2021). Furthermore, selective asymmetry of PKCζ could play a fate decisive role as asymmetric PKCζ distribution was exclusively described upon strong TCR stimulation so far (Chang et al., 2007; Metz et al., 2015). This hypothesis would fit to our results showing that inhibition of PKCζ only affects memory formation after strong TCR stimulation as opposed to weak TCR stimulation. Moreover, it remains to be investigated which mechanisms drive fate divergence upon weak TCR stimulation, as according to our data, ACD does not play a role in this setting. Whether TCR downstream signaling events, such as activation of interleukin-2 inducible tyrosine kinase (ITK), orchestrate a potential threshold of memory versus effector differentiation, which is differentially met by single cells in weak TCR stimulation conditions, but largely overcome in high affinity situations remains to be shown (Conley et al., 2020). It should also be noted that the "asymmetry" of a CD8 T cell division is in our study and has been in previous studies at large defined by an arbitrary threshold (often set as a 50% increased distribution of CD8 in one of the two daughter cells), such that functional asymmetry of a CD8 T cell mitosis would be better defined by physiological endpoints. Indeed, our results confirm that an ACD threshold of 0.2 excludes dividing mother cells after a high affinity stimulation to be able to give rise to mixed fate colonies (Fig. 6F). However, also some mother cells that gave rise to mixed fate colonies exhibited a CD8 ACD rate of below 0.2. This might be attributed to the fact that asymmetric CD8 inheritance is transient (Fig. S3B) and might therefore have been missed in some of the analyzed mitoses

(analysis was only done every 60 min). Thus, a more long-lasting and thus reliable marker of ACD would enable a more precise and long-lasting determination of asymmetric CD8 T cell division and its relevance for future fate determination.

Our imaging approaches allow insights into CD8 T cell differentiation at high resolution. However, emerging new imaging technologies might enable even more precise single-cell tracing experiments, further allowing the combination with downstream manipulations of single cells, such as mitochondrial transfer between living cells, Live-seq or trackSeq (Chen et al., 2022; Gäbelein et al., 2022; Wehling et al., 2022). A general limitation of *in vitro* lineage tracing experiments is the missing link to the physiological *in vivo* environment, which is technically extremely challenging. However, our observation that ACD plays an important role in fate diversification specifically upon strong TCR stimulation provides new perspectives into the regulation of fate diversification during CD8 T cell responses, which can and should in the future be probed and challenged by additional approaches.

Material and Methods

Mice

Six to ten-week-old male or female mice were used for the experiments performed in this study. Wild-type Ly5.2 C57BL/6 mice were obtained from the ETH Phenomics Center or from Janvier Labs. C57BL/6J, Ly5.1 P14 mice (CD8$^+$ T cells with a transgenic TCR with specificity for the glycoprotein GP$_{33-41}$ epitope of lymphocytic choriomeningitis virus (LCMV) in the context of H-2D^b (Pircher et al., 1990), Ly5.1 OTI (CD8$^+$ T cells with a transgenic TCR with specificity for the OVA$_{257-264}$ SIINFEKL peptide)) (Hogquist et al., 1994) and *Tcf7*^{GFP} reporter mice (expressing GFP under the control of the *Tcf7* locus) (Daniel T. Utzschneider et al., 2016) were housed and bred under specific pathogen-free conditions in animal facilities at ETH Zurich, Hönggerberg. P14 *Tcf7*^{GFP} and OTI *Tcf7*^{GFP} mice were obtained by crossing *Tcf7*^{GFP} mice to P14 or OTI mice, respectively. All animal experiments were conducted in accordance with the Swiss federal regulations and were approved by the cantonal veterinary office of Zurich (animal experimental permissions: 115/2017, 022/2020).

Cell lines, virus, viral peptides and infections

Dendritic cells (DC) of the immortalized MuTuDC1940 cell line originate from splenic CD8α conventional DC tumors of C57BL/6J mice and retain all major characteristics of their natural counterparts (Fuertes Marraco et al., 2012). LCMV strain WE was kindly provided by R.M. Zinkernagel (University Hospital Zurich), propagated on baby hamster kidney 21 cells (Ahmed et al., 1984) and viral titers were determined as previously described (Battegay et al., 1991). Acute LCMV infections were conducted by injecting 200 ffu of the LCMV WE strain intravenously into the tail vein of recipient mice. LCMV-derived peptides gp33 (KAVYNFATC) and C6 (KAVYNCATC) and

OVA-derived peptides N4 (SIINFEKL) and L4 (SIILFEKL) were obtained from EMC Microcollections GmbH.

CD8 T cell isolation

CD8 T cells were isolated from spleens and lymph nodes of P14 $Tcf7^{GFP}$ or OTI $Tcf7^{GFP}$ mice using the EasySep^{TM} Mouse CD8$^+$ T cell Isolation Kit (Stemcell Technologies), following manufacturer's instructions.

In vitro CD8 T cell activation

After isolation, CD8 T cells were kept in complete T cell medium (RPMI-1640 (Bioconcept), 2 mM L-Glutamine (Bioconcept), 2% penicillin-streptomycin (Sigma-Aldrich), 1x Non-Essential Amino Acids (Sigma-Aldrich), 1 mM Sodium Pyruvate (Gibco), 10% fetal bovine serum (Omnilab), 25 mM HEPES (Gibco), 50 µM β-Mercaptoethanol (Gibco)). For antibody induced activation, CD8 T cells were stimulated in presence of self-made human IL-2 on α-CD3 (5 µg/ml) (145-2C11, BioLegend), α-CD28 (5 µg/ml) (37.51, BioLegend) and human Fc-ICAM-1 (50 µg/ml) (R&D Biosciences, Bio-Techne AG) coated plates for 30-36h at 37°C and 5% CO_2. To activate CD8 T cells by cognate antigen, adherent MuTuDCs were stimulated with CpG (0.5 µg/ml) and at the same time loaded with the respective peptides at indicated concentrations for 1h at 37°C and 5% CO_2. DCs were washed once with PBS before CD8 T cells were added in the presence of self-made human IL-2 and activated for 28-30h. After initial activation, CD8 T cells were removed from either plate-bound antibodies or adherent dendritic cells and further cultured in complete T cell medium supplemented with IL-7 (10 ng/ml) (eBioscience), IL-15 (5 ng/ml) (eBioscience) and self-made

human IL-2. ACD modulation was conducted by adding 30 µM of MYR PKC Zeta Pseudosubstrate (ThermoFisher) to inhibit PKCζ, or by adding 2 µM of FTY720 (Sigma-Aldrich).

Immunofluorescence staining and confocal microscopy

For tissue section analysis, spleens were incubated in 20% sucrose (Sigma-Aldrich) on a spinning wheel at 4°C for 24 h. Spleens were then embedded in Tissue-Tek® O.C.T. Compound (Sakuraus), snap-frozen in liquid N_2 and stored at -20°C. 10µm slices were obtained using a microtome. Spleen slices were fixed with 2% paraformaldehyde (PFA) (Sigma-Aldrich) for 1 h at room temperature and blocked with 1×PBS containing 1% of rat serum for 1 h at room temperature. Sections were stained in 1×PBS containing 0.1% of rat serum for 1 h at room temperature in the dark. The following fluorophore-conjugated antibodies were purchased from BioLegend (α-CD8 BV421 53-6.7; α-CD45R/B220 FITC RA3-6B2; α-CD169 (Siglec-1) PE 3D6.112; α-CD45.1 APC A20). Stained slices were mounted on ProLong™ Diamond Antifade Mountant (ThermoFisher) and dried overnight in the dark.

For asymmetry analysis, cells were washed with PBS, seeded on poly-l-lysine coated coverslips and incubated for 1 h at 37°C. Fixation of cells was performed by adding 2% PFA (Sigma-Aldrich) for 7 min at room temperature. Cells were then permeabilized with 0.1% Triton X (Sigma-Aldrich) for 10 min and blocked in PBS containing 2% bovine serum albumin (GE Healthcare) and 0.01% Tween 20 (National Diagnostics) for 1 h at room temperature. The following antibodies were used for immunofluorescence staining: mouse α-β-tubulin (Sigma-Aldrich), α-mouse IgG AF488 (Abcam), α-CD8b.2 APC (53-5.8, BioLegend) and α-FOXO1 (C29H4, BioConcept NEB). DAPI (Sigma-Aldrich) was used to identify DNA. Cells were mounted on one drop of ProLong™ Diamond Antifade Mountant (ThermoFisher) onto the microscopy slide and dried overnight in the dark.

Microscopic analyses were conducted with a Visitron Confocal System (inverse confocal microscope, Visitron Systems) equipped with four laser lines (405, 488, 561 and 640nm) allowing visualization of four wavelength spectra: blue (405 - 450nm), green (525 - 550nm), red (605 -

652nm) and far-red (700 - 775nm) fluorophores. For each image, 25 Z-stacks (0.5 µm each) were recorded with 10× (spleen sections) (10× objective, type: plan-neofluar, aperture: 0.3, immersion: Air, contrast Ph1) or 100× (asymmetry analysis) magnification (100× objective, type: plan-neofluar, aperture: 1.3, immersion: oil, contrast Ph3) coupled to Evolve 512 EMCCD cameras (Photometrics). Mitotic cells in phases ranging from late anaphase to late telophase were identified based on nuclear morphology, the presence of a dual microtubule-organizing center on each pole of the cell and on characteristic tubulin bridges between two daughter cells in cytokinetic cells (Fig. 4.S8).

Time-lapse microscopy

For all time-lapse microscopic approaches, cells were cultured at 37°C in a temperature- and CO_2-controlled incubation chamber in complete T cell medium without phenol red (RPMI-1640 (Gibco), 2 mM L-Glutamine (Bioconcept), 2% penicillin-streptomycin (Sigma-Aldrich), 1x Non-Essential Amino Acids (Sigma-Aldrich), 1 mM Sodium Pyruvate (Gibco), 10% fetal bovine serum (Omnilab), 25 mM HEPES (Gibco), 50 µM β-Mercaptoethanol (Gibco)) supplemented with with IL-7 (10 ng/ml) (eBioscience), IL-15 (5 ng/ml) (eBioscience) and self-made human IL-2.

For single-cell continuous imaging after antibody stimulation (Loeffler et al., 2022, 2019), cells were harvested 32-34 h after activation and transferred into µ-slide VI^{0,4} channel slides (IBIDI), pre-coated with 5 µg/ml α-CD43 (eBioR2/60, Invitrogen) and α-CD44 (IRAWB14) (Loeffler et al., 2018). Movie 4.1 and 4.2 were imaged for 3 days using a Nikon-Ti Eclipse equipped with linear-encoded motorized stage, Orca Flash 4.0 V2 (Hamamatsu), and Spectra X fluorescent light source (Lumencor) with CFP (436/20; 455LP; 480/40), GFP (470/40; 495LP; 525/50) and Cy5 (620/60; 660LP; 700/75; all, AHF) filter cubes to detect CD62L-BV421, TCF1-GFP and CD8-APC, respectively. Images were acquired every 40 min in BF and the Cy5 channel and every 90 min in the CFP and GFP channels with a 10× (NA 0.45) CFI Plan Apochromat λ objective.

For single-cell high-throughput imaging, cells were harvested 24 h after initial activation and stained for viability and CD8b-APC before blasted single cells were sorted into wells of a 384-well

plate pre-coated with 5 µg/ml α-CD43 (eBioR2/60, Invitrogen) and α-CD44 (IRAWB14) (Loeffler et al., 2018). Cells were time-lapse imaged using an ImageXpress Micro Confocal Microscope (Molecular Devices) for 24 h in an interval of 1 h to record the first cell division. After 24 h, cells were removed from the microscope and incubated for another 3 days. Single-cell derived colonies were subsequently imaged for fate analysis. Bright-field and fluorescence images were acquired using the 10× objective using MetaXpress software (Molecular Devices).

Microscopy images were analyzed using the ImageJ softwares. Single cell tracking was performed using the tTt software (Hilsenbeck et al., 2016).

Quantification

Wide field and confocal microscopy images were analyzed using the ImageJ software. GFP intensities were measured by subtracting the background signal next to the cell from each individual cell from the signal obtained by the region of interest (ROI) drawn around the cell. Asymmetry rates were calculated based on CD8 signal quantification of both daughter cells (detailed information of determining the ROI in Fig. 4.S8). The raw integrated density (RID) of each daughter cell was first normalized to the respective area. Next, a threshold at 40% was applied on both daughter cells, excluding 60% of dim, potentially unspecific signal (Shimoni et al., 2014). Using this threshold, a new measurement was performed creating updated raw integrated density values. The final formula led us to determine the asymmetry rate (AR) of two daughter cells (Equation 1). Cell divisions were defined as asymmetric when the CD8 signal was 1.5-fold greater in one daughter cell compared to the other, equaling an AR of 0.2.

$$ AR = \frac{(\text{RID (Cell1)} / \text{Area (Cell1)}) - (\text{RID (Cell2)} / \text{Area (Cell2)})}{(\text{RID (Cell1)} / \text{Area (Cell1)}) + (\text{RID (Cell2)} / \text{Area (Cell2)})} $$

Flow cytometry

Inguinal lymph nodes, spleens and lungs were obtained from PBS-perfused mice. Spleens and lymph nodes were smashed through 70 μm strainers (BD Biosciences) using a syringe plunger in order to prepare single-cell suspensions. Lungs were cut into smaller pieces and further incubated in RPMI-1640 (BioConcept) containing 2 mM L-Glutamine (Bioconcept), 2% penicillin-streptomycin (Sigma-Aldrich), 1x Non-Essential Amino Acids (Sigma-Aldrich), 1 mM Sodium Pyruvate (Gibco), 10% fetal bovine serum (Omnilab), 25 mM HEPES (Gibco), 50 μM β-Mercaptoethanol (Gibco) and 2.4 mg/ml collagenase type I (Gibco) and 0.2 mg/ml DNase I (Roche Diagnostics) for 40 min at 37°C. Next, mononuclear cells were obtained by gradient centrifugation over 30% Percoll (Sigma-Aldrich). Erythrocytes were removed by ACK lysis buffer treatment at room temperature for 5 min. When cytokine production was investigated, CD8 T cells were stimulated with 1 μg/ml of gp33 peptide in the presence of 10 μg/ml Brefeldin A (Sigma-Aldrich) at 37°C for 6h. Fluorophore-conjugated antibodies used for flow cytometry stainings were purchased from BD Biosciences (α-CD278 (ICOS) PE 7E.17G9), eBiosciences (α-TNF Pe-Cy7 TN3-19.12), Miltenyi Biotec (α-phospho-Akt (pS473) PE REA359) and BioLegend (α-CD8b.2 APC 53-5.8; α-CD62L PerCP MEL-14; α-CD45.1 APC A20; α-IL-7Rα BV421 A7R34; α-KLRG1 PE-Cy7 2F1; α-CD44 PE IM7; α-CD8 BV510 53-6.7; α-CD11c PE-Cy7 N418; α-CD25 PE 3C7; α-PD-1 PE-Cy7 29F.1A12; α-IL-2 PE JES6-5H4; α-IFNγ Pacific Blue XMG1.2; α-CD366 (Tim-3) PE RMT3-23; α-CD80 PE 16-10A1; α-CD86 APC GL-1; α-CD40 PE-Cy7 3/23; α-CD11c PerCP N418). Identification of viable cells was done by fixable near-IR dead cell staining (Life Technologies). Surface staining was conducted at 4°C for 20 - 30 min. For intracellular cytokine staining, cells were additionally fixed and permeabilized in 2x FACS Lysis Solution (BD Biosciences) with 0.08% Tween 20 (National Diagnostics) at room temperature for 10 min. Intracellular staining was performed at room temperature in the dark for 30 min. In order to investigate phosphoprotein expression, surface staining was followed by fixation with pre-heated 4% PFA (Sigma-Aldrich) at 37°C for 10 min. Cells were then permeabilized with 90% of ice-cold methanol on ice for 30 min and phosphor-staining was conducted at room temperature in the dark for 40 min. Proliferation was analysed by using the Cell Proliferation Dye eFluor™ 670 or Cell Proliferation Dye eFluor® 450 (eBioscience). Following staining, cell suspensions were washed and

stored in PBS containing 2% FBS (Omnilab) and 5 mM of EDTA (Sigma-Aldrich) for acquisition. Multiparameter flow cytometry analysis was performed on a FACS Canto™ (BD Biosciences) cell analyzer and fluorescence-activated cell sorting was performed using a BD FACSAria™ (BD Biosciences) cell sorter with FACS Diva software. Data was analyzed using FlowJo software (FlowJo Enterprise, version 10.0.8, BD Biosciences).

Adoptive transfer

For adoptive transfer, 10 000 or 1000 sorted CD8 T cells were intravenously injected into naïve young CD45.2 C57BL/6 recipient mice.

Extracellular flux analysis

Sorted CD8 T cells were seeded into poly-l-lysine pre-coated wells of a 96-well plate (XFe96 cell culture microplates, Agilent) and incubated at 37°C for 1h before the plate was placed into an Extracellular Flux Analyzer XFe96 (Seahorse, Agilent) for measuring the extracellular acidification rate (ECAR) and the oxygen consumption rate (OCR). For ECAR measurement, the following reagents were diluted in pure XF medium and injected into the plate at the indicated timepoints to achieve the final concentrations: 11.6 mM glucose (Sigma-Aldrich), 0.75 µM Oligomycin (ATP-synthase inhibitor) (Adipogen), 100 mM 2-deoxyglucose (2-DG) (Sigma-Aldrich). Non-glycolytic acidification of media (ECAR following injection of 2-DG) was subtracted to calculate glycolysis (ECAR following injection of glucose) and maximal glycolytic capacity (ECAR following injection of Oligomycin). For OCR measurement, the following reagents were diluted in XF medium containing 25 mM glucose (Sigma-Aldrich), 2 mM L-glutamine (BioConcept) and 1 mM Sodium Pyruvate (Gibco), which was adjusted to pH 7.4 and injected into the plate at the indicated timepoints to

achieve the final concentrations: 0.75 µM Oligomycin (ATP-synthase inhibitor) (Adipogen), 1 µM FCCP (chemical uncoupler) (Sigma-Aldrich), 1 µM Rotenone and Antimycin A (electron transport chain inhibitors) (Sigma-Aldrich). Non-mitochondrial respiration (OCR values following injection of Rotenone and Antimycin A) was subtracted from overall basal (OCR values prior to injection of Oligomycin), uncoupled (OCR values following injection of Oligomycin) and maximal respiration (OCR values prior injection of Oligomycin) to calculate basal, uncoupled, and maximal mitochondrial respiration, respectively. ATP production was calculated by subtracting uncoupled mitochondrial respiration from basal mitochondrial respiration.

Bulk RNAseq

CD62L$^+$TCF1$^+$ and CD62L$^-$TCF1$^-$ P14 cells were sorted on day 6 after *in vitro* activation with either plate-bound antibodies or peptide-loaded dendritic cells (MutuDC1940 cell line). RNA was extracted using the RNeasy Micro Kit (Qiagen) according to the manufacturer's protocol and processed for sequencing at the Functional Genomics Center Zürich (FGCZ). mRNA was sequenced on the Illumina platform. For analysis, RNAseq reads were mapped to the mouse reference genome (Ensembl_GRCm38.75) using the R package Rsubread (v2.8.2) with the default parameters (Liao et al., 2019). The featureCounts function was then used to assign mapped reads to genomic features using NCBI Entrez IDs (Liao et al., 2014). Differential gene expression analysis was performed using the R package edgeR (v3.36.0) (Lun et al., 2016). Principal component analysis was performed using the PCAtools package in R (v2.6.0). Heatmaps were created using the pheatmap package (v1.0.12) and general data visualization was performed using ggplot2 (v3.3.6) and ggrepel (v0.9.1). Gene set enrichment analysis was performed using the R package fgsea (v1.20.0), which uses the adaptive multilevel splitting Monte Carlo approach (Korotkevich et al., 2021). Gene sets used: KAECH_DAY8_EFF_VS_MEMORY_CD8_TCELL_DN and KAECH_DAY8_EFF_VS_MEMORY_CD8_TCELL_UP (Kaech et al., 2002);

GSE8678_IL7R_LOW_VS_HIGH_EFF_CD8_TCELL_DN   and

GSE8678_IL7R_LOW_VS_HIGH_EFF_CD8_TCELL_UP (Joshi et al., 2007).

Statistical analysis

For statistical analysis the unpaired two-tailed Student's t test or, when data did not pass the Shapiro-Wilk normality test, the unpaired two-tailed Mann-Whitney test was performed using GraphPad Prism Software. Statistical significance was determined with $*P < 0.05$; $**P < 0.01$; $***P < 0.001$; $****P < 0.0001$. For animal experiments, sample size varied between 3 to 4 mice per group for each individual experiment.

Supplementary information
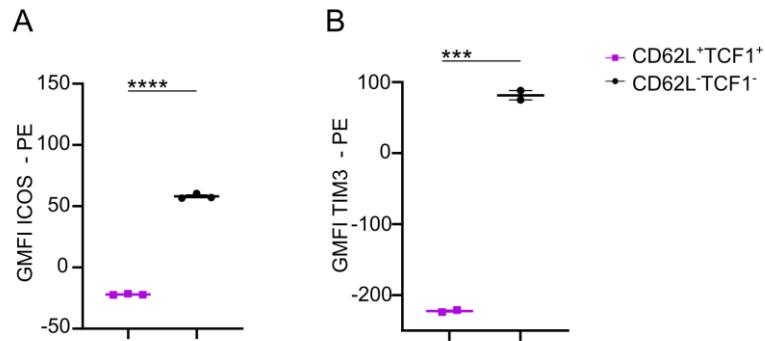
Figure 4.S1: *In vitro* differentiation of P14 TCF1-GFP cells and characterization of CD62L⁺TCF1⁺ and CD62L⁻TCF1⁻ cells.

Geometric Mean of Fluorescence Intensity (GMFI) of CD62L⁺TCF1⁺ and CD62L⁻TCF1⁻ cells expressing ICOS **(A)** and TIM3 **(B)** on day 4 post stimulation. Statistical analysis was performed using the unpaired two-tailed Student's *t* test or, when data did not pass the Shapiro-Wilk normality test, the unpaired two-tailed Mann-Whitney test. *$P < 0.05$; **$P < 0.01$; ***$P < 0.001$; ****$P < 0.0001$.

A
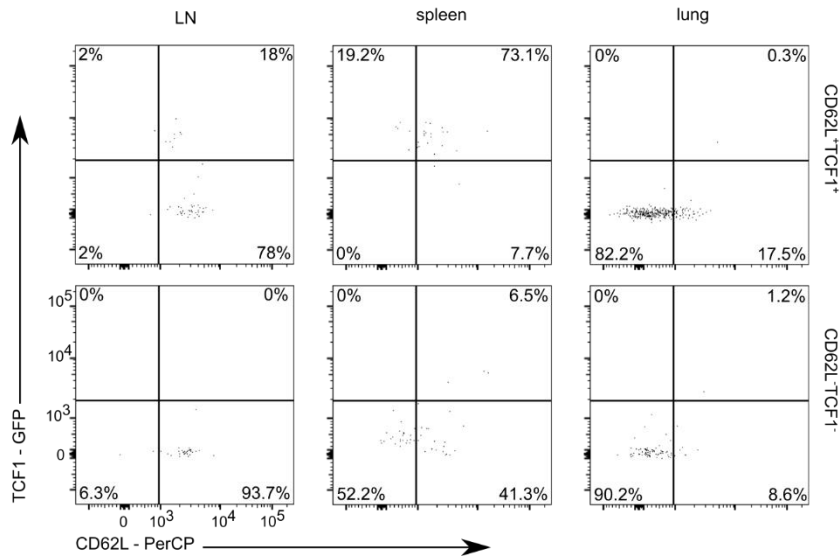
Figure 4.S2: *In vivo* adoptive transfer of CD62L⁺TCF1⁺ and CD62L⁻TCF1⁻ cells leads to changes in expression of CD62L and TCF1.

A P14 TCF1-GFP cells were activated as described in Figure 4.1A and sorted on day 4 post activation into CD62L⁺TCF1⁺ and CD62L⁻TCF1⁻ cells. Sorted subsets were individually transferred at equal numbers into recipient mice. Spleens, lymph nodes and lungs were harvested 8 h post transfer and homing of transferred cells was investigated. Representative FACS plots of TCF1 and CD62L expression of P14 cells in spleens, lymph nodes and lungs of recipient mice 8h post transfer.
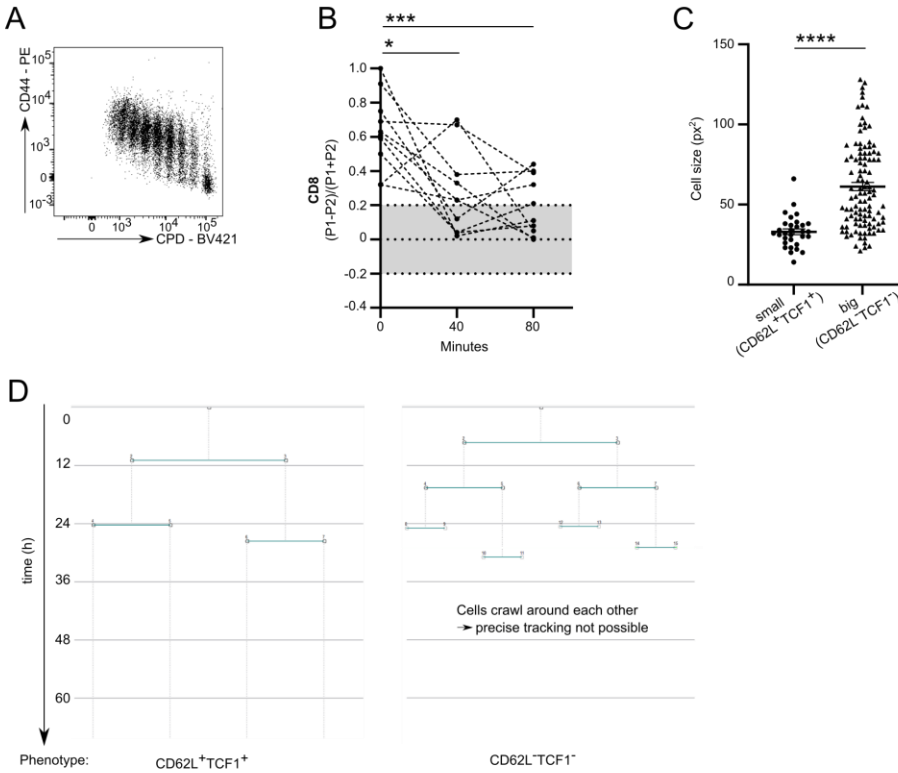
Figure 4.S3: ACD does not promote diversity upon stimulation with TCR agonistic antibodies.

A Naïve P14 TCF1-GFP cells were stimulated as described in Figure 4.1A. Representative plot of CPD dilution against expression of CD44 on day 4 post activation. **B** ACD rates of sister cell pairs (n=10) measured directly after completed mitosis, 40 and 80 min later. **C** Cell size (in square pixels) from P14 TCF1-GFP cells that later formed small-sized (CD62L$^+$TCF1$^+$) (n=31) and big-sized (CD62L$^-$TCF1$^-$) (n=108) colonies. Data are represented as mean ± SEM. **D** Representative family trees of one small-sized colony consisting of CD62L$^+$TCF1$^+$ cells and one big-sized colony consisting of CD62L$^-$TCF1$^-$ cells. Statistical analysis was performed using the paired (in B) or unpaired (for C) two-tailed Student's t test or, when data did not pass the Shapiro-Wilk normality test, the unpaired two-tailed Mann-Whitney test. *$P < 0.05$; **$P < 0.01$; ***$P < 0.001$; ****$P < 0.0001$.
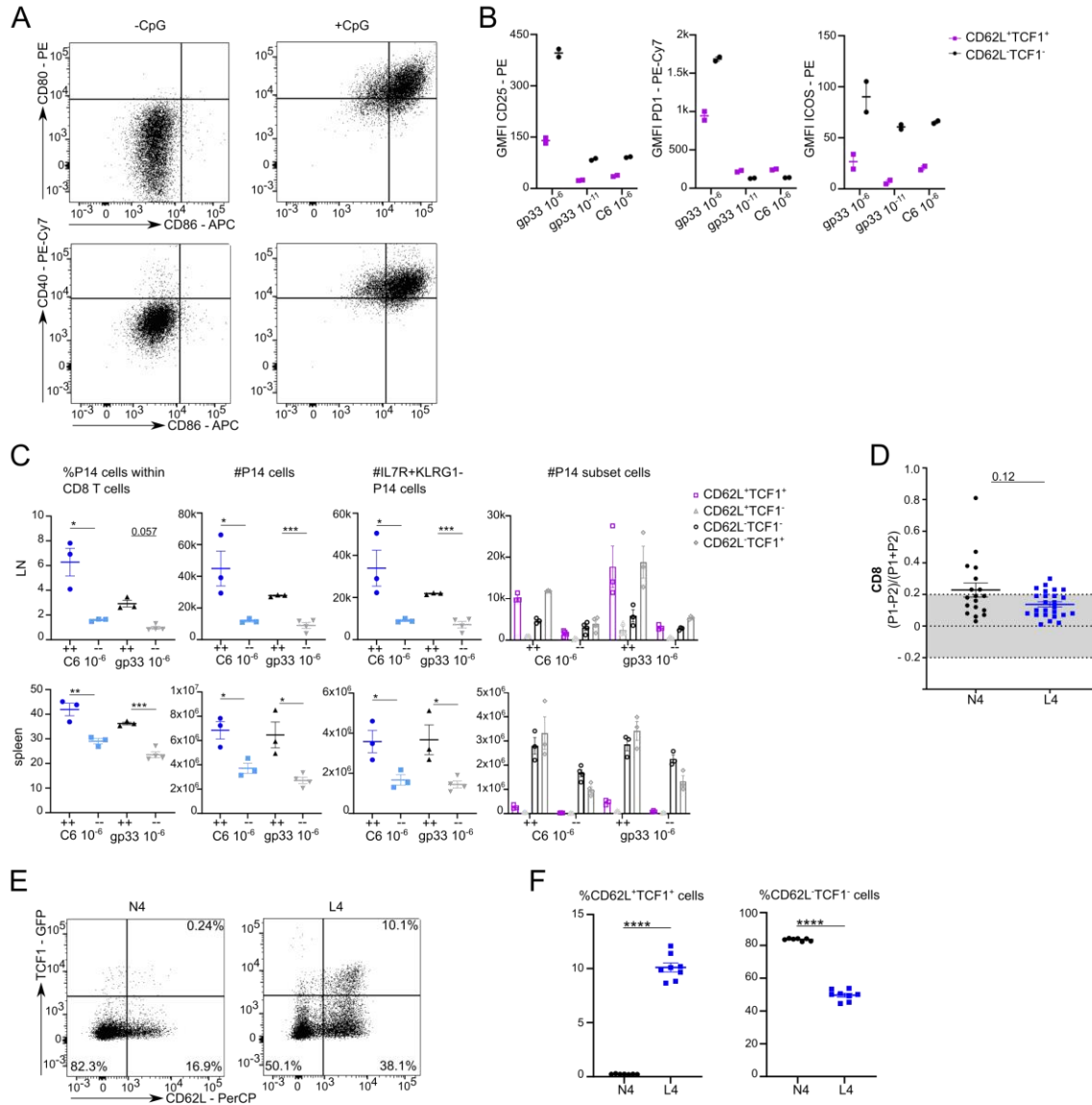
Figure 4.S4: The strength of TCR stimulation impacts ACD and fate.

A MutuDC1940 cells were either stimulated with or without CpG overnight at 37°C. Representative FACS plots of CD80, CD86 and CD40 expression. **B** Geometric Mean of Fluorescence Intensity (GMFI) of CD25, PD1 and ICOS expression by CD62L⁺TCF1⁺ and CD62L⁻TCF1⁻ cells on day 6 post stimulation with gp33 at 10^{-6} M, gp33 at 10^{-11} M or C6 at 10^{-6} M. **C** P14 TCF1-GFP cells were activated with gp33 at 10^{-6} M or C6 at 10^{-6} M and sorted on day 6 post activation into CD62L⁺TCF1⁺ and CD62L⁻TCF1⁻ cells. Sorted subsets were individually transferred at equal numbers into recipient mice followed by acute LCMV WE infection (200 ffu/mouse intravenously) one day later. Spleens, lymph nodes and lungs were harvested 35 days post infection. Frequencies and absolute numbers of P14 cells within spleens and lymph nodes of recipient mice. Absolute numbers of IL7R⁺KLRG1⁻, CD62L⁺TCF1⁺, CD62L⁺TCF1⁻, CD62L⁻TCF1⁻ and CD62L⁻TCF1⁺ cells. **D** ACD

rates from OT-I cells activated with SIINFEKL (N4) (n=18) or SIILFEKL (L4) (n=25). Data are represented as mean ± SEM. **E** Representative FACS plots of TCF1 and CD62L expression. OT-I TCF1-GFP cells were activated and analyzed on day 6. **F** Frequencies of CD62L$^+$TCF1$^+$ and CD62L$^-$TCF1$^-$ OT-I cells on day 6 after stimulation. Statistical analysis was performed using the unpaired two-tailed Student's *t* test or, when data did not pass the Shapiro-Wilk normality test, the unpaired two-tailed Mann-Whitney test. *$P < 0.05$; **$P < 0.01$; ***$P < 0.001$.

A

C

B
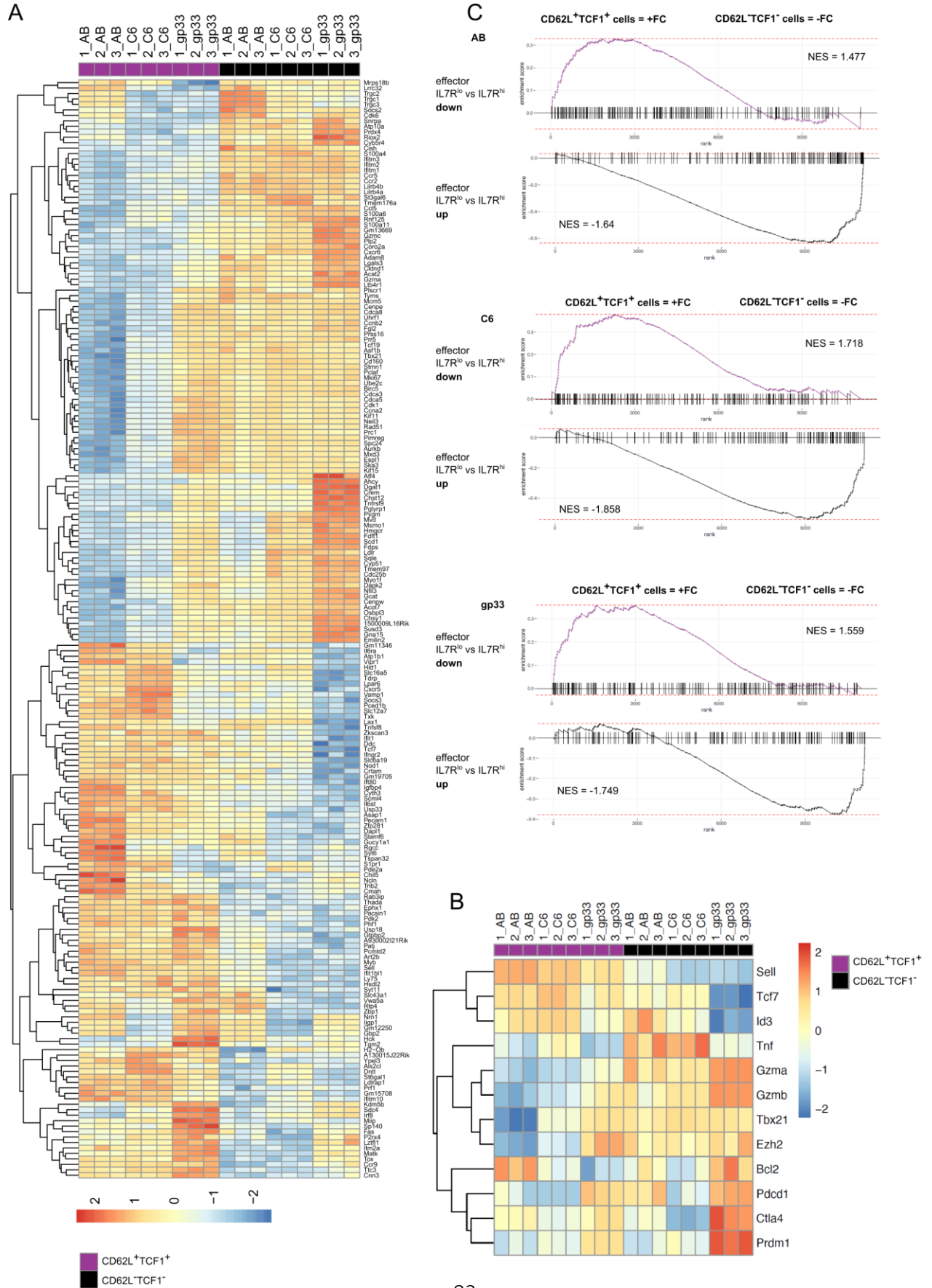
Figure 4.S5: Transcriptional profiling of *in vitro* generated memory and effector precursor cells upon weak and strong TCR stimulation.
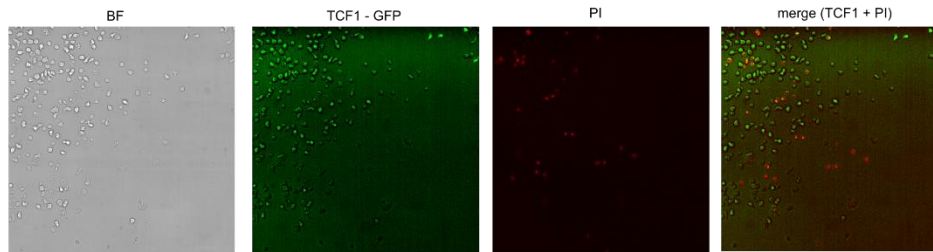
P14 TCF1-GFP cells were activated by plate-bound Fc-ICAM-1, α-CD3 and α-CD28 (AB) or by MutuDC1940 cells, which were stimulated with CpG and either pulsed with gp33 or C6 peptides. P14 cells were cultured in the presence of IL-2 for 30 h before cells were transferred to new wells in medium containing IL-2, IL-7 and IL-15. Cells were cultured for 6 days and CD62L$^+$TCF1$^+$ and CD62L$^-$TCF1$^-$ cells were sorted for RNAseq. 3 biological replicates were used for each condition. **A** Differential expression of genes among CD62L$^+$TCF1$^+$ and CD62L$^-$TCF1$^-$ cells derived from AB, C6 or gp33 activation (top and bottom 50 differentially expressed genes based on the lowest P value) presented as a heatmap. **B** Heatmap of gene expression of selected memory- and effector-specific genes of CD62L$^+$TCF1$^+$ and CD62L$^-$TCF1$^-$ cells derived from AB, C6 or gp33 activation. Individual biological replicates are shown. **C** Gene set enrichment analysis (GSEA) plots and normalized enrichment score (NES) of differential gene expression displayed in Fig. 4.5C using gene sets describing 6/7 days post acute LCMV infection IL7R^{lo} short-lived effector cells (SLECs) and IL7R^{hi} memory precursor effector cells (MPECs), respectively (GSE8678) (Joshi et al., 2007).

A

B

| BF | TCF1 - GFP | PI | merge (TCF1 + PI) |

C

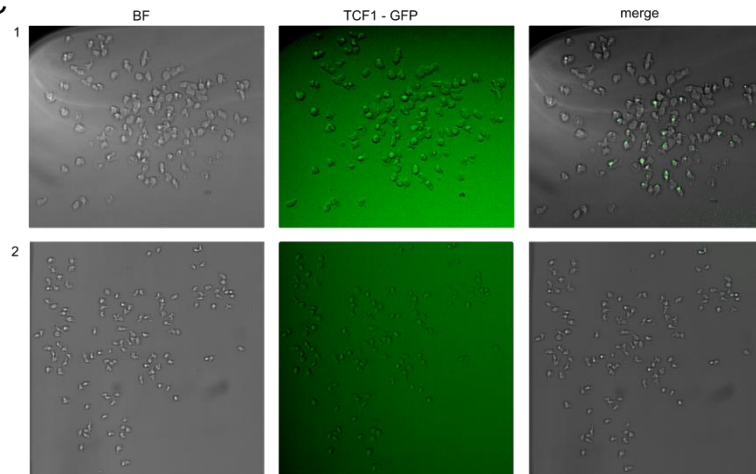| BF | TCF1 - GFP | merge |

1

2

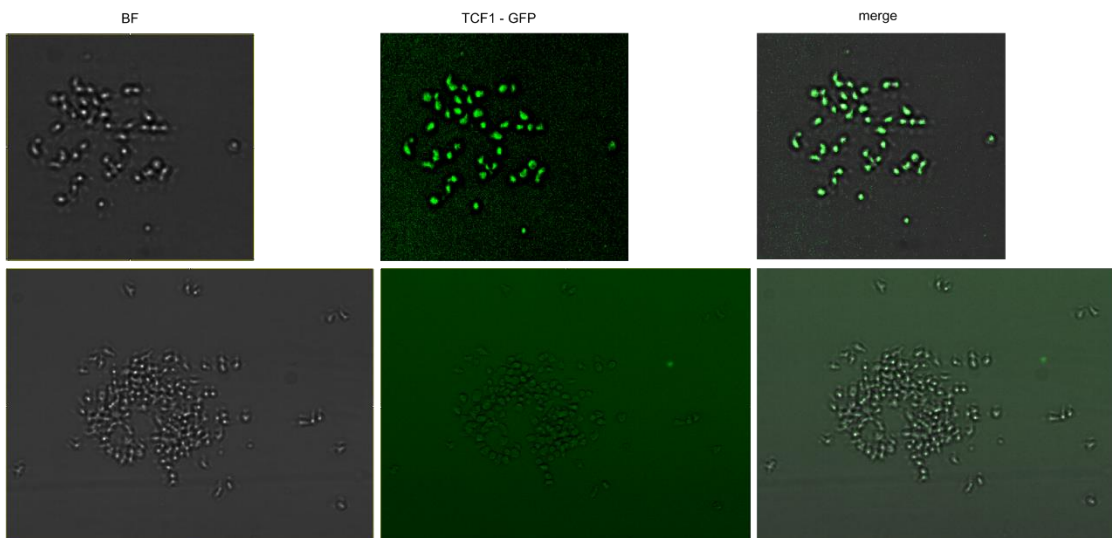D

| BF | TCF1 - GFP | merge |
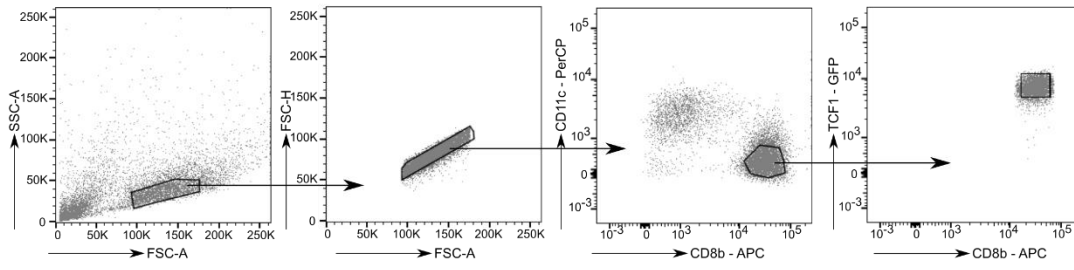
Figure 4.S6: Strong TCR stimulation results in single-cell derived mixed-fate colonies.

A Gating strategy for sorting of blasted P14 CD8 TCF1-GFP cells 24 h after stimulation. **B** Propidium Iodide (PI) staining of colonies on day 5 after initial stimulation. **C** Representative BF and green channel (TCF1-GFP) images of established P14 TCF1-GFP cell colonies stemming from one single mother cell on day 5 post gp33 activation. **D** Representative BF and green channel (TCF1-GFP) images of established P14 TCF1-GFP cell colonies stemming from one single mother cell on day 5 post C6 activation.
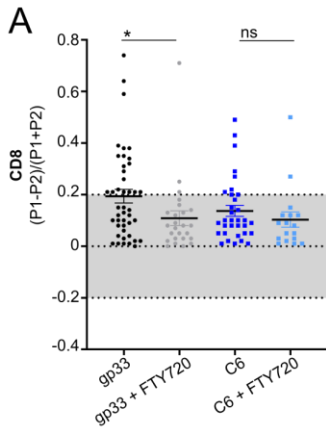

Figure 4.S7: Inhibition of ACD markedly curtails memory precursor formation upon strong TCR stimulation. A ACD rates from P14 cells activated with gp33 or C6 in the presence or absence of 2 μM FTY720. Data are represented as mean ± SEM (gp33, n=44; gp33 + FTY720, n=25; C6, n=33; C6 + FTY720, n=17). Statistical analysis was performed using the unpaired two-tailed Student's *t* test or, when data did not pass the Shapiro-Wilk normality test, the unpaired two-tailed Mann-Whitney test. *$P < 0.05$.
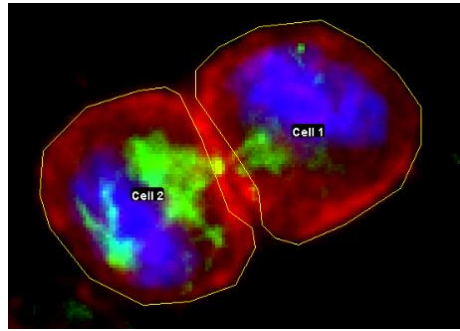
Figure 4.S8. Identification of mitotic cells and determination of regions of interest (ROI).

Mitotic cells were selected based on nuclear (DAPI, blue staining) and β-tubulin (green staining) structures and imaged from late anaphase to telophase when daughter cells could be distinguished. The cell with higher intensities of CD8 (red staining) was defined as P1. The ROI was drawn around each cell excluding the contact area between the two cells. The ACD ratio (P1-P2)/(P1+P2) was calculated. A cell division was considered asymmetric when the CD8 intensity was 50% higher in one daughter cell compared to the other, leading to the threshold of 0.2.

Establishment of a high-resolution single cell analysis of CD8 T cells using Fluidic Force Microscopy (FluidFM)

Fabienne Gräbnitz[1], Orane Guillaume-Gentil[1], Ioana Sandu[1], Julia Vorholt[1] and Annette Oxenius[1]

[1] Institute of Microbiology, ETH Zurich, Vladimir-Prelog-Weg 4, 8093 Zurich, Switzerland

Abstract

CD8 T cell responses comprise heterogeneous populations of activated cells that differ in their phenotype, longevity, function, metabolism and localization. One mechanism that contributes to the generation of cellular diversity is asymmetric cell division (ACD). To date, the precise link between ACD and subsequent asymmetric fate is missing due to technical limitations. Here, we explored two high-resolution *in vitro* live image-based single cell approaches for lineage tracing and kinship analysis of primary CD8 T cells upon activation using fluidic force microscopy (FluidFM). In the first approach, asymmetrically divided sister cells were physically separated after completed mitosis. Isolated cells were cultured and monitored for several days until establishment of a progeny colony was observed. Using confocal microscopy, the fate of cells within the established colony was subsequently determined by using effector and memory specific markers. In the second approach, we examined the feasibility of cytoplasm extraction of individual ACD-derived sister cells followed by scRNAseq. These two approaches allow precise tracing and fate determination of the progeny of ACD-derived sister cells as well as the recording of their transcriptomic profiles directly after completed cell division.

Introduction

Cellular heterogeneity within the CD8 T cell response is fundamental for efficient immunity. Upon acute infection, naïve virus-specific CD8 T cells are activated and initiate transcriptional and metabolic changes allowing for proliferation and differentiation. A remarkable cellular diversification occurring throughout the course of a viral infection has been reported for CD8 T cells (Y. Chen et al., 2018). Besides the generation of effector CD8 T cells (T_E), which are responsible for viral clearance and are short-lived, the generation of different memory subsets has been described that differ in their phenotypic, transcriptomic and metabolic characteristics, specifically effector memory (T_{EM}), central memory (T_{CM}), stem cell memory (T_{SCM}) and tissue-resident memory (T_{RM}) CD8 T cells (Chung et al., 2021). Interestingly, it has been shown that a single naïve CD8 T cell can give rise to effector and memory CD8 T cells upon activation (Buchholz et al., 2013; Gerlach et al., 2013, 2010; Plumlee et al., 2013; Stemberger et al., 2007). However, how this cellular diversification is mechanistically generated remains to be investigated. Different models propose various factors or mechanisms that contribute to the establishment of cellular heterogeneity, including asymmetric cell division (ACD) (Y. Chen et al., 2018; Kaech and Cui, 2012). ACD is characterized by the unequal distribution of effector and memory fate-related molecules leading to two daughter cells that differ in phenotype, metabolism and in the composition of cell organelles and transcription factors (Chang et al., 2011, 2007; Y.-H. Chen et al., 2018; Ciocca et al., 2012; King et al., 2012; Pollizzi et al., 2016; Verbist et al., 2016). While one daughter cell is destined to differentiate into an effector cell, the other daughter cell is endowed with memory features. Previous studies provided evidence that ACD serves as a mechanism for fate-diversification by using bulk sorting of cells either expressing the marker of interest at a high or low level after the first cell division upon activation, followed by subsequent functional analysis (Borsa et al., 2019; Guo et al., 2022; Pollizzi et al., 2016; Verbist et al., 2016). The transcriptional heterogeneity within CD8 T cells that have undergone their first mitosis upon activation further supports early fate divergence, potentially mediated by ACD (Borsa et al., 2019; Kakaradov et al., 2017). However, a direct link between ACD and subsequent asymmetric fate on a single cell level is missing. Therefore, tracing of individual daughter cells after ACD and their future differentiation is necessary. While

current *in vitro* imaging technologies allow tracing of single cell derived colonies as well as the identification of subsequent fate, the precise link to ACD remains elusive, mostly due to the difficulty to monitor the progeny of individual daughter cells long-term (Plambeck et al., 2021). Therefore, we aimed to establish an image-guided single cell manipulation approach based on fluidic force microscopy (FluidFM) (Guillaume-Gentil et al., 2014a; Meister et al., 2009). FluidFM enables live cell microscopy-imaging and single cell micromanipulations with a microfluidic probe, such as cell isolation, cell content extraction and cell organelle transplantation between living cells (Gäbelein et al., 2022; Guillaume-Gentil et al., 2016, 2014b). Further, it has recently been described that repetitive cell content extraction for scRNAseq from the same cell, while preserving its viability, is possible using FluidFM. This elegant approach termed Live-seq transforms scRNAseq from an end-point to a temporal analysis (Chen et al., 2022). Here, we adapted the FluidFM-based isolation approach to primary CD8 T cells and established a colony formation assay for isolated daughter cells. In addition, we assessed the feasibility of performing Live-seq on primary CD8 T cells. Specifically, within this study, we performed time-lapse imaging of ACDs and physically separated the two emerging daughter cells into individual microwells, followed by a colony formation assay in order to determine the fate of the progeny cells. Furthermore, we defined optimal conditions for cytoplasm extraction followed by scRNAseq. These two approaches allow high-resolution analyses of asymmetrically divided daughter cells during their individual future fate diversification as well as analysis of their potentially different transcriptomic profiles directly after mitosis.

Results

Image-based selection and isolation of divided sister CD8 T cells followed by colony formation assay and fate determination

Considering the current technical challenges in the field of asymmetric T cell division research in precisely tracking the progeny of divided sister cells and follow their fate, we set out to develop a high-resolution colony formation assay of isolated sister cells after cell division using the FluidFM technology. Therefore, we activated TCR transgenic CD8 T cells (P14 cells), which recognize the LCMV GP-derived epitope gp_{33-41} / H-2D^b (gp33) by gp33-loaded dendritic cells (DCs) for 24h. The P14 cells expressed in addition a TCF1-GFP reporter (P14 TCF1-GFP). Thereafter, we separated the P14 TCF1-GFP cells from the DCs by FACS sorting of single, undivided and blasted CD8 T cells. Sorted cells were seeded onto a cover glass, glued into a μ-Dish pre-coated with α-CD44 and α-CD43 antibodies to provide adhesion. While isolation of divided CD8 T cells directly from the DC-T cell co-culture proved feasible, sorting the undivided blasted T cells and thereby removing the DCs facilitated enhanced precision-monitoring of the divisions and limited the contamination of colony wells by DCs. Similarly, seeding the cells on a coverslip allowed for removing the cell culture after the isolations and therefore limited contamination of the forming colonies in the microwells. We recorded cell divisions during the following 3-5h with 80× magnification and determined asymmetry based on CD8 surface distribution, which has been used as a reliable proxy to measure ACD in numerous studies (Borsa et al., 2021, 2019; Chang et al., 2007; Pollizzi et al., 2016). Cell divisions were defined as asymmetric when the CD8 signal was 1.5-fold greater in one daughter cell compared to the other. After completed first cell division, we physically separated the two daughter cells by picking up each cell individually and transporting it into a microwell for subsequent individual colony formation for 4 days (Fig. 5.1A-B, Movie 5.1). We monitored colony formation every 1 to 2 days until day 5 after initial stimulation. Our established protocol maintained viability and proliferation potential of the cells, resulting in the establishment of a progeny colony (Fig. 5.1C). In order to characterize the adopted fate of individual cells within the established population, we analyzed expression of TCF1 and CD62L by confocal imaging (Fig. 5.1D). While

93

expression of TCF1 and CD62L identifies memory precursor cells, the absence of these markers characterizes effector precursor cells. The majority of cells within the emerging colony downregulated TCF1 over time, however in some colonies, few cells maintained TCF1 expression (Fig. 5.1E). So far, we isolated 2 daughter cells from symmetric and 2 daughter cells from asymmetric cell divisions in order to have a direct comparison of later fate divergence resulting from either SCD or ACD progeny. Interestingly, both CD8^{hi} sister cells, which derived from an ACD died during the manipulation process, either during transportation or shortly after deposition into the microwell. The CD8^{lo} sister cell, instead, could be successfully isolated and subsequently formed a colony. Whether the observation that the CD8^{hi} daughter cell dies after mitosis is a real biological characteristic of ACD, needs to be further validated. Of note, although we could successfully isolate 1 of the 2 symmetrically divided sister cells each, the other sister cell survived, however, unfortunately was lost during the transportation process and could therefore not be further monitored. The formed colonies comprised either cells of both, effector (CD62L$^-$TCF1$^-$) and memory (CD62L$^+$TCF1$^+$) precursor cells or only effector precursor cells. However, these preliminary findings remain to be validated in further experimental repetitions and it remains to be shown whether the offspring of ACD-derived daughter cells indeed establish colonies of differential fates. Taken together, we established a high-resolution image-based approach allowing the physical separation of asymmetrically divided sister cells upon completed mitosis and further individual colony formation with subsequent fate determination of the established offspring population.
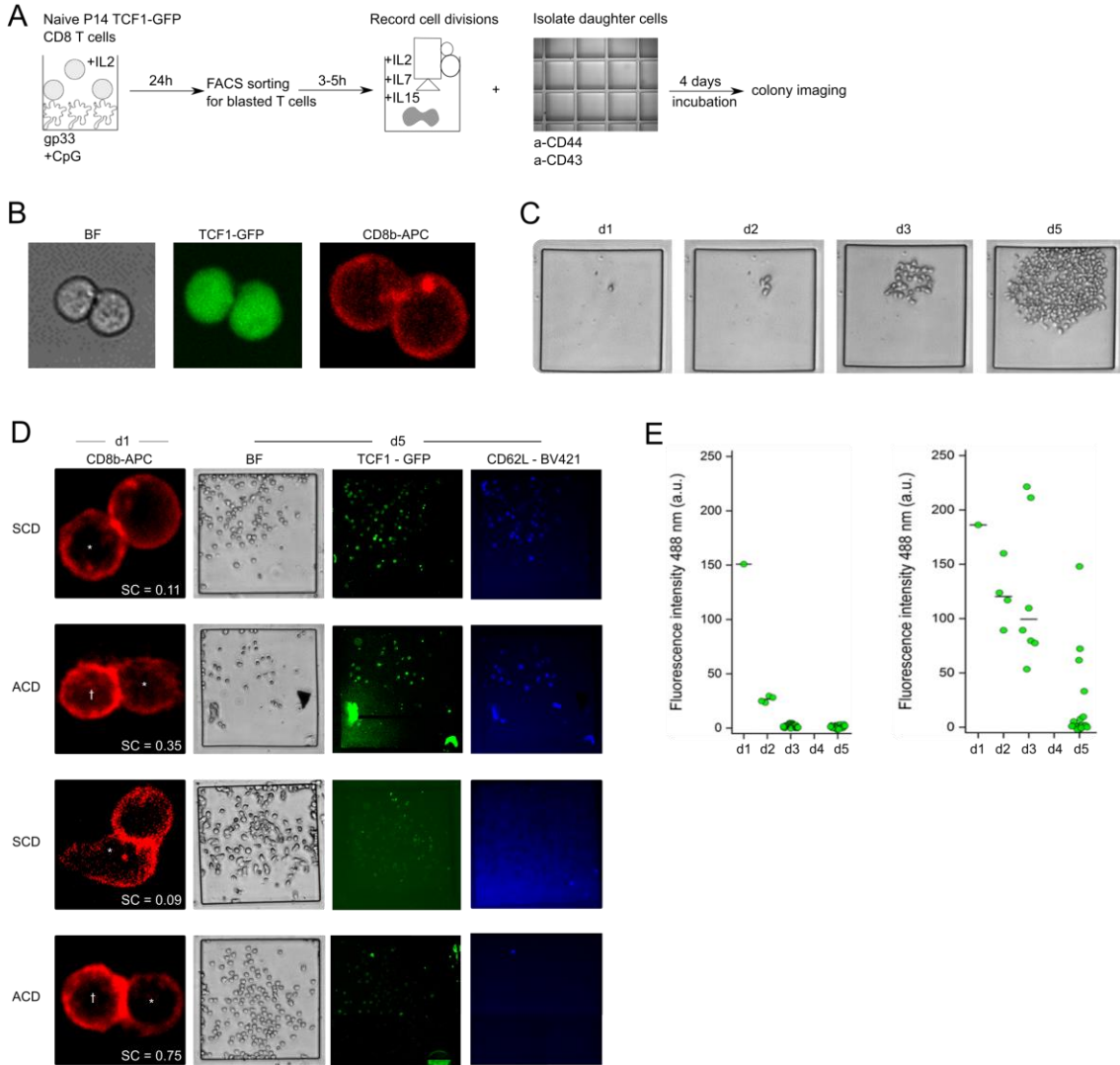
Figure 5.1: Isolation of divided sister CD8 T cells followed by colony formation assay.

A Experimental setup. MutuDC1940 dendritic cells were stimulated with CpG and pulsed with gp33 peptide before P14 TCF1-GFP cells were added. P14 cells were activated in the presence of IL-2 for 24h before blasted single cells were sorted. Sorted cells were seeded onto an α-CD44 and α-CD43 antibody coated cover glass in a culture dish containing medium supplemented with IL-2, IL-7 and IL-15. Cell divisions were imaged and daughter cells were individually picked up and transferred into microwells using FluidFM. Cells were separately cultured and colony formation was monitored every 1-2 days. **B** Representative images of P14 TCF1-GFP cells in BF, GFP (TCF1) and red channel (CD8b-APC) recorded directly after cell division was completed. **C** Representative BF-images of a forming colony stemming from a single isolated daughter cell after cell division. **D** Representative images of asymmetrically (ACD) and symmetrically (SCD) (based on

CD8b-APC signal) divided P14 TCF1-GFP cells on day 1 post activation prior to physical separation and their resulting formed colonies on day 5 post activation. Colonies are depicted in BF, green channel (TCF1-GFP) and blue channel (CD62L-BV421). * indicates the isolated cell. † indicates death of the cell. **E** Two representative graphs showing TCF1-GFP intensities of individual cells measured at 488nm over time.

Cytoplasmic extraction of single CD8 T cells after cell division followed by scRNAseq

Although previous studies reported remarkable differences in the transcriptional profiles of cells that have undergone one cell division after activation, the direct link of whether these cells are indeed stemming from an ACD is missing (Borsa et al., 2019; Kakaradov et al., 2017). In order to close this gap, we aimed to establish an experimental system, which enables the combination of imaging data and transcriptomic data for a detailed analysis of ACD on a transcriptional level. Therefore, we established a protocol for single cell (sc) RNA sequencing of asymmetrically divided sister cells. We stimulated P14 cells as described in Figure 5.1A before we started time-lapse imaging of cell divisions and determination of asymmetry based on CD8 surface distribution. After completed cell division, the entire cytoplasmic content of each CD8 daughter cell was individually extracted using the FluidFM probe preloaded with sampling buffer in order to directly mix the cytoplasm with RNase inhibitors (Fig. 5.2A). Next, the cytoplasmic extract collected in the probe was released into a microliter of RNAseq lysis buffer droplet (Fig. 5.2B). The droplet was then manually pipetted into a PCR tube for downstream sample processing using a scRNA-seq protocol, which was specifically developed for low input material obtained by FluidFM (Chen et al., 2022). While cytoplasmic extraction with FluidFM was never previously performed on non-adherent cells, we successfully collected cytoplasmic biopsies from 5 individual CD8 T cells. For 2 out of 5 extracts, cDNA was successfully generated, yielding a concentration of 0.7 and 1.2 ng/uL, which corresponds to 40% efficiency, similar to the Live-seq efficiency reported for other cell types (Fig. 5.2C) (Chen et al., 2022). The two libraries were further sequenced and 1478 and 2576 expressed unique genes were detected, while no mitochondrial genes were identified, suggesting an acceptable quality of the data (Fig. 5.2D). As expected, the detected expressed genes (at least in 1 cell) included well-

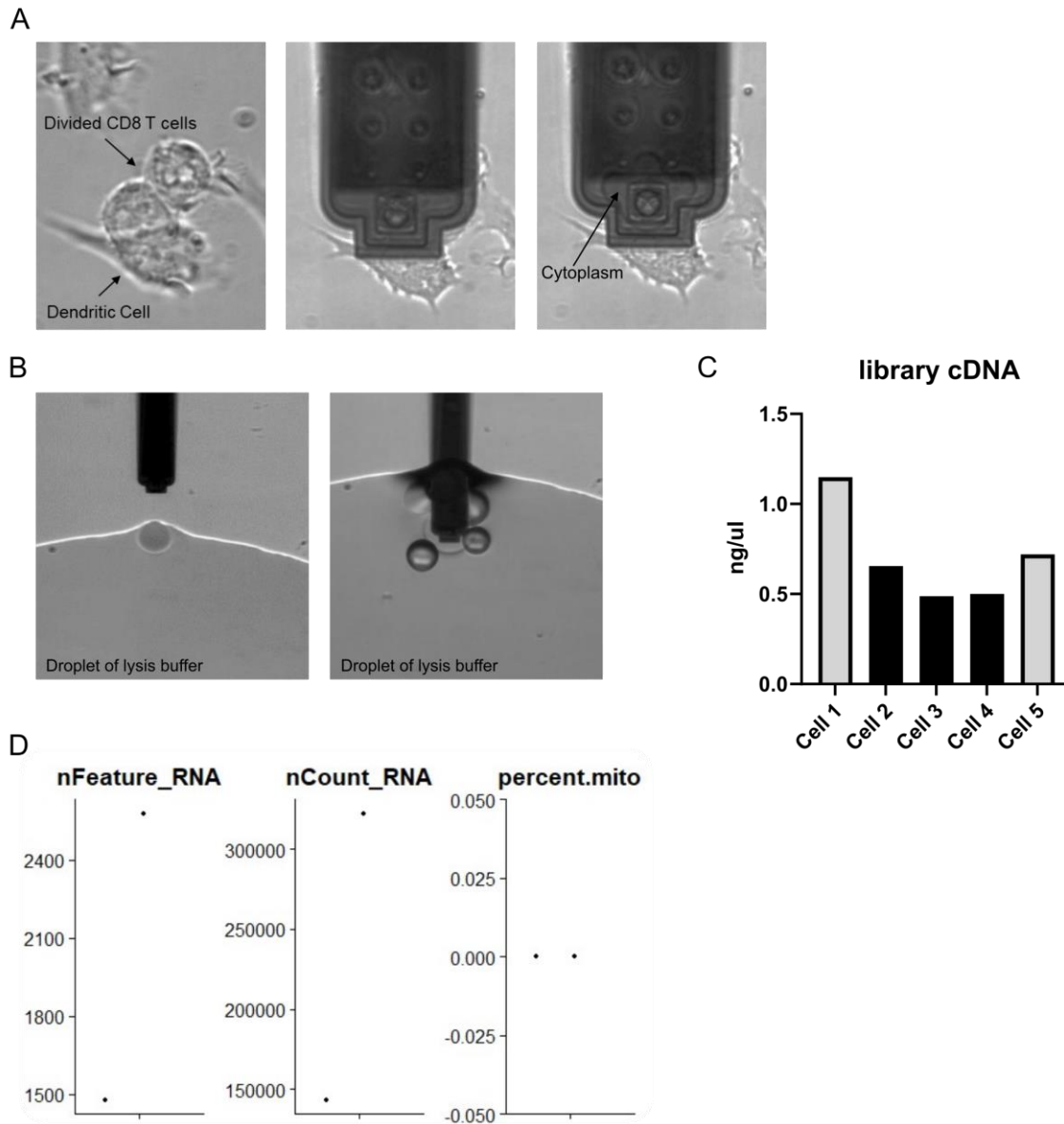known CD8 T cell genes such as CD8α, IL2Rγ, CD69, Tbx21, Gzmb, Id2, IL7R and Hif1α (data not shown).

Figure 5.2. Cytoplasmic extraction of single CD8 T cells after cell division followed by scRNAseq.

A Divided target CD8 T cells were still attached to the dendritic cell. The FluidFM probe was preloaded with sample buffer containing RNase inhibitors before the entire CD8 T cell cytoplasm was extracted. **B** The loaded probe was moved to a microliter of RNAseq lysis buffer droplet and the cytoplasmic fluid was released. **C** cDNA concentration of 5 extracted cells after cDNA library preparation. **D** Cell 1 and cell 5 were sequenced. Plots show detected genes and reads as well as detected mitochondrial genes.

Discussion

The increasing knowledge about the cellular heterogeneity between different cell types and cell subsets emphasizes the need to investigate cellular function, phenotype and plasticity at the single cell level. In order to study kinship and track differentiation, fate mapping- and lineage tracing approaches are essential. In the present study, we established a high-resolution image-based single cell analysis approach for primary CD8 T cells using Fluidic Force Microscopy (FluidFM) (Guillaume-Gentil et al., 2014a; Meister et al., 2009). While there are existing high-throughput live imaging approaches for CD8 T cells, the here established experimental procedure allows for more precise and detailed analysis at higher resolution (Plambeck et al., 2021). Using confocal and time-lapse microscopy, we show that upon completed cell division, asymmetrically divided CD8 sister cells can be successfully separated and isolated into microwells, while cell viability and subsequent proliferation is maintained. Repetitive imaging of the single cell culture over time allows accurate recording of colony formation and using fluorescence confocal imaging enables the determination of the adopted fate of the progeny cells. Thus, this approach allows the precise analysis of offspring cells derived from asymmetrically divided sister cells and thereby excludes potential mixing of cells, which might occur in culture conditions in which divided cells are not physically separated from each other. Several studies addressed the mechanistic role of ACD on fate diversification by bulk sorting of cells based on the expression of fate related molecules at a low or high level, followed by subsequent functional analysis (Borsa et al., 2019; Guo et al., 2022; Pollizzi et al., 2016; Verbist et al., 2016). However, this approach lacks the information whether the investigated cells are indeed stemming from an ACD. The established single cell isolation approach for CD8 T cells described within this study would allow for the separated collection of monoclonal and proven ACD-derived CD8^{hi} and CD8^{lo} (or other molecules) daughter cells that are specific for a given antigen. These cells could subsequently be transferred into recipient mice followed by challenge with their cognate antigen and their fate adoption could be analyzed *in vivo*. Another aspect of current research on CD8 T cell ACD that might be improved are the thresholds used for calling a cell division asymmetric. These thresholds are mostly arbitrary and randomly set to a certain value. Our presented approach would allow for a reasonable and functional data-based determination of

an ACD, by defining an ACD threshold that leads to asymmetric fates. Moreover, similar to a recent study combining single cell tracking with transcriptional profiling in HSCs (Wehling et al., 2022), our established protocol for extracting cytoplasm of asymmetrically divided CD8 sister T cells would provide new insights into potential transcriptional differences between daughter cells that emerge from an ACD, which might provide new findings on ACD in CD8 T cells. So far, a major limitation of scRNA sequencing is that it is an end-point analysis, as the cells have to be lysed before the sequencing protocol can be initiated. It has recently been reported that FluidFM can be used for a new application termed Live-seq (Chen et al., 2022). Herewith, cellular cytoplasm can be repetitively extracted from the same cell and submitted to scRNA sequencing while keeping the cell alive. This technology allows for the analysis of transcriptomic changes in the same cell over time and in response to different stimuli. However, whether this method is applicable for primary CD8 T cells remains to be shown. The repetitive transcriptional analysis of the same CD8 T cell during its differentiation process would open remarkable insights into the kinetics of fate choice, which are intensively studied in current research. Specifically, in the field of ACD, it would be a ground-breaking technology in order to unravel how already described unequal segregation of certain molecules, such as transcription factors, further translate into the transcriptomic profiles of the sister cells over time and finally lead to different functional phenotypes. The ongoing improvements of *in vitro* technologies providing the tools for investigating the functional, transcriptomic and phenotypic changes of single cells over time allow for a remarkable amount of new discoveries. However, a general limitation of *in vitro* studies is the artificial environment in which the cells of interest are cultured. It is well described that the tissue, in which the cells are physiologically residing in, has a large impact on cellular behavior as it provides various inputs such as cytokine signaling or interactions with surrounding other cell types that impact the current and future state of the cell (Joshi et al., 2007; Plumlee et al., 2013). Although *in vitro* experimental approaches are able to partially compensate for this, for instance by adding certain cytokines, the establishment of precise single cell imaging approaches that allow single cell tracking and manipulations *in vivo* remains to be developed.

Material and Methods

FluidFM setup

The FluidFM system composed of a FlexAFM-NIR scan head and a C3000 controller driven by the EasyScan2 software (Nanosurf), and a digital pressure controller unit (ranging from -800 to + 1000 mbar) operated by a digital controller software (Cytosurge) was used. FluidFM micropipettes with a circular aperture of 4 μm in diameter (Cytosurge) were used for single cell isolation. For cytoplasmic extraction, we used FluidFM Rapid Prototyping probes with a microchannel height of 800 nm and a pyramidal tip (Cytosurge). A 400 nm wide triangular aperture was custom-milled by a focused ion beam near the apex of the pyramidal tips and imaged by scanning electron microscopy as previously described (Guillaume-Gentil et al., 2016). The FluidFM micropipettes for isolation were coated with the anti-fouling polymer PLL(20)-g[3.5]- PEG(2) (SuSoS, surface technology) at 80°C for 60 min. The probes for extraction were coated with Sigmacote as previously described (Guillaume-Gentil et al., 2016). The FluidFM scan head was mounted on an inverted AxioObserver microscope equipped with a temperature-controlled incubation chamber (Zeiss) and coupled to a spinning disc confocal microscope (Visitron) with a Yokogawa CSU-W1 confocal unit and an EMCCD camera system (Andor).

CD8 T cell preparation

Splenic and lymph node naïve P14 TCF1-GFP cells were activated on CpG-activated and gp33-loaded dendritic cells (MutuDC1940) for 24h. For single cell isolations, 10 000 - 15 000 activated and undivided P14 TCF1-GFP cells were sorted and seeded in complete imaging T cell medium containing self-made IL-2, 10 ng/ml IL-7 and 5 ng/ml IL-15 onto a cover glass glued into a 50 mm culture μ-Dish (Ibidi). For cytoplasm extractions, the DC-T cell co-culture, was directly cultured on

the cover glass. The cover glass was pre-coated with 5 µg/ml α-CD43 (eBioR2/60, Invitrogen) and α-CD44 (IRAWB14). In order to trace dividing cells, time-lapse imaging in BF was initiated and as soon as a cell division was completed, a Z-Stack image was taken of the CD8b-APC signal for asymmetry measurement of the daughter cells.

Cell isolation by FluidFM and colony formation assay

In close proximity to the cover glass presenting the CD8 T cells, 250 µm microwells (Microsurfaces) pre-coated with 5 µg/ml α-CD43 (eBioR2/60, Invitrogen) and α-CD44 (IRAWB14) (Loeffler et al., 2018) were placed. Target cells were picked up by the FluidFM probe by approaching the cell with a force of 20 nN, applying -100 mbar of under-pressure and then lifting up the probe with the immobilized cell. During subsequent transport of the cell to the microwell, the under-pressure was released. The probe was then approached to the wall of the microwell with a force of 100 nM and an overpressure of 1000 mbar was applied to efficiently release the cell into the microwell. Once cell isolation was finished, the cover glass was removed from the culture dish and cells were incubated at 37°C and 5% CO_2 until formed colonies were imaged. Phase-contrast and fluorescence images were acquired using 10×, 20× and 40× (0.6 na) objectives and a 2× lens switcher using VisiView software (Visitron). Microscopy images were analyzed using the ImageJ softwares.

Cytoplasmic extraction of divided CD8 T cells by FluidFM and scRNAseq

The FluidFM probe was preloaded with 0.5 pl sample buffer containing RNase inhibitors (Chen et al., 2022). The target cell was visualized by light microscopy and the tip of the FluidFM probe was inserted into the cytoplasm by a forward force spectroscopy routine driven by the Z-piezo with a force setpoint of 100 nN. The probe was kept inside the cell at constant force and under-pressure

of 600 mbar was applied to aspirate the CD8 T cell cytoplasm into the probe. Next, the probe was inserted into 1 µl drop of lysis buffer and by applying overpressure, the cytoplasmic fluid was released into the droplet. The microchannel of the probe was rinsed three times by suction and release of the lysis buffer before the droplet was manually pipetted into a PCR tube containing 3.2 µl of the same lysis buffer. The solution was spun down and stored at -80°C until further processing. The enhanced Smart-seq2 protocol was applied for sample processing for single cell RNAseq (Chen et al., 2022).

General discussion

Asymmetric Cell Division - A safeguard mechanism for the generation of memory?

Asymmetric cell division - an evolutionary conserved mechanism

The generation of cellular diversity is a basic requirement for the development of multicellular organisms. Cellular diversification can be induced by asymmetric cell division (ACD), during which the two daughter cells emerging after a mitosis unequally distribute lineage specific cargo (including transcription factors, receptors for specific signaling inputs, metabolic platforms and possibly different epigenetic landscapes), resulting in two daughter cells endowed with different fates. ACD was first discovered in early ascidian embryos in 1905 by Edwin Conklin who observed that yellow cytoplasm localizes asymmetrically in order to drive muscle cell fate and ever since the knowledge and interest in ACD increased constantly (Conklin, 1905). Asymmetric partitioning of RNA for Actin isoforms - also reported in early ascidian embryos for the first time by using *in situ* hybridization - was consequently confirmed by several studies using more advanced technologies such as fluorescence *in situ* hybridization (FISH) or the combination of cell fractionation with RNA sequencing (Benoit Bouvrette et al., 2018; Jeffery et al., 1983; Lécuyer et al., 2007). Polarized distribution of cellular components by ACD was further characterized in Drosophila melanogaster by differential segregation of the cell fate determinant Numb during CNS development in 1994 (Rhyu et al., 1994; Spana et al., 1995). Moreover, other studies were conducted in Caenorhabditis elegans, which demonstrated asymmetric partitioning of polarization inducing PAR proteins (Boyd et al., 1996; Etemad-Moghadam et al., 1995; Guo and Kemphues, 1995; Hung and Kemphues, 1999). Furthermore, ACD has been described to occur in prokaryotic as well as eukaryotic unicellular organisms including bacteria and yeast (Ackermann et al., 2003; McFaline-Figueroa et al., 2011; Radhakrishnan et al., 2008; Stewart et al., 2005). Upon ACD in budding yeast, the mother cell continues ageing while the daughter bud retains the full lifespan independently of the age of the mother cell, at least until the last few mother cell divisions (Jazwinski, 1990; Kennedy et al.,

1994). The eukaryotic organism yeast has been instrumental to advance our knowledge of ACD in fate determination and how this knowledge can be extended to other mammalian cells.

Asymmetric cell division in mammalian stem cells - the instructor of cell fate

Besides occurring in invertebrates and unicellular organisms, ACD has been shown to serve as a mechanism for cell diversification in mammalian cell subsets, especially in cell subsets that are linked to stemness such as hematopoietic stem cells (HSCs), embryonic stem cells (ESCs), mammary stem cells (MSCs) and neural stem cells (NSCs) (Chhabra and Booth, 2021; Fuentealba et al., 2008; Loeffler and Schroeder, 2021; Moore and Jessberger, 2017).

ACD in HSCs leads to a self-renewing daughter cell maintaining stemness features while the other daughter cell is enabled to differentiate into one of all blood lineages (Sunchu and Cabernard, 2020). Unequal partitioning of the cellular degradation machinery, specifically lysosomes, autophagosomes and mitophagosomes, together with Numb have been observed to destine the daughter cell that inherits less of these components to differentiate into cells with less stem cell potential (Loeffler et al., 2019).

Similar to the findings of ACD in yeast, asymmetric cell division in murine NSCs has been shown to unequally segregate senescence factors, such as damaged proteins, between the two emerging daughter cells maintaining the self-renewing stem cell free from damage, while the other sibling is destined to differentiate into neurons, astrocytes or oligodendrocytes (Moore et al., 2015; Moore and Jessberger, 2017).

Thus, multiple studies provide evidence for ACD as a mechanism in stem cells driving lineage choice and cell specialization in one daughter cell, while ensuring self-renewing potential of the other daughter cell. However, ACD has also been reported for cells that have already differentiated into a certain cell type, such as B cells and T cells in the hematopoietic system. For instance, although T cells have undergone already some level of differentiation during their development in the

thymus, they can still be viewed as "stem cells" as their progeny can adopt different cell fates upon T cell receptor (TCR) mediated activation.

Studies on ACD in these partially differentiated subsets lend support to the hypothesis that also here, ACD might be involved in further fate diversification (Alampi et al., 2022; Borsa et al., 2021, 2019; Chang et al., 2011, 2007; Nish et al., 2016; Pollizzi et al., 2016; Thaunat et al., 2012; Verbist et al., 2016). However, precise evidence on the single cell level is missing. Furthermore, there is also work describing segregation of cellular identity in these subsets that is mediated by other factors than ACD, such as the overall TCR signal strength, including affinity of the TCR towards the peptide MHC complex, extent of co-stimulation and exposure to inflammatory signals (Chin et al., 2022; King et al., 2012; Knudson et al., 2013; Marchingo et al., 2016, 2014; Solouki et al., 2020; Zehn et al., 2009).

Although certain differentiated cell subsets, such as naïve and memory CD8 T cells, retain the ability to give rise to heterogeneous progeny upon stimulation, the precise role of ACD serving as a mechanism for the generation of cellular diversity is not completely proven and therefore still a matter of current research.

Asymmetric cell division in differentiated cells - different perspectives on ACD's role

Besides occurring in stem cells, ACD is described to happen in cell subsets, which have already undergone a lineage choice earlier during their development, such as T cells and B cells. Fate-related transcription factors, cell organelles and surface receptors were found to partition unequally between emerging daughter cells during an ACD, leading to two cells that are differentially equipped and fate-imprinted for their individual future differentiation. Leishmania-specific CD4 T cells, which were activated with L. major were found to unequally segregate LFA-1, CD4 and the receptor for interferon-γ (IFNγR), suggesting an instructive role of ACD for divergence into the different CD4 T helper subsets (Chang et al., 2011, 2007).

Similarly, asymmetric inheritance of CD8, LFA-1, IFNγR, CD25 as well as the transcription factor T-bet and metabolism instructing factors, such as c-myc, were observed for CD8 T cells, leading to one daughter cell being destined for an effector fate, while the other daughter cell is endowed with memory cell features (Chang et al., 2011, 2007; Ciocca et al., 2012; Verbist et al., 2016). The surface receptor CD8 has been identified as a reliable readout for asymmetry and thus been used as a proxy to measure ACD in numerous studies (Borsa et al., 2021, 2019; Chang et al., 2007; Pollizzi et al., 2016).

Strong evidence for a specific role of first mitosis ACD in future fate diversification has been found for CD8 T cells by different research groups. However, in these studies, the correlation of first mitosis asymmetry with later fate outcome is based on using bulk sorting of cells either expressing the marker of interest at a high or low level after the first cell division upon activation, followed by downstream analysis (Borsa et al., 2019; Guo et al., 2022; Pollizzi et al., 2016; Verbist et al., 2016). Therefore, this approach lacks the precise history and information of whether the investigated cells indeed emerged from an asymmetric cell division and points out the need for single cell lineage tracing experiments.

Another important decisive contributor of CD8 T cell differentiation is the affinity of the T cell receptor (TCR) towards its specific antigen. While strong TCR stimulation leads to elevated ACD rates, it simultaneously induces preferential effector differentiation compared to weak TCR stimulation (King et al., 2012). The latter instead induces higher frequencies of memory precursor cells and lower ACD rates (Chin et al., 2022; King et al., 2012; Smith-Garvin et al., 2010; Solouki et al., 2020). However, the reason for elevated ACD rates upon strong TCR stimulation combined with preferential effector differentiation is not completely understood so far.

Therefore, in order to address these questions and close the gap between first mitosis ACD and later fate outcome, we used image-based live single cell approaches to unravel the interplay between ACD and TCR signal strength as well as the role of ACD in fate diversification upon different activation conditions. In line with previous findings, we observed that high affinity ligand-induced activation of the TCR leads to elevated ACD rates during the first mitosis upon activation and increased effector differentiation, compared to weak TCR stimulation. Strikingly, we found that only single cells, which were activated by strong TCR stimulation and underwent an ACD,

established "mixed-fate" colonies consisting of memory (CD62L$^+$TCF1$^+$) and effector (CD62L$^-$TCF1$^-$) precursor cells. Additionally, impairing ACD by inhibition of PKCζ prevented memory formation upon strong TCR stimulation. In contrast, single cells upon weak TCR stimulation formed "single-fate" colonies, comprising either effector or memory precursor cells, independent of the asymmetry degree of the first cell division upon activation and inhibition of ACD did not impact memory formation. These findings allow the conclusion that ACD serves as a safeguard mechanism for the establishment of a robust memory CD8 T cell pool specifically upon strong TCR stimulation, in which cells are destined to preferentially differentiate into effector cells at the expense of memory formation (Figure 6.1).
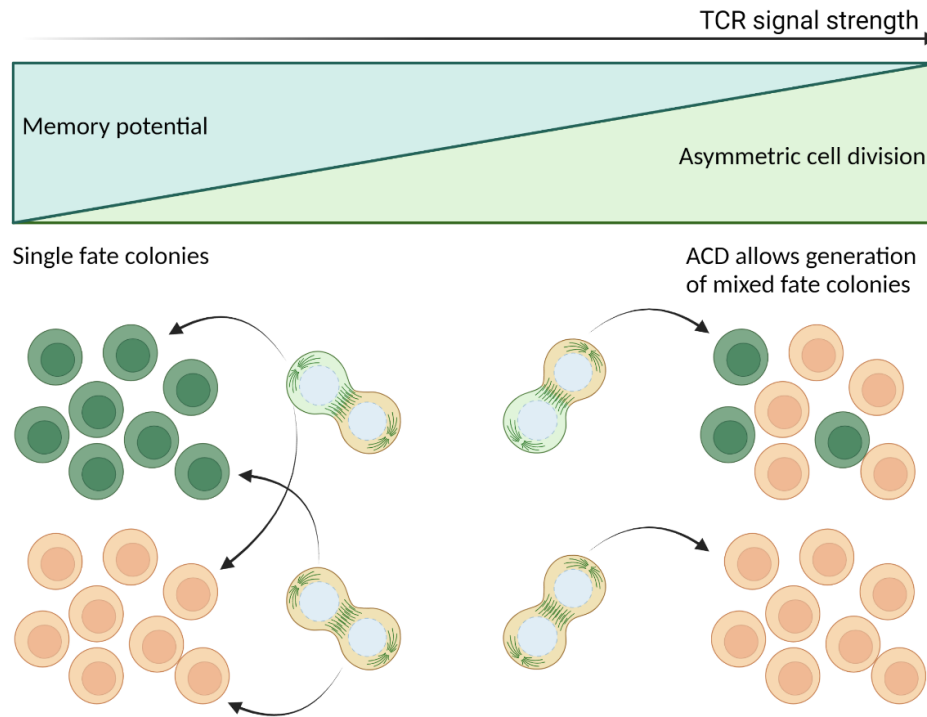
Figure 6.1. ACD functions as a safeguard mechanism for CD8 T cell memory formation specifically upon strong TCR stimulation.

Orange indicates suggested effector fate, green indicates suggested memory fate. Single cells give rise to single fate colonies (either comprising effector or memory precursor cells) upon weak TCR stimulation, independent of the initial asymmetry/symmetry of their first mitosis. In contrast, ACD-derived single cells activated by strong TCR stimulation give rise to mixed fate colonies.

We next set out to investigate whether fate-related implications of ACD are restricted to the first mitosis upon activation. Most of the studies addressing ACD in CD8 T cells analyzed differential segregation of specific molecules during the first mitosis (Chang et al., 2011, 2007; Y.-H. Chen et al., 2018; Ciocca et al., 2012; King et al., 2012; Pollizzi et al., 2016; Verbist et al., 2016). However, asymmetric segregation of the transcription factors IRF4 and TCF1 was described to occur only in later cell divisions (Lin et al., 2015). Transient prevention of ACD during the first mitosis after strong TCR stimulation by inhibition of PKCζ strongly curtailed memory formation upon subsequent *in vivo* cell transfer and LCMV challenge. This observation was specific for impairing ACD during the first

cell division after activation as prolonged prevention of ACD by persistent PKCζ inhibition did not lead to a further decrease in memory formation. In contrast, neither transient nor persistent inhibition of ACD upon weak TCR stimulation did affect memory potential, emphasizing a specific role for ACD upon high affinity interaction in inducing fate diversification.

These observations lead to the conclusion that asymmetric segregation of fate-related markers during the first mitosis upon strong TCR stimulation in CD8 T cells is crucial for the generation of a functional CD8 memory T cell pool.

It remains to be elucidated whether the quality of ACD-dependent memory T cell clones emerging after high affinity stimulation is comparable or superior to those of low affinity memory T cell clones with regard to giving rise to potent cytotoxic effector T cell clones and generating secondary long-lived memory T cell clones. If so, it could be assumed that besides generally rescuing the generation of memory cells in strong stimulation conditions, ACD might function as a selection mechanism for qualitatively superior cells that are equipped with survival factors and stemness features, allowing them to respond in an optimal manner during recall responses.

Asymmetric cell division in differentiated cells - a safeguard mechanism for the generation of robust and long-lived memory cells?

While there is strong evidence for a specific role of ACD in fate diversification in cell subsets that retain stemness, another perspective about the role of ACD is a potential involvement in the generation of a robust population of daughter cells that is equipped with enhanced survival features. One study performed in B cells lends support to this hypothesis. Barnett and colleagues describe ACD during the germinal centre (GC) reaction, where refinement of antibody responses takes place and high affinity B cell clones are selected to proliferate and differentiate into antibody-secreting plasma cells and memory B cells (MacLennan, 1994; Nutt and Tarlinton, 2011). They find that Bcl6, the IL12R and PKCζ are selectively distributed to one high affinity daughter cell suggesting that ACD in this scenario serves as a mechanism to ensure lifelong fitness of a self-renewing high affinity B cell (Barnett et al., 2012). While ACD in B cells does not seem to be linked with the

establishment of fate divergence between memory B cells and plasma cells, ACD might therefore rather play a role in equipping one daughter B cell with survival and self-renewing features (Duffy et al., 2012; Hawkins et al., 2013). Accordingly, we found that ACD functions as a safeguard mechanism for the establishment of a robust memory CD8 T cell pool specifically upon strong TCR stimulation mediated by high affinity TCR-peptide/MHC interactions. Thus, ACD might, in addition, possibly serve as a mechanism for the generation of high-quality memory T cells upon specific stimulation conditions.

Interestingly, analysis of the potential of CD8 T cells in different differentiation states to undergo ACD, which were generated either by acute or chronic infection, revealed remarkable differences between those differentiation states. While memory CD8 T cells performed ACD to a similar extent compared to naïve CD8 T cells, terminally differentiated effector and exhausted CD8 T cells were drastically impaired in their ability to undergo ACD (Borsa et al., 2019; Ciocca et al., 2012). As naïve and memory CD8 T cells are both able to give rise to diverse progeny upon activation, this finding raises the idea of different layers of stemness, which are related to the level of cellular differentiation. Furthermore, ageing has been shown to diminish the ability of CD8 T cells, HSCs and NSCs to undergo asymmetric cell division, adding another contributor to the loss of stemness potential (Borsa et al., 2021; Florian et al., 2018; Moore et al., 2015). In summary, these findings suggest that the ability of cells to perform ACD inversely correlates with increasing age and terminal differentiation.

Taken together, we propose a model in which ACD exerts different functions depending on the state of the cell and stimulation signal strength. The state of the cell is influenced by age, differentiation history and stemness potential. With advanced ageing and differentiation as well as decreased stemness potential, the ability of cells to undergo ACD is gradually diminished. The current state of research shows that stem cells perform ACD to drive one daughter cell into a specific lineage allowing specialization whereas the other daughter cell retains the self-renewing and stemness potential. This cellular state is called state 1. State 2 would comprise cells with a defined history of differentiation, implying a certain age and loss of stemness potential to a specific degree. GC B cells, naïve T cells (T_N) and memory T cells (T_M) would fall into this category. While activation of GC B cells, T_N and T_M by their specific antigens results in diversification of their

progeny, ACD might be particularly required in situations where it is of utmost importance to ensure a robust long-lived daughter cell. This would be the case for strong TCR stimulation conditions for instance, in which high affinity T cell clones preferentially differentiate into effector cells at the expense of memory cells. Here, ACD safeguards the general establishment of memory cells, while possibly at the same time leading to the generation of high affinity memory T cell clones with enhanced survival and self-renewing features potentially giving rise to effector cells with enhanced effector functions during recall responses. Cells that are either older, such as cells from aged individuals, or cells that underwent a longer path of differentiation, such as terminally differentiated effector T cells (T_E) and exhausted T cells (T_{EX}), would be categorized into state 3. Aged cells, such as old T_N and old HSCs intrinsically lost the ability to perform ACD, which is due to increased activity of cell division control protein 42 (Cdc42) in ageing HSCs (Borsa et al., 2021; Florian et al., 2018). In addition, terminally differentiated cells reached the endpoint in their differentiation trajectory and lost plastic potential. Thus, ACD is not necessary for further cellular diversification or generation of cells with enhanced survival and stemness features anymore. (Figure 6.2).
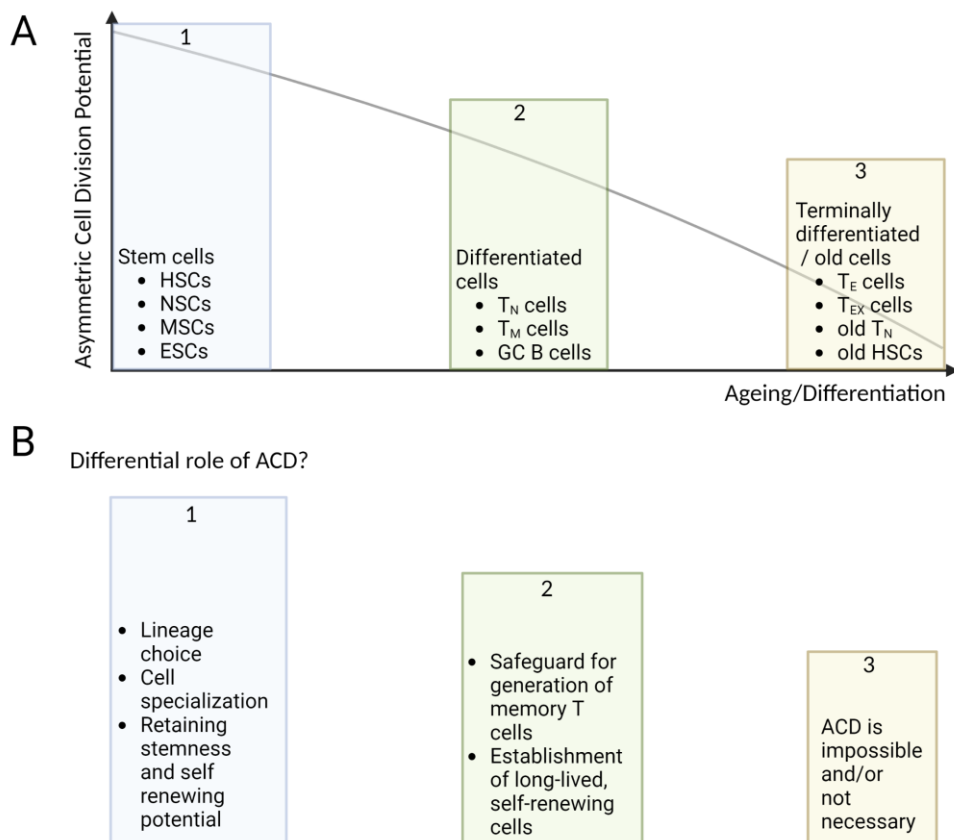
Figure 6.2. Differential roles of asymmetric cell division depending on the cellular state.

A Asymmetric cell division potential decreases with ageing, with advanced differentiation and with reduced stemness potential. Depending on the state of a cell implied by these three factors, ACD has different roles. **B** In state 1, comprising stem cells, ACD functions as a lineage defining mechanism allowing cell specialization in one daughter cell while the other retains stemness and self-renewing potential. Partially differentiated cells, such as naïve T cells (T_N), memory T cells (T_M) and GC B cells fall into state 2. Here, ACD functions as a safeguard mechanism in CD8 T cells for the generation of memory cells upon strong TCR stimulation or for the establishment of cells equipped with enhanced long term survival factors and high affinity receptors in GC B cells and potentially CD8 T cells. Cells categorized into state 3, such as old cells, terminal effector T cells (T_E) or exhausted T cells (T_{EX}), do not perform ACD, either due to their age-dependent intrinsic loss of ACD performance or advanced differentiation history.

Several *in vivo* studies provide evidence for a model in which certain effector CD8 T cells de-differentiate into central memory CD8 T cells upon viral clearance (Bannard et al., 2009; Youngblood et al., 2017). However, it is not resolved whether these de-differentiating effector CD8 T cells received a prior imprint that orchestrates their de-differentiation ability. This ability could have been imprinted by ACD and/or the inflammatory milieu (Chang et al., 2007; Joshi et al., 2007). In contrast, recent work has described the emergence of central memory precursor cells, which occur early during the expansion phase after acute viral infection and lack cytolytic differentiation (Johnnidis et al., 2021; Pais Ferreira et al., 2020). Interestingly, the early established CD62L^{hi} subset that later yields T$_{CM}$ cells, displayed evidence of stronger TCR signalling despite restrained proliferation during the expansion phase. Furthermore, although T$_{CM}$ cells were generated in the absence of this specific cell subset, a following memory CD8 T cell recall response was diminished compared to T$_{CM}$ cells that originated from the early CD62L^{hi} subset (Johnnidis et al., 2021). It remains to be elucidated whether early memory precursors that are established during the expansion phase upon acute infection, stem from strong TCR stimulation induced ACD and might potentially be equipped with enhanced memory and survival features, possibly representing high-quality central memory cells with enhanced recall response capacity in the later T$_{CM}$ pool. Thus, ACD might indeed function as a mechanism for ensuring the development of qualitatively superior high-affinity memory CD8 T cell clones, while also ensuring the general establishment of a robust memory T cell pool (Figure 6.2).

Taken together, the current work on CD8 T cell differentiation suggests different layers of regulatory mechanisms as well as various conditions under which the latter are employed. While the tissue niche and the inflammatory milieu certainly have large impacts on CD8 T cell differentiation, ACD might mediate the formation of qualitatively enhanced memory CD8 T cells enabled by the strong affinity of the TCR towards its cognate antigen. It remains to be shown whether those ACD dependent high-affinity memory CD8 T cells are equipped with enhanced survival and self-renewal features and whether they generate effector cells with increased effector functions during recall responses. It would be of interest to perform single cell tracing experiments in high and low affinity memory CD8 T cells after stimulation with either high or low affinity ligands and observe whether single cells form mixed fate or single fate colonies. It is described, that despite

pronounced expansion capacity, low affinity memory CD8 T cells responding to low affinity ligands are impaired in their effector functions (expression of Granzyme B, IFNγ, Tbet and Eomes) upon secondary expansion, while remaining reactive against high-affinity ligands (Knudson et al., 2013). Thus, given the fact, that low affinity memory clones are less reactive to low affinity ligands, it could be that the amount of single cell derived effector colonies might be diminished compared to its naïve counterparts stimulated with low affinity ligands as well as compared to stimulation of low affinity memory T cell clones with high affinity ligands. Consequently, stimulation of low affinity memory T cells with low affinity ligands would increase the abundancy of single cell derived memory colonies. In contrast, high affinity memory CD8 T cell clones robustly expanded and exerted potent effector functions in response to high and low affinity ligands, with only a slight decrease in production of IFNγ upon low affinity ligand stimulation (Knudson et al., 2013). Therefore, we would not expect major differences in the fate adoption of cells within high affinity memory CD8 T single cell derived colonies compared to those of their naïve counterparts.

Further, the precise underlying mechanisms of ACD establishment have not been fully described so far and are therefore currently investigated. Our present knowledge of the drivers of ACD will be summarized in the next section.

Drivers of asymmetric cell division

The exact drivers and regulators of asymmetric cell division are not yet fully defined. However, intrinsic regulators can be distinguished from external drivers. External regulators describe the impact of other cells or the tissue niche a cell is residing in on the dividing cell. Upon interaction of the cell with external ligands, a polarization axis is induced. Along the polarization axis, conserved polarity complexes as well as spindle orientation control the localization of fate-related molecules. In CD8 T cells, a polarization axis is induced by the interaction of the CD8 T cell with an antigen-presenting cell (APC) presenting the cognate antigen on MHC-I to the specific T cell receptor (TCR) (Oliaro et al., 2010). This interaction leads to the recruitment of other costimulatory and

adherence-providing molecules, such as ICAM-1, to the cell interface and finally to the formation of the immune synapse (IS). It has been elegantly described that inhibition of the formation of the IS by ICAM-1 deficiency abrogates ACD (Chang et al., 2007). Following successful establishment of the IS, the conserved polarity proteins Scribble and Par complexes antagonistically segregate into the two emerging daughter cells, with Scribble localizing into the IS-proximal daughter cell and Par3 into the IS-distal daughter cell (Oliaro et al., 2010). Another external contributor of ACD is the strength of TCR activation, also orchestrated via the IS, which prolongs the interaction between the CD8 T cell and the APC, potentially leading to increased ACD (King et al., 2012; Ozga et al., 2016).

In addition, an ER-diffusion barrier has been reported as a cell intrinsic regulator of asymmetric cell division. This lateral ER diffusion barrier is composed of sphingolipids and has been observed to form in the nuclear and ER membrane in yeast, in the ER membrane of NSCs and recently in the ER membrane of activated CD8 T cells where it facilitates the unequal segregation of certain molecules, such as aggregated or misfolded proteins in yeast (Clay et al., 2014; Emurla et al., 2021; Moore et al., 2015).

Furthermore, it has been shown that PKCζ activity is essential for ACD and that during an ACD, PKCζ localizes into the IS-distal CD8 daughter T cell, which is destined to differentiate into a memory cell (Chang et al., 2011, 2007; Metz et al., 2015). Of note, studies that show the latter have been performed upon strong TCR activation conditions. Our results show that, besides preventing ACD, inhibition of PKCζ during the first mitosis upon activation leads to decreased memory potential specifically upon strong TCR stimulation. In contrast, we did not observe any effect of PKCζ inhibition on fate outcome upon weak TCR stimulation. These findings raise the question whether PKCζ is potentially only segregated asymmetrically upon strong TCR stimulation, possibly in order to guide ACD. If so, it remains to be investigated how PKCζ mechanistically regulates ACD resulting in asymmetric fates. Even though ACD occurs after weak TCR stimulation at low levels, it does not lead to single cell derived mixed fate colonies, suggesting that other cues (potentially some differences in the relative strength of activation or differences in the exposure to differentiation-inducing cytokines) than ACD are responsible for fate determination. In contrast, upon strong TCR stimulation, single cell derived mixed fate colonies emerge particularly from single activated CD8

T cells that show an ACD in their first mitosis, which might potentially be mediated by selective asymmetric distribution of PKCζ. Thus, despite the identification of several contributors and regulatory mechanisms for the establishment of ACD, their individual importance as well as their interplay in fate diversification remains to be investigated.

Translating asymmetric cell division into clinical applications

CD8 T cells play critical roles in immune responses against acute and chronic viral infections as well as in anti-tumour responses. In order to improve and develop new successful vaccination strategies as well as immunotherapies against cancer, such as chimeric antigen receptor (CAR) T cell therapy or adoptive cell transfer therapy, it is essential to understand the biological mechanisms of CD8 T cell differentiation. As ACD is suggested to be a strong contributor of cell diversification into effector and memory subsets, its modulation provides potential for controlled and directed differentiation into a specific fate trajectory and might therefore be useful in clinical applications. For instance, it has been shown that transient mTOR inhibition by rapamycin treatment during activation of naïve CD8 T cells leads to enhanced ACD rates and improved memory potential (Borsa et al., 2019). Furthermore, it is well described that ageing leads to the loss of cellular ACD potential in HSCs, NSCs and CD8 T cells (Borsa et al., 2021; Florian et al., 2018; Moore et al., 2015). For aged CD8 T cells, it has been shown that also here, transient mTOR inhibition during activation is able to restore ACD potential, leading to improved memory potential of these cells (Borsa et al., 2021). This might be of particular relevance for the elderly population with regard to decreased vaccination efficacy and increased tumour incidence. Enhancement of diffusion barrier strength by rapamycin treatment has been observed in yeast cells and CD8 T cells and this correlated with increased ACD, at least for CD8 T cells (Baldi et al., 2017; Emurla et al., 2021). Whether the impact of rapamycin treatment would result in enhanced ACD in stem cells, such as in HSCs and NSCs as well, remains to be shown. However, the ongoing refinement of current as well as the development of new single cell-based technologies together with the increasing knowledge about the regulation

of CD8 T cell differentiation provides promising potential for the successful design of precise and individualized clinical applications, such as for CAR T cell therapy or vaccination.

References

Ackermann, M., Stearns, S.C., Jenal, U., 2003. Senescence in a Bacterium with Asymmetric Division. Science 300, 1920–1920. https://doi.org/10.1126/science.1083532

Adams, W.C., Chen, Y.-H., Kratchmarov, R., Yen, B., Nish, S.A., Lin, W.-H.W., Rothman, N.J., Luchsinger, L.L., Klein, U., Busslinger, M., Rathmell, J.C., Snoeck, H.-W., Reiner, S.L., 2016. Anabolism-Associated Mitochondrial Stasis Driving Lymphocyte Differentiation over Self-Renewal. Cell Reports 17, 3142–3152. https://doi.org/10.1016/j.celrep.2016.11.065

Ahmed, R., Salmi, A., Butler, L.D., Chiller, J.M., Oldstone, M.B., 1984. Selection of genetic variants of lymphocytic choriomeningitis virus in spleens of persistently infected mice. Role in suppression of cytotoxic T lymphocyte response and viral persistence. J Exp Med 160, 521–540. https://doi.org/10.1084/jem.160.2.521

Al Khabouri, S., Gerlach, C., 2020. T cell fate mapping and lineage tracing technologies probing clonal aspects underlying the generation of CD8 T cell subsets. Scand J Immunol 92. https://doi.org/10.1111/sji.12983

Alampi, G., Vignali, D., Centorame, I., Canu, A., Cosorich, I., Filoni, J., Di Dedda, C., Monti, P., 2022. Asymmetric T cell division of GAD65 specific naive T cells contribute to an early divergence in the differentiation fate into memory T cell subsets. Immunology imm.13537. https://doi.org/10.1111/imm.13537

Alanio, C., Lemaitre, F., Law, H.K.W., Hasan, M., Albert, M.L., 2010. Enumeration of human antigen-specific naive CD8+ T cells reveals conserved precursor frequencies. Blood 115, 3718–3725. https://doi.org/10.1182/blood-2009-10-251124

Andreotti, A.H., Schwartzberg, P.L., Joseph, R.E., Berg, L.J., 2010. T-cell signaling regulated by the Tec family kinase, Itk. Cold Spring Harb Perspect Biol 2, a002287. https://doi.org/10.1101/cshperspect.a002287

Arsenio, J., Metz, P.J., Chang, J.T., 2015. Asymmetric Cell Division in T Lymphocyte Fate Diversification. Trends in Immunology 36, 670–683. https://doi.org/10.1016/j.it.2015.09.004

Baldi, S., Bolognesi, A., Meinema, A.C., Barral, Y., 2017. Heat stress promotes longevity in budding yeast by relaxing the confinement of age-promoting factors in the mother cell. Elife 6. https://doi.org/10.7554/eLife.28329

Bannard, O., Kraman, M., Fearon, D.T., 2009. Secondary replicative function of CD8+ T cells that had developed an effector phenotype. Science 323, 505–509. https://doi.org/10.1126/science.1166831

Barnett, B.E., Ciocca, M.L., Goenka, R., Barnett, L.G., Wu, J., Laufer, T.M., Burkhardt, J.K., Cancro, M.P., Reiner, S.L., 2012. Asymmetric B cell division in the germinal center reaction. Science 335, 342–344. https://doi.org/10.1126/science.1213495

Battegay, M., Cooper, S., Althage, A., Bänziger, J., Hengartner, H., Zinkernagel, R.M., 1991. Quantification of lymphocytic choriomeningitis virus with an immunological focus assay in 24- or 96-well plates. J Virol Methods 33, 191–198. https://doi.org/10.1016/0166-0934(91)90018-u

Benoit Bouvrette, L.P., Cody, N.A.L., Bergalet, J., Lefebvre, F.A., Diot, C., Wang, X., Blanchette, M., Lécuyer, E., 2018. CeFra-seq reveals broad asymmetric mRNA and noncoding RNA distribution profiles in Drosophila and human cells. RNA 24, 98–113. https://doi.org/10.1261/rna.063172.117

Berdyshev, E.V., Gorshkova, I., Skobeleva, A., Bittman, R., Lu, X., Dudek, S.M., Mirzapoiazova, T., Garcia, J.G.N., Natarajan, V., 2009. FTY720 inhibits ceramide synthases and up-regulates dihydrosphingosine 1-phosphate formation in human lung endothelial cells. J Biol Chem 284, 5467–5477. https://doi.org/10.1074/jbc.M805186200

Borsa, M., Barandun, N., Gräbnitz, F., Barnstorf, I., Baumann, N.S., Pallmer, K., Baumann, S., Stark, D., Balaz, M., Oetiker, N., Wagen, F., Wolfrum, C., Simon, A.K., Joller, N., Barral, Y., Spörri, R., Oxenius, A., 2021. Asymmetric cell division shapes naive and virtual memory T-cell immunity during ageing. Nat Commun 12, 2715. https://doi.org/10.1038/s41467-021-22954-y

Borsa, M., Barnstorf, I., Baumann, N.S., Pallmer, K., Yermanos, A., Gräbnitz, F., Barandun, N., Hausmann, A., Sandu, I., Barral, Y., Oxenius, A., 2019. Modulation of asymmetric cell division as a mechanism to boost CD8 $^+$ T cell memory. Sci. Immunol. 4, eaav1730. https://doi.org/10.1126/sciimmunol.aav1730

Boyd, L., Guo, S., Levitan, D., Stinchcomb, D.T., Kemphues, K.J., 1996. PAR-2 is asymmetrically distributed and promotes association of P granules and PAR-1 with the cortex in C. elegans embryos. Development 122, 3075–3084. https://doi.org/10.1242/dev.122.10.3075

Buchholz, V.R., Flossdorf, M., Hensel, I., Kretschmer, L., Weissbrich, B., Gräf, P., Verschoor, A., Schiemann, M., Höfer, T., Busch, D.H., 2013. Disparate Individual Fates Compose Robust CD8 $^+$ T Cell Immunity. Science 340, 630–635. https://doi.org/10.1126/science.1235454

Capece, T., Walling, B.L., Lim, K., Kim, K.-D., Bae, S., Chung, H.-L., Topham, D.J., Kim, M., 2017. A novel intracellular pool of LFA-1 is critical for asymmetric CD8+ T cell activation and differentiation. Journal of Cell Biology 216, 3817–3829. https://doi.org/10.1083/jcb.201609072

Chang, J.T., Ciocca, M.L., Kinjyo, I., Palanivel, V.R., McClurkin, C.E., DeJong, C.S., Mooney, E.C., Kim, J.S., Steinel, N.C., Oliaro, J., Yin, C.C., Florea, B.I., Overkleeft, H.S., Berg, L.J., Russell, S.M., Koretzky, G.A., Jordan, M.S., Reiner, S.L., 2011. Asymmetric Proteasome Segregation as a Mechanism for Unequal Partitioning of the Transcription Factor T-bet during T Lymphocyte Division. Immunity 34, 492–504. https://doi.org/10.1016/j.immuni.2011.03.017

Chang, J.T., Palanivel, V.R., Kinjyo, I., Schambach, F., Intlekofer, A.M., Banerjee, A., Longworth, S.A., Vinup, K.E., Mrass, P., Oliaro, J., Killeen, N., Orange, J.S., Russell, S.M., Weninger, W., Reiner, S.L., 2007. Asymmetric T Lymphocyte Division in the Initiation of Adaptive Immune Responses. Science 315, 1687–1691. https://doi.org/10.1126/science.1139393

Chang, J.T., Wherry, E.J., Goldrath, A.W., 2014. Molecular regulation of effector and memory T cell differentiation. Nature Immunology 15, 1104–1115. https://doi.org/10.1038/ni.3031

Chen, W., Guillaume-Gentil, O., Rainer, P.Y., Gäbelein, C.G., Saelens, W., Gardeux, V., Klaeger, A., Dainese, R., Zachara, M., Zambelli, T., Vorholt, J.A., Deplancke, B., 2022. Live-seq enables temporal transcriptomic recording of single cells. Nature 608, 733–740. https://doi.org/10.1038/s41586-022-05046-9

Chen, Y., Zander, R., Khatun, A., Schauder, D.M., Cui, W., 2018. Transcriptional and Epigenetic Regulation of Effector and Memory CD8 T Cell Differentiation. Front. Immunol. 9, 2826. https://doi.org/10.3389/fimmu.2018.02826

Chen, Y.-H., Kratchmarov, R., Lin, W.-H.W., Rothman, N.J., Yen, B., Adams, W.C., Nish, S.A., Rathmell, J.C., Reiner, S.L., 2018. Asymmetric PI3K Activity in Lymphocytes Organized by a PI3K-Mediated Polarity Pathway. Cell Reports 22, 860–868. https://doi.org/10.1016/j.celrep.2017.12.087

Chhabra, S.N., Booth, B.W., 2021. Asymmetric cell division of mammary stem cells. Cell Division 16, 5. https://doi.org/10.1186/s13008-021-00073-w

Chin, S.S., Guillen, E., Chorro, L., Achar, S., Ng, K., Oberle, S., Alfei, F., Zehn, D., Altan-Bonnet, G., Delahaye, F., Lauvau, G., 2022. T cell receptor and IL-2 signaling strength control memory CD8+ T cell functional fitness via chromatin remodeling. Nat Commun 13, 2240. https://doi.org/10.1038/s41467-022-29718-2

Chung, H.K., McDonald, B., Kaech, S.M., 2021. The architectural design of CD8+ T cell responses in acute and chronic infection: Parallel structures with divergent fates. Journal of Experimental Medicine 218, e20201730. https://doi.org/10.1084/jem.20201730

Ciocca, M.L., Barnett, B.E., Burkhardt, J.K., Chang, J.T., Reiner, S.L., 2012. Cutting Edge: Asymmetric Memory T Cell Division in Response to Rechallenge. J.I. 188, 4145–4148. https://doi.org/10.4049/jimmunol.1200176

Clay, L., Caudron, F., Denoth-Lippuner, A., Boettcher, B., Buvelot Frei, S., Snapp, E.L., Barral, Y., 2014. A sphingolipid-dependent diffusion barrier confines ER stress to the yeast mother cell. Elife 3, e01883. https://doi.org/10.7554/eLife.01883

Conklin, E.G., 1905. The organization and cell-lineage of the ascidian egg. Academy of Natural Sciences.

Conley, J.M., Gallagher, M.P., Berg, L.J., 2016. T Cells and Gene Regulation: The Switching On and Turning Up of Genes after T Cell Receptor Stimulation in CD8 T Cells. Frontiers in Immunology 7.

Conley, J.M., Gallagher, M.P., Rao, A., Berg, L.J., 2020. Activation of the Tec Kinase ITK Controls Graded IRF4 Expression in Response to Variations in TCR Signal Strength. J Immunol 205, 335–345. https://doi.org/10.4049/jimmunol.1900853

Corse, E., Gottschalk, R.A., Allison, J.P., 2011. Strength of TCR–Peptide/MHC Interactions and In Vivo T Cell Responses. J. Immunol. 186, 5039. https://doi.org/10.4049/jimmunol.1003650

de Greef, P.C., Oakes, T., Gerritsen, B., Ismail, M., Heather, J.M., Hermsen, R., Chain, B., de Boer, R.J., 2020. The naive T-cell receptor repertoire has an extremely broad distribution of clone sizes. Elife 9. https://doi.org/10.7554/eLife.49900

Denton, A.E., Wesselingh, R., Gras, S., Guillonneau, C., Olson, M.R., Mintern, J.D., Zeng, W., Jackson, D.C., Rossjohn, J., Hodgkin, P.D., Doherty, P.C., Turner, S.J., 2011. Affinity thresholds for naive CD8+ CTL activation by peptides and engineered influenza A viruses. J Immunol 187, 5733–5744. https://doi.org/10.4049/jimmunol.1003937

D'Souza, W.N., Hedrick, S.M., 2006. Cutting Edge: Latecomer CD8 T Cells Are Imprinted with a Unique Differentiation Program. J. Immunol. 177, 777. https://doi.org/10.4049/jimmunol.177.2.777

Duffy, K.R., Wellard, C.J., Markham, J.F., Zhou, J.H.S., Holmberg, R., Hawkins, E.D., Hasbold, J., Dowling, M.R., Hodgkin, P.D., 2012. Activation-Induced B Cell Fates Are Selected by Intracellular Stochastic Competition. Science 335, 338–341. https://doi.org/10.1126/science.1213230

Emurla, H., Barral, Y., Oxenius, A., 2021. Role of mitotic diffusion barriers in regulating the asymmetric division of activated CD8 T cells (preprint). Immunology. https://doi.org/10.1101/2021.09.10.458880

Etemad-Moghadam, B., Guo, S., Kemphues, K.J., 1995. Asymmetrically distributed PAR-3 protein contributes to cell polarity and spindle alignment in early C. elegans embryos. Cell 83, 743–752. https://doi.org/10.1016/0092-8674(95)90187-6

Florian, M.C., Klose, M., Sacma, M., Jablanovic, J., Knudson, L., Nattamai, K.J., Marka, G., Vollmer, A., Soller, K., Sakk, V., Cabezas-Wallscheid, N., Zheng, Y., Mulaw, M.A., Glauche, I., Geiger, H., 2018. Aging alters the epigenetic asymmetry of HSC division. PLoS Biol 16, e2003389. https://doi.org/10.1371/journal.pbio.2003389

Fuentealba, L.C., Eivers, E., Geissert, D., Taelman, V., De Robertis, E.M., 2008. Asymmetric mitosis: Unequal segregation of proteins destined for degradation. Proc Natl Acad Sci U S A 105, 7732–7737. https://doi.org/10.1073/pnas.0803027105

Fuertes Marraco, S.A., Grosjean, F., Duval, A., Rosa, M., Lavanchy, C., Ashok, D., Haller, S., Otten, L.A., Steiner, Q.-G., Descombes, P., Luber, C.A., Meissner, F., Mann, M., Szeles, L., Reith, W., Acha-Orbea, H., 2012. Novel murine dendritic cell lines: a powerful auxiliary tool for dendritic cell research. Front Immunol 3, 331. https://doi.org/10.3389/fimmu.2012.00331

Gäbelein, C.G., Feng, Q., Sarajlic, E., Zambelli, T., Guillaume-Gentil, O., Kornmann, B., Vorholt, J.A., 2022. Mitochondria transplantation between living cells. PLOS Biology 20, e3001576. https://doi.org/10.1371/journal.pbio.3001576

Gattinoni, L., Lugli, E., Ji, Y., Pos, Z., Paulos, C.M., Quigley, M.F., Almeida, J.R., Gostick, E., Yu, Z., Carpenito, C., Wang, E., Douek, D.C., Price, D.A., June, C.H., Marincola, F.M., Roederer, M., Restifo, N.P., 2011. A human memory T cell subset with stem cell-like properties. Nat Med 17, 1290–1297. https://doi.org/10.1038/nm.2446

Geltink, R.I.K., Kyle, R.L., Pearce, E.L., 2018. Unraveling the Complex Interplay Between T Cell Metabolism and Function. Annu Rev Immunol 36, 461–488. https://doi.org/10.1146/annurev-immunol-042617-053019

Gerlach, C., Rohr, J.C., Perié, L., van Rooij, N., van Heijst, J.W.J., Velds, A., Urbanus, J., Naik, S.H., Jacobs, H., Beltman, J.B., de Boer, R.J., Schumacher, T.N.M., 2013. Heterogeneous Differentiation Patterns of Individual CD8 + T Cells. Science 340, 635–639. https://doi.org/10.1126/science.1235487

Gerlach, C., van Heijst, J.W.J., Swart, E., Sie, D., Armstrong, N., Kerkhoven, R.M., Zehn, D., Bevan, M.J., Schepers, K., Schumacher, T.N.M., 2010. One naive T cell, multiple fates in CD8+ T cell differentiation. Journal of Experimental Medicine 207, 1235–1246. https://doi.org/10.1084/jem.20091175

Gourley, T.S., Wherry, E.J., Masopust, D., Ahmed, R., 2004. Generation and maintenance of immunological memory. Semin Immunol 16, 323–333. https://doi.org/10.1016/j.smim.2004.08.013

Guillaume-Gentil, O., Grindberg, R.V., Kooger, R., Dorwling-Carter, L., Martinez, V., Ossola, D., Pilhofer, M., Zambelli, T., Vorholt, J.A., 2016. Tunable Single-Cell Extraction for Molecular Analyses. Cell 166, 506–516. https://doi.org/10.1016/j.cell.2016.06.025

Guillaume-Gentil, O., Potthoff, E., Ossola, D., Franz, C.M., Zambelli, T., Vorholt, J.A., 2014a. Force-controlled manipulation of single cells: from AFM to FluidFM. Trends in Biotechnology 32, 381–388. https://doi.org/10.1016/j.tibtech.2014.04.008

Guillaume-Gentil, O., Zambelli, T., Vorholt, J.A., 2014b. Isolation of single mammalian cells from adherent cultures by fluidic force microscopy. Lab Chip 14, 402–414. https://doi.org/10.1039/C3LC51174J

Guo, A., Huang, H., Zhu, Z., Chen, M.J., Shi, H., Yuan, S., Sharma, P., Connelly, J.P., Liedmann, S., Dhungana, Y., Li, Z., Haydar, D., Yang, M., Beere, H., Yustein, J.T., DeRenzo, C., Pruett-Miller, S.M., Crawford, J.C., Krenciute, G., Roberts, C.W.M., Chi, H., Green, D.R., 2022. cBAF complex components and MYC cooperate early in CD8+ T cell fate. Nature 607, 135–141. https://doi.org/10.1038/s41586-022-04849-0

Guo, S., Kemphues, K.J., 1995. par-1, a gene required for establishing polarity in C. elegans embryos, encodes a putative Ser/Thr kinase that is asymmetrically distributed. Cell 81, 611–620. https://doi.org/10.1016/0092-8674(95)90082-9

Hawkins, E.D., Oliaro, J., Kallies, A., Belz, G.T., Filby, A., Hogan, T., Haynes, N., Ramsbottom, K.M., Van Ham, V., Kinwell, T., Seddon, B., Davies, D., Tarlinton, D., Lew, A.M., Humbert, P.O., Russell, S.M., 2013. Regulation of asymmetric cell division and polarity by Scribble is not required for humoral immunity. Nature Communications 4, 1801. https://doi.org/10.1038/ncomms2796

Hilsenbeck, O., Schwarzfischer, M., Skylaki, S., Schauberger, B., Hoppe, P.S., Loeffler, D., Kokkaliaris, K.D., Hastreiter, S., Skylaki, E., Filipczyk, A., Strasser, M., Buggenthin, F., Feigelman, J.S., Krumsiek, J., van den Berg, A.J.J., Endele, M., Etzrodt, M., Marr, C., Theis, F.J., Schroeder, T., 2016. Software tools for single-cell tracking and quantification of cellular and molecular properties. Nat Biotechnol 34, 703–706. https://doi.org/10.1038/nbt.3626

Hogquist, K.A., Jameson, S.C., Heath, W.R., Howard, J.L., Bevan, M.J., Carbone, F.R., 1994. T cell receptor antagonist peptides induce positive selection. Cell 76, 17–27. https://doi.org/10.1016/0092-8674(94)90169-4

Hu, B., Guo, H., Zhou, P., Shi, Z.-L., 2021. Characteristics of SARS-CoV-2 and COVID-19. Nature Reviews Microbiology 19, 141–154. https://doi.org/10.1038/s41579-020-00459-7

Huang, F., Huang, W., Briggs, J., Chew, T., Bai, Y., Deol, S., August, A., 2015. The tyrosine kinase Itk suppresses CD8+ memory T cell development in response to bacterial infection. Scientific Reports 5, 7688. https://doi.org/10.1038/srep07688

Hung, T.J., Kemphues, K.J., 1999. PAR-6 is a conserved PDZ domain-containing protein that colocalizes with PAR-3 in Caenorhabditis elegans embryos. Development 126, 127–135. https://doi.org/10.1242/dev.126.1.127

Huseby, E.S., Teixeiro, E., 2022. The perception and response of T cells to a changing environment are based on the law of initial value. Sci Signal 15, eabj9842. https://doi.org/10.1126/scisignal.abj9842

Jameson, S.C., 2005. T cell homeostasis: keeping useful T cells alive and live T cells useful. Semin Immunol 17, 231–237. https://doi.org/10.1016/j.smim.2005.02.003

Jameson, S.C., Masopust, D., 2018. Understanding Subset Diversity in T Cell Memory. Immunity 48, 214–226. https://doi.org/10.1016/j.immuni.2018.02.010

Jameson, S.C., Masopust, D., 2009. Diversity in T cell memory: an embarrassment of riches. Immunity 31, 859–871. https://doi.org/10.1016/j.immuni.2009.11.007

Jazwinski, S.M., 1990. Aging and senescence of the budding yeast Saccharomyces cerevisiae. Molecular Microbiology 4, 337–343. https://doi.org/10.1111/j.1365-2958.1990.tb00601.x

Jeffery, W.R., Tomlinson, C.R., Brodeur, R.D., 1983. Localization of actin messenger RNA during early ascidian development. Dev Biol 99, 408–417. https://doi.org/10.1016/0012-1606(83)90290-7

Johnnidis, J.B., Muroyama, Y., Ngiow, S.F., Chen, Z., Manne, S., Cai, Z., Song, S., Platt, J.M., Schenkel, J.M., Abdel-Hakeem, M., Beltra, J.-C., Greenplate, A.R., Ali, M.-A.A., Nzingha, K., Giles, J.R., Harly, C., Attanasio, J., Pauken, K.E., Bengsch, B., Paley, M.A., Tomov, V.T., Kurachi, M., Vignali, D.A.A., Sharpe, A.H., Reiner, S.L., Bhandoola, A., Johnson, F.B., Wherry, E.J., 2021. Inhibitory signaling sustains a distinct early memory CD8 $^+$ T cell precursor that is resistant to DNA damage. Sci. Immunol. 6, eabe3702. https://doi.org/10.1126/sciimmunol.abe3702

Joshi, N.S., Cui, W., Chandele, A., Lee, H.K., Urso, D.R., Hagman, J., Gapin, L., Kaech, S.M., 2007. Inflammation directs memory precursor and short-lived effector CD8(+) T cell fates via the graded expression of T-bet transcription factor. Immunity 27, 281–295. https://doi.org/10.1016/j.immuni.2007.07.010

Kaech, S.M., Cui, W., 2012. Transcriptional control of effector and memory CD8+ T cell differentiation. Nat Rev Immunol 12, 749–761. https://doi.org/10.1038/nri3307

Kaech, S.M., Hemby, S., Kersh, E., Ahmed, R., 2002. Molecular and Functional Profiling of Memory CD8 T Cell Differentiation. Cell 111, 837–851. https://doi.org/10.1016/S0092-8674(02)01139-X

Kaech, S.M., Tan, J.T., Wherry, E.J., Konieczny, B.T., Surh, C.D., Ahmed, R., 2003. Selective expression of the interleukin 7 receptor identifies effector CD8 T cells that give rise to long-lived memory cells. Nat Immunol 4, 1191–1198. https://doi.org/10.1038/ni1009

Kakaradov, B., Arsenio, J., Widjaja, C.E., He, Z., Aigner, S., Metz, P.J., Yu, B., Wehrens, E.J., Lopez, J., Kim, S.H., Zuniga, E.I., Goldrath, A.W., Chang, J.T., Yeo, G.W., 2017. Early transcriptional and epigenetic regulation of CD8+ T cell differentiation revealed by single-cell RNA sequencing. Nat Immunol 18, 422–432. https://doi.org/10.1038/ni.3688

Kavazović, I., Han, H., Balzaretti, G., Slinger, E., Lemmermann, N.A.W., ten Brinke, A., Merkler, D., Koster, J., Bryceson, Y.T., de Vries, N., Jonjić, S., Klarenbeek, P.L., Polić, B., Eldering, E., Wensveen, F.M., 2020. Eomes broadens the scope of CD8 T-cell memory by inhibiting apoptosis in cells of low affinity. PLOS Biology 18, e3000648. https://doi.org/10.1371/journal.pbio.3000648

Kennedy, B.K., Austriaco, N.R.J., Guarente, L., 1994. Daughter cells of Saccharomyces cerevisiae from old mothers display a reduced life span. J Cell Biol 127, 1985–1993. https://doi.org/10.1083/jcb.127.6.1985

Kim, M.V., Ouyang, W., Liao, W., Zhang, M.Q., Li, M.O., 2013. The transcription factor Foxo1 controls central-memory CD8+ T cell responses to infection. Immunity 39, 286–297. https://doi.org/10.1016/j.immuni.2013.07.013

King, C.G., Koehli, S., Hausmann, B., Schmaler, M., Zehn, D., Palmer, E., 2012. T Cell Affinity Regulates Asymmetric Division, Effector Cell Differentiation, and Tissue Pathology. Immunity 37, 709–720. https://doi.org/10.1016/j.immuni.2012.06.021

Kinjyo, I., Qin, J., Tan, S.-Y., Wellard, C.J., Mrass, P., Ritchie, W., Doi, A., Cavanagh, L.L., Tomura, M., Sakaue-Sawano, A., Kanagawa, O., Miyawaki, A., Hodgkin, P.D., Weninger, W., 2015. Real-time tracking of cell cycle progression during CD8+ effector and memory T-cell differentiation. Nat Commun 6, 6301. https://doi.org/10.1038/ncomms7301

Knudson, K.M., Goplen, N.P., Cunningham, C.A., Daniels, M.A., Teixeiro, E., 2013. Low-Affinity T Cells Are Programmed to Maintain Normal Primary Responses but Are Impaired in Their Recall to Low-Affinity Ligands. Cell Reports 4, 554–565. https://doi.org/10.1016/j.celrep.2013.07.008

Korotkevich, G., Sukhov, V., Budin, N., Shpak, B., Artyomov, M.N., Sergushichev, A., 2021. Fast gene set enrichment analysis. bioRxiv. https://doi.org/10.1101/060012

Kretschmer, L., Flossdorf, M., Mir, J., Cho, Y.-L., Plambeck, M., Treise, I., Toska, A., Heinzel, S., Schiemann, M., Busch, D.H., Buchholz, V.R., 2020. Differential expansion of T central memory precursor and effector subsets is regulated by division speed. Nat Commun 11, 113. https://doi.org/10.1038/s41467-019-13788-w

Lanzavecchia, A., Sallusto, F., 2005. Understanding the generation and function of memory T cell subsets. Curr Opin Immunol 17, 326–332. https://doi.org/10.1016/j.coi.2005.04.010

Lécuyer, E., Yoshida, H., Parthasarathy, N., Alm, C., Babak, T., Cerovina, T., Hughes, T.R., Tomancak, P., Krause, H.M., 2007. Global analysis of mRNA localization reveals a prominent role in organizing cellular architecture and function. Cell 131, 174–187. https://doi.org/10.1016/j.cell.2007.08.003

Liao, Y., Smyth, G.K., Shi, W., 2019. The R package Rsubread is easier, faster, cheaper and better for alignment and quantification of RNA sequencing reads. Nucleic Acids Res 47, e47. https://doi.org/10.1093/nar/gkz114

Liao, Y., Smyth, G.K., Shi, W., 2014. featureCounts: an efficient general purpose program for assigning sequence reads to genomic features. Bioinformatics 30, 923–930. https://doi.org/10.1093/bioinformatics/btt656

Liedmann, S., Liu, X., Guy, C.S., Crawford, J.C., Rodriguez, D.A., Kuzuoğlu-Öztürk, D., Guo, A., Verbist, K.C., Temirov, J., Chen, M.J., Ruggero, D., Zhang, H., Thomas, P.G., Green, D.R., 2022. Localization of a TORC1-eIF4F translation complex during CD8+ T cell activation drives divergent cell fate. Molecular Cell 82, 2401-2414.e9. https://doi.org/10.1016/j.molcel.2022.04.016

Lin, W.-H.W., Adams, W.C., Nish, S.A., Chen, Y.-H., Yen, B., Rothman, N.J., Kratchmarov, R., Okada, T., Klein, U., Reiner, S.L., 2015. Asymmetric PI3K Signaling Driving Developmental and Regenerative Cell Fate Bifurcation. Cell Reports 13, 2203–2218. https://doi.org/10.1016/j.celrep.2015.10.072

Loeffler, D., Schneiter, F., Schroeder, T., 2020. Pitfalls and requirements in quantifying asymmetric mitotic segregation. Annals of the New York Academy of Sciences 1466, 73–82. https://doi.org/10.1111/nyas.14284

Loeffler, D., Schneiter, F., Wang, W., Wehling, A., Kull, T., Lengerke, C., Manz, M.G., Schroeder, T., 2022. Asymmetric organelle inheritance predicts human blood stem cell fate. Blood 139, 2011–2023. https://doi.org/10.1182/blood.2020009778

Loeffler, D., Schroeder, T., 2021. Symmetric and asymmetric activation of hematopoietic stem cells. Curr Opin Hematol 28, 262–268. https://doi.org/10.1097/MOH.0000000000000644

Loeffler, D., Wang, W., Hopf, A., Hilsenbeck, O., Bourgine, P.E., Rudolf, F., Martin, I., Schroeder, T., 2018. Mouse and human HSPC immobilization in liquid culture by CD43- or CD44-antibody coating. Blood 131, 1425–1429. https://doi.org/10.1182/blood-2017-07-794131

Loeffler, D., Wehling, A., Schneiter, F., Zhang, Y., Müller-Bötticher, N., Hoppe, P.S., Hilsenbeck, O., Kokkaliaris, K.D., Endele, M., Schroeder, T., 2019. Asymmetric lysosome inheritance predicts activation of haematopoietic stem cells. Nature 573, 426–429. https://doi.org/10.1038/s41586-019-1531-6

Lun, A.T.L., Chen, Y., Smyth, G.K., 2016. It's DE-licious: A Recipe for Differential Expression Analyses of RNA-seq Experiments Using Quasi-Likelihood Methods in edgeR. Methods Mol Biol 1418, 391–416. https://doi.org/10.1007/978-1-4939-3578-9_19

MacLennan, I.C., 1994. Germinal centers. Annu Rev Immunol 12, 117–139. https://doi.org/10.1146/annurev.iy.12.040194.001001

Mandala, S., Hajdu, R., Bergstrom, J., Quackenbush, E., Xie, J., Milligan, J., Thornton, R., Shei, G.-J., Card, D., Keohane, C., Rosenbach, M., Hale, J., Lynch, C.L., Rupprecht, K., Parsons, W., Rosen, H., 2002. Alteration of lymphocyte trafficking by sphingosine-1-phosphate receptor agonists. Science 296, 346–349. https://doi.org/10.1126/science.1070238

Marchingo, J.M., Kan, A., Sutherland, R.M., Duffy, K.R., Wellard, C.J., Belz, G.T., Lew, A.M., Dowling, M.R., Heinzel, S., Hodgkin, P.D., 2014. Antigen affinity, costimulation, and cytokine inputs sum linearly to amplify T cell expansion. Science 346, 1123–1127. https://doi.org/10.1126/science.1260044

Marchingo, J.M., Prevedello, G., Kan, A., Heinzel, S., Hodgkin, P.D., Duffy, K.R., 2016. T-cell stimuli independently sum to regulate an inherited clonal division fate. Nat Commun 7, 13540. https://doi.org/10.1038/ncomms13540

Martinez, R.J., Evavold, B.D., 2015. Lower Affinity T Cells are Critical Components and Active Participants of the Immune Response. Front. Immunol. 6. https://doi.org/10.3389/fimmu.2015.00468

Masopust David, Vezys Vaiva, Marzo Amanda L., Lefrançois Leo, 2001. Preferential Localization of Effector Memory Cells in Nonlymphoid Tissue. Science 291, 2413–2417. https://doi.org/10.1126/science.1058867

Matloubian, M., Lo, C.G., Cinamon, G., Lesneski, M.J., Xu, Y., Brinkmann, V., Allende, M.L., Proia, R.L., Cyster, J.G., 2004. Lymphocyte egress from thymus and peripheral lymphoid organs is dependent on S1P receptor 1. Nature 427, 355–360. https://doi.org/10.1038/nature02284

McFaline-Figueroa, J.R., Vevea, J., Swayne, T.C., Zhou, C., Liu, C., Leung, G., Boldogh, I.R., Pon, L.A., 2011. Mitochondrial quality control during inheritance is associated with lifespan and mother-daughter age asymmetry in budding yeast. Aging Cell 10, 885–895. https://doi.org/10.1111/j.1474-9726.2011.00731.x

Meister, A., Gabi, M., Behr, P., Studer, P., Vörös, J., Niedermann, P., Bitterli, J., Polesel-Maris, J., Liley, M., Heinzelmann, H., Zambelli, T., 2009. FluidFM: Combining Atomic Force Microscopy and Nanofluidics in a Universal Liquid Delivery System for Single Cell Applications and Beyond. Nano Lett. 9, 2501–2507. https://doi.org/10.1021/nl901384x

Mescher, M.F., Curtsinger, J.M., Agarwal, P., Casey, K.A., Gerner, M., Hammerbeck, C.D., Popescu, F., Xiao, Z., 2006. Signals required for programming effector and memory development by CD8+ T cells. Immunol Rev 211, 81–92. https://doi.org/10.1111/j.0105-2896.2006.00382.x

Metz, P.J., Arsenio, J., Kakaradov, B., Kim, S.H., Remedios, K.A., Oakley, K., Akimoto, K., Ohno, S., Yeo, G.W., Chang, J.T., 2015. Regulation of Asymmetric Division and CD8^{+} T Lymphocyte Fate Specification by Protein Kinase Cζ and Protein Kinase Cλ/ι. J.I. 194, 2249–2259. https://doi.org/10.4049/jimmunol.1401652

Moore, D., Pilz, G., Araúzo-Bravo, M., Barral, Y., Jessberger, S., 2015. A mechanism for the segregation of age in mammalian neural stem cells. Science 349, 1334–1338. https://doi.org/10.1126/science.aac9868

Moore, D.L., Jessberger, S., 2017. Creating Age Asymmetry: Consequences of Inheriting Damaged Goods in Mammalian Cells. Trends Cell Biol 27, 82–92. https://doi.org/10.1016/j.tcb.2016.09.007

Mueller, S.N., Mackay, L.K., 2016. Tissue-resident memory T cells: local specialists in immune defence. Nat Rev Immunol 16, 79–89. https://doi.org/10.1038/nri.2015.3

Nayar, R., Enos, M., Prince, A., Shin, H., Hemmers, S., Jiang, J., Klein, U., Thomas, C.J., Berg, L.J., 2012. TCR signaling via Tec kinase ITK and interferon regulatory factor 4 (IRF4) regulates CD8+ T-cell differentiation. Proc Natl Acad Sci U S A 109, E2794-2802. https://doi.org/10.1073/pnas.1205742109

Neitzke-Montinelli, V., Calôba, C., Melo, G., Frade, B.B., Caramez, E., Mazzoccoli, L., Gonçalves, A.N.A., Nakaya, H.I., Pereira, R.M., Werneck, M.B.F., Viola, J.P.B., 2022. Differentiation of Memory CD8 T Cells Unravel Gene Expression Pattern Common to Effector and Memory Precursors. Front Immunol 13, 840203. https://doi.org/10.3389/fimmu.2022.840203

Nish, S.A., Zens, K.D., Kratchmarov, R., Lin, W.-H.W., Adams, W.C., Chen, Y.-H., Yen, B., Rothman, N.J., Bhandoola, A., Xue, H.-H., Farber, D.L., Reiner, S.L., 2016. CD4+ T cell effector commitment coupled to self-renewal by asymmetric cell divisions. Journal of Experimental Medicine 214, 39–47. https://doi.org/10.1084/jem.20161046

Nutt, S.L., Tarlinton, D.M., 2011. Germinal center B and follicular helper T cells: siblings, cousins or just good friends? Nat Immunol 12, 472–477. https://doi.org/10.1038/ni.2019

Oliaro, J., Van Ham, V., Sacirbegovic, F., Pasam, A., Bomzon, Z., Pham, K., Ludford-Menting, M.J., Waterhouse, N.J., Bots, M., Hawkins, E.D., Watt, S.V., Cluse, L.A., Clarke, C.J.P., Izon, D.J., Chang, J.T., Thompson, N., Gu, M., Johnstone, R.W., Smyth, M.J., Humbert, P.O., Reiner, S.L., Russell, S.M., 2010. Asymmetric Cell Division of T Cells upon Antigen Presentation Uses Multiple Conserved Mechanisms. J.I. 185, 367–375. https://doi.org/10.4049/jimmunol.0903627

Ozga, A.J., Moalli, F., Abe, J., Swoger, J., Sharpe, J., Zehn, D., Kreutzfeldt, M., Merkler, D., Ripoll, J., Stein, J.V., 2016. pMHC affinity controls duration of CD8+ T cell-DC interactions and imprints timing of effector differentiation versus expansion. J Exp Med 213, 2811–2829. https://doi.org/10.1084/jem.20160206

Pais Ferreira, D., Silva, J.G., Wyss, T., Fuertes Marraco, S.A., Scarpellino, L., Charmoy, M., Maas, R., Siddiqui, I., Tang, L., Joyce, J.A., Delorenzi, M., Luther, S.A., Speiser, D.E., Held, W., 2020. Central memory CD8+ T cells derive from stem-like Tcf7hi effector cells in the absence of cytotoxic differentiation. Immunity 53, 985-1000.e11. https://doi.org/10.1016/j.immuni.2020.09.005

Pearce, E.L., Poffenberger, M.C., Chang, C.-H., Jones, R.G., 2013. Fueling immunity: insights into metabolism and lymphocyte function. Science 342, 1242454. https://doi.org/10.1126/science.1242454

Pircher, H., Ohashi, P., Miescher, G., Lang, R., Zikopoulos, A., Bürki, K., Mak, T.W., MacDonald, H.R., Hengartner, H., 1990. T cell receptor (TcR) beta chain transgenic mice: studies on allelic exclusion and on the TcR+ gamma/delta population. Eur J Immunol 20, 417–424. https://doi.org/10.1002/eji.1830200227

Plambeck, M., Kazeroonian, A., Loeffler, D., Schroeder, T., Busch, D.H., Flossdorf, M., Buchholz, V.R., 2021. Heritable changes in division speed accompany the diversification of single T cell fate (preprint). Immunology. https://doi.org/10.1101/2021.07.28.454102

Plumlee, C.R., Sheridan, B.S., Cicek, B.B., Lefrançois, L., 2013. Environmental cues dictate the fate of individual CD8+ T cells responding to infection. Immunity 39, 347–356. https://doi.org/10.1016/j.immuni.2013.07.014

Pollizzi, K.N., Sun, I.-H., Patel, C.H., Lo, Y.-C., Oh, M.-H., Waickman, A.T., Tam, A.J., Blosser, R.L., Wen, J., Delgoffe, G.M., Powell, J.D., 2016. Asymmetric inheritance of mTORC1 kinase activity during division dictates CD8+ T cell differentiation. Nat Immunol 17, 704–711. https://doi.org/10.1038/ni.3438

Prlic, M., Hernandez-Hoyos, G., Bevan, M.J., 2006. Duration of the initial TCR stimulus controls the magnitude but not functionality of the CD8+ T cell response. J Exp Med 203, 2135–2143. https://doi.org/10.1084/jem.20060928

Radhakrishnan, S.K., Thanbichler, M., Viollier, P.H., 2008. The dynamic interplay between a cell fate determinant and a lysozyme homolog drives the asymmetric division cycle of Caulobacter crescentus. Genes Dev 22, 212–225. https://doi.org/10.1101/gad.1601808

Rhyu, M.S., Jan, L.Y., Jan, Y.N., 1994. Asymmetric distribution of numb protein during division of the sensory organ precursor cell confers distinct fates to daughter cells. Cell 76, 477–491. https://doi.org/10.1016/0092-8674(94)90112-0

Sallusto, F., Geginat, J., Lanzavecchia, A., 2004. Central memory and effector memory T cell subsets: function, generation, and maintenance. Annu Rev Immunol 22, 745–763. https://doi.org/10.1146/annurev.immunol.22.012703.104702

Sallusto, F., Lenig, D., Lanzavecchia, A., 1999. Two subsets of memory T lymphocytes with distinct homing potentials and effector functions 401, 5.

Sarkar, S., Kalia, V., Haining, W.N., Konieczny, B.T., Subramaniam, S., Ahmed, R., 2008. Functional and genomic profiling of effector CD8 T cell subsets with distinct memory fates. Journal of Experimental Medicine 205, 625–640. https://doi.org/10.1084/jem.20071641

Shakiba, M., Zumbo, P., Espinosa-Carrasco, G., Menocal, L., Dündar, F., Carson, S.E., Bruno, E.M., Sanchez-Rivera, F.J., Lowe, S.W., Camara, S., Koche, R.P., Reuter, V.P., Socci, N.D., Whitlock, B., Tamzalit, F., Huse, M., Hellmann, M.D., Wells, D.K., Defranoux, N.A., Betel, D., Philip, M., Schietinger, A., 2022. TCR signal strength defines distinct mechanisms of T cell dysfunction and cancer evasion. Journal of Experimental Medicine 219, e20201966. https://doi.org/10.1084/jem.20201966

Shimoni, R., Pham, K., Yassin, M., Ludford-Menting, M.J., Gu, M., Russell, S.M., 2014. Normalized Polarization Ratios for the Analysis of Cell Polarity. PLoS ONE 9, e99885. https://doi.org/10.1371/journal.pone.0099885

Skokos, D., Shakhar, G., Varma, R., Waite, J.C., Cameron, T.O., Lindquist, R.L., Schwickert, T., Nussenzweig, M.C., Dustin, M.L., 2007. Peptide-MHC potency governs dynamic interactions between T cells and dendritic cells in lymph nodes. Nature Immunology 8, 835–844. https://doi.org/10.1038/ni1490

Smith-Garvin, J.E., Burns, J.C., Gohil, M., Zou, T., Kim, J.S., Maltzman, J.S., Wherry, E.J., Koretzky, G.A., Jordan, M.S., 2010. T-cell receptor signals direct the composition and function of the memory CD8+ T-cell pool. Blood 116, 5548–5559. https://doi.org/10.1182/blood-2010-06-292748

Solouki, S., Huang, W., Elmore, J., Limper, C., Huang, F., August, A., 2020. TCR Signal Strength and Antigen Affinity Regulate CD8 $^+$ Memory T Cells. J.I. 205, 1217–1227. https://doi.org/10.4049/jimmunol.1901167

Spana, E.P., Kopczynski, C., Goodman, C.S., Doe, C.Q., 1995. Asymmetric localization of numb autonomously determines sibling neuron identity in the Drosophila CNS. Development 121, 3489–3494. https://doi.org/10.1242/dev.121.11.3489

Sprent, J., Cho, J.-H., Boyman, O., Surh, C.D., 2008. T cell homeostasis. Immunology & Cell Biology 86, 312–319. https://doi.org/10.1038/icb.2008.12

Stemberger, C., Huster, K.M., Koffler, M., Anderl, F., Schiemann, M., Wagner, H., Busch, D.H., 2007. A single naive CD8+ T cell precursor can develop into diverse effector and memory subsets. Immunity 27, 985–997. https://doi.org/10.1016/j.immuni.2007.10.012

Stewart, E.J., Madden, R., Paul, G., Taddei, F., 2005. Aging and death in an organism that reproduces by morphologically symmetric division. PLoS Biol 3, e45. https://doi.org/10.1371/journal.pbio.0030045

Sunchu, B., Cabernard, C., 2020. Principles and mechanisms of asymmetric cell division. Development 147, dev167650. https://doi.org/10.1242/dev.167650

Surh, C.D., Sprent, J., 2008. Homeostasis of naive and memory T cells. Immunity 29, 848–862. https://doi.org/10.1016/j.immuni.2008.11.002

Thaunat, O., Granja, A.G., Barral, P., Filby, A., Montaner, B., Collinson, L., Martinez-Martin, N., Harwood, N.E., Bruckbauer, A., Batista, F.D., 2012. Asymmetric Segregation of Polarized Antigen on B Cell Division Shapes Presentation Capacity. Science 335, 475–479. https://doi.org/10.1126/science.1214100

Turner, M.J., Jellison, E.R., Lingenheld, E.G., Puddington, L., Lefrançois, L., 2008. Avidity maturation of memory CD8 T cells is limited by self-antigen expression. J Exp Med 205, 1859–1868. https://doi.org/10.1084/jem.20072390

Utzschneider, Daniel T, Alfei, F., Roelli, P., Barras, D., Chennupati, V., Darbre, S., Delorenzi, M., Pinschewer, D.D., Zehn, D., 2016. High antigen levels induce an exhausted phenotype in a chronic infection without impairing T cell expansion and survival. J Exp Med 213, 1819–1834. https://doi.org/10.1084/jem.20150598

Utzschneider, Daniel T., Charmoy, M., Chennupati, V., Pousse, L., Ferreira, D.P., Calderon-Copete, S., Danilo, M., Alfei, F., Hofmann, M., Wieland, D., Pradervand, S., Thimme, R., Zehn, D., Held, W., 2016. T Cell Factor 1-Expressing Memory-like CD8+ T Cells Sustain the Immune Response to Chronic Viral Infections. Immunity 45, 415–427. https://doi.org/10.1016/j.immuni.2016.07.021

van der Windt, G.J.W., Pearce, E.L., 2012. Metabolic switching and fuel choice during T-cell differentiation and memory development. Immunol Rev 249, 27–42. https://doi.org/10.1111/j.1600-065X.2012.01150.x

Verbist, K.C., Guy, C.S., Milasta, S., Liedmann, S., Kamiński, M.M., Wang, R., Green, D.R., 2016. Metabolic maintenance of cell asymmetry following division in activated T lymphocytes. Nature 532, 389–393. https://doi.org/10.1038/nature17442

Wagner, D.E., Klein, A.M., 2020. Lineage tracing meets single-cell omics: opportunities and challenges. Nat Rev Genet 21, 410–427. https://doi.org/10.1038/s41576-020-0223-2

Wehling, A., Loeffler, D., Zhang, Y., Kull, T., Donato, C., Szczerba, B., Ortega, G.C., Lee, M., Moor, A., Göttgens, B., Aceto, N., Schroeder, T., 2022. Combined single-cell tracking and omics improves blood stem cell fate regulator identification. Blood. https://doi.org/10.1182/blood.2022016880

Wherry, E.J., Teichgräber, V., Becker, T.C., Masopust, D., Kaech, S.M., Antia, R., von Andrian, U.H., Ahmed, R., 2003. Lineage relationship and protective immunity of memory CD8 T cell subsets. Nature Immunology 4, 225–234. https://doi.org/10.1038/ni889

Wiesel, M., WALTON, S., RICHTER, K., OXENIUS, A., 2009. Virus-specific CD8 T cells: activation, differentiation and memory formation. APMIS 117, 356–381. https://doi.org/10.1111/j.1600-0463.2009.02459.x

Winkelstein, W.J., 1992. Not just a country doctor: Edward Jenner, scientist. Epidemiol Rev 14, 1–15. https://doi.org/10.1093/oxfordjournals.epirev.a036081

Youngblood, B., Hale, J.S., Kissick, H.T., Ahn, E., Xu, X., Wieland, A., Araki, K., West, E.E., Ghoneim, H.E., Fan, Y., Dogra, P., Davis, C.W., Konieczny, B.T., Antia, R., Cheng, X., Ahmed, R., 2017. Effector CD8 T cells dedifferentiate into long-lived memory cells. Nature 552, 404–409. https://doi.org/10.1038/nature25144

Zehn, D., Lee, S.Y., Bevan, M.J., 2009. Complete but curtailed T-cell response to very low-affinity antigen. Nature 458, 211–214. https://doi.org/10.1038/nature07657

Zhang, L., Romero, P., 2018. Metabolic Control of CD8(+) T Cell Fate Decisions and Antitumor Immunity. Trends Mol Med 24, 30–48. https://doi.org/10.1016/j.molmed.2017.11.005

Zhang, S.-Q., Parker, P., Ma, K.-Y., He, C., Shi, Q., Cui, Z., Williams, C.M., Wendel, B.S., Meriwether, A.I., Salazar, M.A., Jiang, N., 2016. Direct measurement of T cell receptor affinity and sequence from naïve antiviral T cells. Sci Transl Med 8, 341ra77. https://doi.org/10.1126/scitranslmed.aaf1278

Zhao, D.-M., Yu, S., Zhou, X., Haring, J.S., Held, W., Badovinac, V.P., Harty, J.T., Xue, H.-H., 2010. Constitutive activation of Wnt signaling favors generation of memory CD8 T cells. J Immunol 184, 1191–1199. https://doi.org/10.4049/jimmunol.0901199

Zikherman, J., Au-Yeung, B., 2015. The role of T cell receptor signaling thresholds in guiding T cell fate decisions. Curr Opin Immunol 33, 43–48. https://doi.org/10.1016/j.coi.2015.01.012

Abbreviations

α alpha, anti

ACD asymmetric cell division

ACT adoptive cell transfer

APC antigen-presenting cell

β beta

°C degree Celsius

CAR chimeric antigen receptor

CCR C-C motif chemokine receptor

CD cluster of differentiation

DC dendritic cell

DMSO dimethysulfoxide

EDTA ethylenediaminetetraacetic acid

Eomes eomesodermin

ER endoplasmic reticulum

ESC embryonic stem cell

FACS fluorescence-activated cell sorting

ffu focus forming unit

FOXO1 forkhead box O1

γ gamma

g gram

GMFI geometric mean of fluorescence intensity

gp glycoprotein

h hour / hours

hi high

HSC hematopoietic stem cell

ICAM intercellular adhesion molecule

IFN interferon

IL interleukin

IS immune/immunological synapse

KLRG killer cell lectin-like receptor

RNA ribonucleic acid

L ligand

LCMV lymphocytic choriomeningitis virus

LFA lymphocyte function-associated antigen

LN lymph node

lo low

µg microgram

µl microliter

µm micrometer

µM micromolar

M molar

mg milligram

mM millimolar

MHC major histocompatibility complex

min minute

ml milliliter

MPEC memory precursor effector cell

MSC mammary stem cell

mTOR mammalian target of rapamycin

ng nanogram

nM nanomolar

NSC neuronal stem cell

OVA ovalbumin

OXPHOS oxidative phosphorylation

p- phosphorylated

PBS phosphate buffered saline

PD programmed cell death

PFA paraformaldehyde

PI3K phosphatidylinositol 3-kinase

PKC protein kinase C

R receptor

ROI region of interest

ROS reactive oxygen species

RPMI Roswell Park Memorial Institute

S6 S6 kinase beta-1

SEM standard error mean

SLEC short-lived effector cell

SPF specific pathogen free

SPR surface plasmon resonance

T-bet T-box transcription factor

TCF T cell factor

T_{cm} central memory T cell

TCR T cell receptor

T_e effector T cell

T_{em} effector memory T cell

T_n naive T cell

T_{rm} resident memory T cell

T_{SCM} memory stem T cell

TIM T cell Ig and mucin domain

TNF tumor necrosis factor

ζ zeta

Acknowledgements

First and foremost, I would like to express my deepest appreciation to **Annette Oxenius**. I am sincerely grateful for having been accepted in her research group as a PhD candidate. Her motivating spirit and fascinating mind were extremely encouraging for me during the last 4.5 years. Personally, I cannot imagine a better supervision. While giving me a lot of freedom and thereby teaching me how to work independently and organize myself, Annette was always immediately available as soon as I needed help or questions arose that I could not answer by myself. With her positive energy and amazing support, I extremely enjoyed my PhD project and I am more than grateful for all the skills I learned from her, also besides the fascinating scientific part.

I am very grateful to **Mariana Borsa** – my mother cell – who taught me about asymmetric cell division (ACD) during my semester project when I joined the lab for the first time 5 years ago. She passed on her passion about ACD to me and strongly supported me during my first time as a young PhD daughter cell before she proceeded to Oxford for her PostDoc. Nevertheless, she became part of my PhD Committee and I was lucky to continue to benefit from her valuable expertise. Not only scientifically, but also personally, I deeply appreciate Mariana for her kind, positive and inspiring personality.

I am especially thankful to **Federica Sallusto** and **Timm Schroeder** for their tremendous support and valuable scientific advice as well as positive criticism as members of my PhD committee.

I am very grateful for the friendly and supportive atmosphere in the Oxenius group and all the insightful discussions we had during our lab meetings and lunch breaks. Many thanks to **Roman Spörri** for amazing scientific input and great support. I appreciate the scientific advice of the members of the **Joller**, **Sallusto** and **Latorre groups** during our shared lab meetings. I truly believe our daily lab work would be much harder without **Nathalie Oetiker** and **Franziska Wagen**. I deeply appreciate their work and effort in the lab by providing everything we need on a daily basis, including the never-ending mouse typings. I am also very grateful to the **Institute of Microbiology**, the **RCHCI team**, especially **Manuela Graf,** and **EPIC** for providing a wonderfully organized environment for scientific working. I am thankful to **Judith Zingg** for a great coordination of the MIM PhD program facilitating stimulating courses and scientific as well as social events.

Curriculum Vitae

FABIENNE GRÄBNITZ

Limmattalstrasse 244, CH 8049 Zürich 📍

graebnif@biol.ethz.ch @
fabienne.graebnitz@gmx.net (private)

www.linkedin.com/in/fabienne-graebnitz 💼

+41 77 916 70 78 📞

21.12.1992 – Munich, Germany ✧

EXPERTISE

immunology and tumor immunology

basic research: T cell differentiation
applied research: immunotherapy | vaccine development

interdisciplinary collaborations

presentation of scientific projects on conferences

supervision and guidance of master students

mentoring new PhD students

METHODS

mouse models and handling | flow cytometry (FACS) | microscopy | cell culture | FluidFM | RNAseq

LANGUAGES

German mother tongue
English fluent
French intermediate

BESIDES SCIENCE

running | cooking | mountaineering | music

PERSONAL PROFILE

Proven and motivated immunologist with a focus on the field of T cell differentiation. Creative and enthusiastic biologist with four years of experience in pharmaceutical industry. Strong expertise in designing and performing experiments, drug screening, researching literature, writing scientific reports and presenting complex data. Excellent analytical and communication skills.

EDUCATION

Swiss Federal Institute of Technology (ETH) Zurich, Zurich, Switzerland
PhD in Immunology

Ludwig-Maximilians-Universität (LMU) München, Munich, Germany
Biology, Master of Science

Friedrich-Alexander-Universität (FAU) Erlangen-Nürnberg, Erlangen, Germany
Biology, Bachelor of Science

Ernst-Mach-Gymnasium Haar, Munich, Germany
High School diploma

WORK EXPERIENCE

2022
Infection Immunology lab, ETH Zurich
Research assistant
Prof. Annette Oxenius, PhD

Lineage tracing of CD8 T cells upon asymmetric cell division

2018
Bavarian Nordic GmbH, Martinsried, Munich,
Working student
Department Immunology Research

Investigation of the rMVA-41BBL mediated anti-tumor response and characterization of rMVA activated NK cells regarding activation, cytotoxic effector functions and migration

2015
Bavarian Nordic GmbH, Martinsried, Munich,
Working student
Department Immunology Research

Immunological characterization of novel, recombinant vaccine vectors based on Modified Vaccinia Virus Ankara

2012

2011

PUBLICATIONS

Gräbnitz, F., Stark, D., Shlesinger, D., Petkidis, A., Borsa, M., Yermanos A., Carr, A., Barandun N., Wehling, A., Balaz, M., Schroeder, T., Oxenius, A., 2022. Asymmetric cell division safeguards memory CD8 T cell development. Sci. In preparation.

Borsa, M., Barandun, N., **Gräbnitz, F.**, Barnstorf, I., Baumann, N.S., Pallmer, K., Baumann, S., Stark, D., Balaz, M., Oetiker, N., Wagen, F., Wolfrum, C., Simon, A.K., Joller, N., Barral, Y., Spörri, R., Oxenius, A., 2021. Asymmetric cell division shapes naive and virtual memory T-cell immunity during ageing. Nat Commun 12, 2715

Müller, M., **Gräbnitz, F.**, Barandun, N., Shen, Y., Wendt, F., Steiner, S.N., Severin, Y., Vetterli, S.U., Mondal, M., Prudent, J.R., Hofmann, R., van Oostrum, M., Sarott, R.C., Nesvizhskii, A.I., Carreira, E.M., Bode, J.W., Snijder, B., Robinson, J.A., Loessner, M.J., Oxenius, A., Wollscheid, B., 2021. Light-mediated discovery of surfaceome nanoscale organization and intercellular receptor interaction networks. Nat Commun 12, 7036.

Hinterberger, M., Giessel, R., Fiore, G., **Gräbnitz, F.**, Bathke, B., Wennier, S., Chaplin, P., Melero, I., Suter, M., Lauterbach, H., Berraondo, P., Hochrein, H., Medina-Echeverz, J., 2021. Intratumoral virotherapy with 4-1BBL armed modified vaccinia Ankara eradicates solid tumors and promotes protective immune memory. J Immunother Cancer 9.

Stoycheva, D., Sandu, I., **Gräbnitz, F.**, Amorim, A., Borsa, M., Weber, S., Becher, B., Oxenius, A., 2021. Non-neutralizing antibodies protect against chronic LCMV infection by promoting infection of inflammatory monocytes in mice. Eur J Immunol 51, 1423–1435.

Borsa, M., Barnstorf, I., Baumann, N.S., Pallmer, K., Yermanos, A., **Gräbnitz, F.**, Barandun, N., Hausmann, A., Sandu, I., Barral, Y., Oxenius, A., 2019. Modulation of asymmetric cell division as a mechanism to boost CD8 + T cell memory. Sci. Immunol. 4, eaav1730.

Medina-Echeverz, J., Hinterberger, M., Testori, M., Geiger, M., Giessel, R., Bathke, B., Kassub, R., **Gräbnitz, F.**, Fiore, G., Wennier, S.T., Chaplin, P., Suter, M., Hochrein, H., Lauterbach, H., 2019. Synergistic cancer immunotherapy combines MVA-CD40L induced innate and adaptive immunity with tumor targeting antibodies. Nat Commun 10, 5041.

Sanos, S.L., Kassub, R., Testori, M., Geiger, M., Pätzold, J., Giessel, R., Knallinger, J., Bathke, B., **Gräbnitz, F.**, Brinkmann, K., Chaplin, P., Suter, M., Hochrein, H., Lauterbach, H., 2017. NLRC4 Inflammasome-Driven Immunogenicity of a Recombinant MVA Mucosal Vaccine Encoding Flagellin. Front Immunol 8, 1988.

PARTICIPATION IN SCIENTIFIC MEETINGS

Gräbnitz F., Guillaume-Gentil, O., Schroeder, T., Vorholt, J., Oxenius, A. Lineage tracing of CD8 T cells upon asymmetric cell division. In: Bridging Innovation and Translation in T cell Immunotherapy – Immunoctoberfest 2022, Munich, Germany. Poster. *SSAI Travel Grant.*

Gräbnitz, F., Barandun, N., Oxenius, A. Asymmetric cell division and differentiation of CD8 T cells. In: ETH D-BIOL Symp., 2022, Davos, Switzerland. Poster.

Gräbnitz, F., Oxenius, A. Lineage tracing of CD8 T cells upon asymmetric cell division. In:Wolfsberg Meeting, 2019, Wolfsberg, Switzerland.
2019: Poster.
2020 and 2021: Oral presentation